

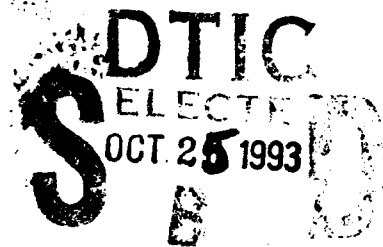
AD-A271 337



2

NAVAL POSTGRADUATE SCHOOL

Monterey, California



THESIS

FSR BASED FORCE TORQUE
TRANSDUCER DESIGN

by

Charles A. Gunzel-III

June, 1993

Thesis Advisor:

Morris R. Driels

Approved for public release; distribution is unlimited

93-25413



93 10 21 006

**Best
Available
Copy**

UNCLASSIFIED

SECURITY CLASSIFICATION OF THIS PAGE

REPORT DOCUMENTATION PAGE												
1a. REPORT SECURITY CLASSIFICATION Unclassified			1b. RESTRICTIVE MARKINGS									
2a. SECURITY CLASSIFICATION AUTHORITY			3. DISTRIBUTION/AVAILABILITY OF REPORT Approved for public release; distribution is unlimited.									
2b. DECLASSIFICATION/DOWNGRADING SCHEDULE												
4. PERFORMING ORGANIZATION REPORT NUMBER(S)			5. MONITORING ORGANIZATION REPORT NUMBER(S)									
6a. NAME OF PERFORMING ORGANIZATION Naval Postgraduate School		6b. OFFICE SYMBOL (If applicable) 34	7a. NAME OF MONITORING ORGANIZATION Naval Postgraduate School									
6c. ADDRESS (City, State, and ZIP Code) Monterey, CA 93943-5000			7b. ADDRESS (City, State, and ZIP Code) Monterey, CA 93943-5000									
8a. NAME OF FUNDING/SPONSORING ORGANIZATION		8b. OFFICE SYMBOL (If applicable)	9. PROCUREMENT INSTRUMENT IDENTIFICATION NUMBER									
8c. ADDRESS (City, State, and ZIP Code)			10. SOURCE OF FUNDING NUMBERS									
			<table border="1"> <tr> <td>Program Element No</td> <td>Project No</td> <td>Task No</td> <td>Work Unit Accession Number</td> </tr> <tr> <td></td> <td></td> <td></td> <td></td> </tr> </table>		Program Element No	Project No	Task No	Work Unit Accession Number				
Program Element No	Project No	Task No	Work Unit Accession Number									
11. TITLE (Include Security Classification) FSR BASED FORCE TORQUE TRANSDUCER DESIGN												
12. PERSONAL AUTHOR(S) Charles A. Gunzel-III												
13a. TYPE OF REPORT Master's Thesis		13b. TIME COVERED From To	14. DATE OF REPORT (year, month, day) June 1993	15. PAGE COUNT 135								
16. SUPPLEMENTARY NOTATION The views expressed in this thesis are those of the author and do not reflect the official policy or position of the Department of Defense or the U.S. Government.												
17. COSATI CODES			18. SUBJECT TERMS (continue on reverse if necessary and identify by block number)									
FIELD	GROUP	SUBGROUP	Force Control, Force-Torque Transducer, Force Sensing Resistor, Joystick									
19. ABSTRACT (continue on reverse if necessary and identify by block number) This thesis report discusses the design, construction and calibration of two force-torque transducers for use in a force control override of a rate control system. Pre-loaded force sensing resistors were used in a computer model to determine the number and location of sensors necessary to resolve three forces and three moments. An analysis was conducted on this full order model to determine redundancy limits. A reduced order model was then used to determine the sensor configuration required to resolve three forces and only one moment. Prototypes of the reduced order model were then built in two different sizes, and used to sense and display applied forces and moments.												
20. DISTRIBUTION/AVAILABILITY OF ABSTRACT <input checked="" type="checkbox"/> UNCLASSIFIED/UNLIMITED <input type="checkbox"/> SAME AS REPORT <input type="checkbox"/> DTIC USERS			21. ABSTRACT SECURITY CLASSIFICATION Unclassified									
22a. NAME OF RESPONSIBLE INDIVIDUAL Driels, Morris R.			22b. TELEPHONE (Include Area code) (408)656-3383	22c. OFFICE SYMBOL ME/dr								

DD FORM 1473, 84 MAR

83 APR edition may be used until exhausted
All other editions are obsoleteSECURITY CLASSIFICATION OF THIS PAGE
UNCLASSIFIED

Approved for public release; distribution is unlimited.

FSR BASED FORCE TORQUE
TRANSDUCER DESIGN

by

Charles A. Gunzel-III
Lieutenant, United States Navy
B.S., Oregon State University, 1986


Submitted in partial fulfillment
of the requirements for the degree of

MASTER OF SCIENCE IN MECHANICAL ENGINEERING
from the

NAVAL POSTGRADUATE SCHOOL


June 1993

Author:


Charles A. Gunzel-III

Approved by:


Morris R. Driels, Thesis Advisor


Matthew Kelleher, Chairman
Department of Mechanical Engineering

ABSTRACT

This thesis report discusses the design, construction and calibration of two force-torque transducers for use in a force control override of a rate control system. Pre-loaded force sensing resistors were used in a computer model to determine the number and location of sensors necessary to resolve three forces and three moments. An analysis was conducted on this full order model to determine redundancy limits. A reduced order model was then used to determine the sensor configuration required to resolve three forces and only one moment. Prototypes of the reduced order model were then built in two different sizes, and used to sense and display applied forces and moments.

DTIC QUALITY INSPECTED 2

Accession For	
NTIS GRA&I	<input checked="" type="checkbox"/>
DTIC TAB	<input type="checkbox"/>
Unannounced	<input type="checkbox"/>
Justification	
By	
Distribution/	
Availability Codes	
Dist	Avail and/or Special
A-1	

TABLE OF CONTENTS

I. INTRODUCTION	1
II. PRELIMINARY WORK	4
A. FORCE OVERRIDE RATE CONTROL	4
1. Concept	4
2. Background	4
B. SENSOR DEVELOPMENT	7
1. Force Sensing Resistor	7
a. Description	7
(1) Construction	7
(2) Characteristics	8
2. Transducer	11
a. Principle	11
b. Sensor Equations	13
c. Sensor Placement	16
d. Early Results	16
III. PRE-LOADED SENSOR TRANSDUCER DEVELOPMENT	19
A. SINGLE FSR PROTOTYPE	19
1. Objective	19
2. Design and Construction	19
a. Mechanical Device	19

b. Electronic Interface	21
3. Response Test	22
a. Data Collection	22
b. Results	23
B. INITIAL TRANSDUCER CONFIGURATION	24
1. Arrangement	24
2. Sensor Equations	26
3. Sensor Placement	29
4. Results	31
C. COMPARISON WITH PRELIMINARY WORK	32
1. Arrangement	32
2. Sensor Equations	32
3. Sensor Placement	34
4. Results	34
D. MODIFIED PRELIMINARY CONFIGURATION	35
1. Arrangement	35
2. Sensor Equations	36
3. Sensor Placement	37
4. Results	37
IV. REDUNDANCY ANALYSIS	38
A. GOAL	38
B. THEORY	39
1. Sensor Configuration	39
2. Algorithm	44
C. FORTRAN PROGRAM	45

D.	RESULTS	47
V.	REDUCED ORDER TRANSDUCER THEORY	48
A.	MOTIVATION	48
B.	SENSOR CONFIGURATION	48
	1. Arrangement	48
	2. Equations	49
	3. Sensor Placement	50
	4. Results	51
VI.	PROTOTYPE TRANSDUCER	53
A.	4 INCH REDUCED ORDER VERSION	53
	1. Objective	53
	2. Design and Construction	53
	a. Mechanical Design	53
	b. Electronic Interface	55
	3. Calibration and Testing	56
	a. Apparatus	56
	b. Technique	57
	c. Data Acquisition	58
	d. Results	59
B.	2 INCH REDUCED ORDER VERSION	62
	1. Objective	62
	2. Shortened FSR	62
	a. Methods	62
	b. Test and Comparison	64

c. Drift Analysis	67
(1) Description	67
(2) Test Conducted	68
(3) Results	69
3. Design and Construction	71
a. Mechanical Device	71
b. Electronic Interface	72
4. Calibration and Testing	73
 VII. DISCUSSION OF RESULTS	 75
A. DRIFT PHENOMENON	75
B. PROTOTYPE PERFORMANCE	76
1. Single FSR Prototype	76
2. Transducer Prototypes	77
C. REDUNDANCY ALGORITHM	80
 VIII. CONCLUSIONS AND RECOMMENDATIONS	 82
A. CONCLUSIONS	82
B. RECOMMENDATIONS	82
 APPENDIX A	 83
 APPENDIX B	 88
 APPENDIX C	 104

APPENDIX D	107
APPENDIX E	114
LIST OF REFERENCES	121
INITIAL DISTRIBUTION LIST	122

LIST OF FIGURES

Figure 1.	Hydraulic Force Override Rate Control System	5
Figure 2.	One DOF Force Override Rate Control of a PUMA 560 Manipulator	5
Figure 3.	A Bonded Strain Gauge	6
Figure 4.	Typical Force Sensing Resistor	8
Figure 5.	Typical FSR Force/Resistance Characteristic	9
Figure 6.	FSR Longevity Test	9
Figure 7.	FSR-Based Transducer Conceptual Design . . .	12
Figure 8.	Planar Joystick	15
Figure 9.	Arrangement for Full Order Transducer . . .	17
Figure 10.	Arrangement for Reduced Order Transducer . .	18
Figure 11.	Single Pre-loaded FSR Prototype	20
Figure 12.	FSR Current-to-Voltage Converter	21
Figure 13.	Force vs. V_{OUT} Curves	23
Figure 14.	Pre-load FSR Test #1 Result	24
Figure 15.	Initial Transducer Configuration	26
Figure 16.	Initial Minimum Sensor Transducer Configuration	31
Figure 17.	12 Sensor Preliminary Work Configuration . .	33
Figure 18.	Modified 12 Sensor Preliminary Work Configuration	35
Figure 19.	First Sequential Cube Face Numbering Scheme	40
Figure 20.	Second Sequential Cube Face Numbering Scheme	42

Figure 21. Successful Sequential Cube Face Numbering Scheme	43
Figure 22. Redundancy Analysis Flowchart	46
Figure 23. Positive Face Pre-Loaded Sensor Reduced Order Transducer	52
Figure 24. Negative Face Pre-Loaded Sensor Reduced Order Transducer	52
Figure 25. Generic Prototype Transducer	54
Figure 26. Transducer Test and Calibration Apparatus .	56
Figure 27. Icon Arrangement for Real Time Matrix Multiplication	60
Figure 28. Shortened FSR Performance Test Results . . .	64
Figure 29. Shortened FSR Performance Tests at Various Pre-Loads	65
Figure 30. Unaltered FSR Test at Three Different Pre-Loads	67

ACKNOWLEDGEMENT

I wish to express my appreciation to NASA for their sponsorship of the Force Override Rate Control project. Also, I am grateful for the leadership and instruction of Professor Driels which were invaluable to me during my research endeavors here at NPGS. Additionally, I would like to thank the Mechanical Engineering Department's laboratory manager, Tom McChord, and his staff for their eager, indispensable support. In particular, Jim Schofield's patience and technical expertise were key elements to the successful completion of this thesis.

I owe LCDR Jeffrey M. Nevels, USN, a big debt of gratitude for his loyal friendship, handy computer, convenient office, and support as a diligent and discerning reader of my writings. Finally, my deepest gratitude is to my loving, supportive wife, Cheryl, for her immeasurable support of the aspirations and quests in my life. And, for her crucial efforts in raising our children in the ever challenging environment of a military career.

I. INTRODUCTION

The objective of this thesis is to design, construct and calibrate a pair of reduced order force-torque transducers based on force sensing resistor technology. This is one branch of a two branch robotics research project. The work done in parallel is a separate study of how a hybrid force override rate control system can be used to enable operation of robotic manipulators.

The motivation for this research is that robotic applications such as the Space Shuttle Manipulator Arm require more than just rate and position control to perform certain assembly tasks. The ability to detect and control interaction forces and moments is necessary in poorly defined environments such as space. To accomplish various tasks without damage to the surrounding objects or the manipulator, the contact forces must be sensed and used in a feedback loop to regulate the conventional rate and position control. Further, with the use of force override control systems, human intervention, which may be hazardous, impractical or even impossible, could be entirely eliminated. This offers the potential for reducing costs, protecting human life and enabling the accomplishment of tasks never before possible.

In order to develop a practical, simple and durable system, the design of the force-torque transducer in this project is based on the **Force Sensing Resistor™** (FSR) rather than the strain gauge. FSRs provide a relatively inexpensive, vibration insensitive, durable and adaptable source of resistance changes from various force applications. To harness this technology in the design of a force-torque transducer, it was necessary to determine a basic configuration which enables the desired forces and moments to be extracted from various sensor signals. A design which enables the resolution of three forces and three moments was developed. This design was then modified to provide three forces and only one moment in the likely scenario of applications requiring only these four commonly used degrees of freedom. Also, the redundancy of the basic six degrees of freedom transducer was analyzed keeping in mind the practical use of such a device. A scheme allowing multiple levels of redundancy, in the event of individual sensor failure, was developed to demonstrate the functional reliability of a force-torque transducer designed using force sensing resistor technology.

Finally, the four degree of freedom transducer and associated electronic interfaces were constructed and tested in two versions. One was a design requiring no alterations to the readily available FSR. The other required a new, shorter FSR not currently available from the manufacturer. To overcome

this obstacle the available FSRs were modified in order to build a force-torque transducer of reduced proportions. This was done due to the payload limitations of the PUMA 560 robotic manipulator arm.

II. PRELIMINARY WORK

A. FORCE OVERRIDE RATE CONTROL

1. Concept

The general concept of a force override rate control system is that the contact forces between a robotic manipulator end effector and the object being moved can be used to generate a feedback signal. This signal is in the form of a voltage change which is used to alter the control input signal of a conventional rate or position control system. This gives conventionally controlled manipulators the ability to reflect the forces applied by the operator on the control device.

2. Background

This concept has been tested using a single degree of freedom hydraulic system [Ref.1:pp. 5-12], a single degree of freedom PUMA 560 manipulator system and a three degree of freedom PUMA 560 manipulator system [Ref. 2;pp.-27-54]. Figure 1 provides a general description of the hydraulic system [Ref. 1:p.6]. Figure 2 shows the general arrangement of the PUMA system [Ref. 3:p. 23]. These systems utilize resistance strain gauges to generate voltage signals which are proportional to the end effector contact forces.

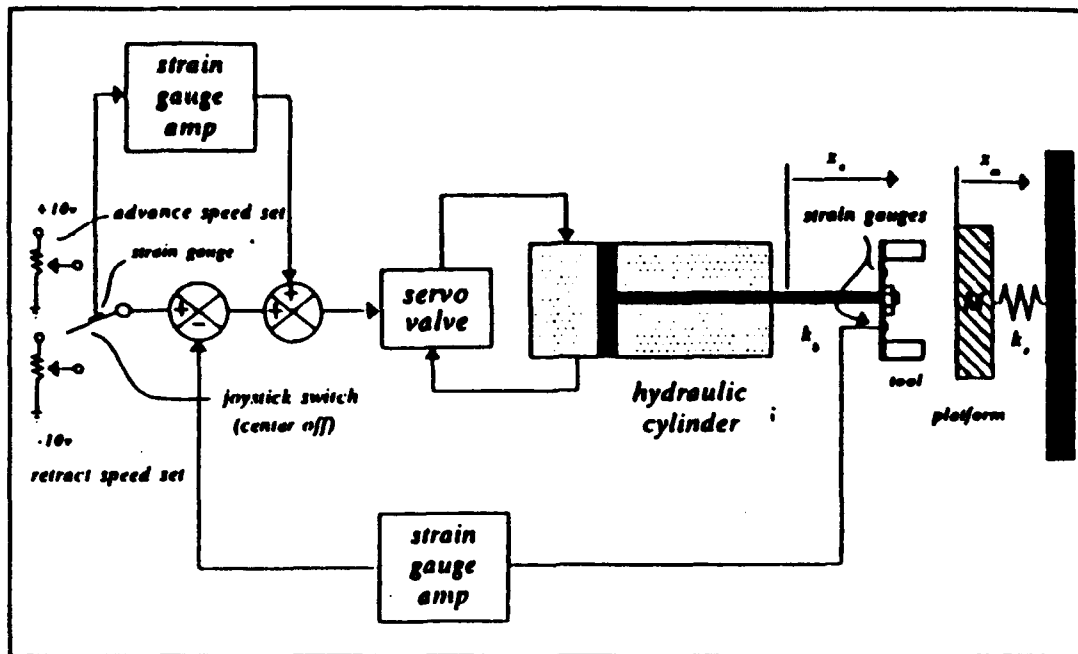


Figure 1
Hydraulic Force Override Rate Control System [Ref.2:p.28]

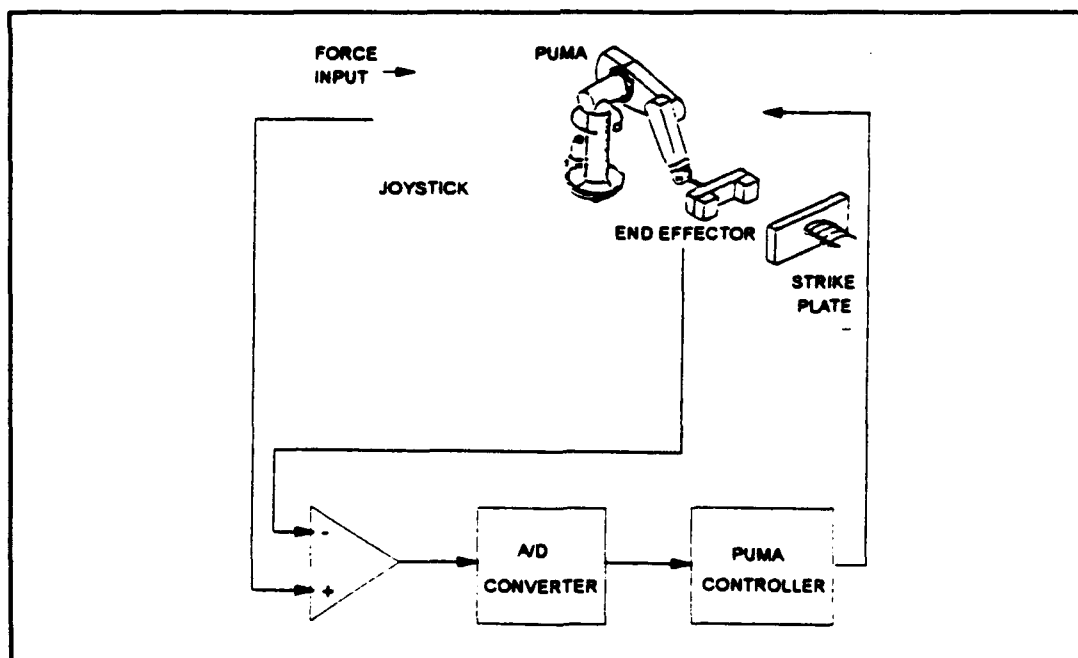


Figure 2
One DOF Force Override Rate Control of a PUMA 560 Manipulator [Ref. 2:p. 34]

In general a strain gauge is used to determine the actual stress experienced on the surface of the member to which it is bonded. The device consists of a folded wire assembly that exhibits a resistance change as the length and cross sectional area change according to:

$$R = \rho L / A \quad (1)$$

Where ρ is the resistivity of the material. L and A represent the wire length and cross sectional area. Figure 3 shows an enlarged view of a strain gauge. These resistance changes are small and temperature effects must be compensated for by use of a second unstrained gauge as part of the system. Also, the

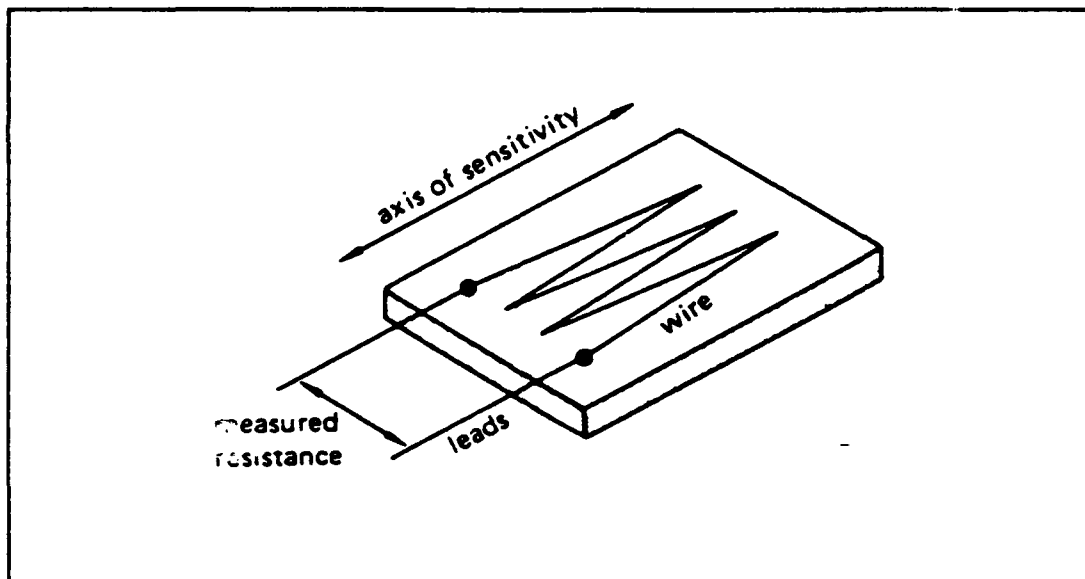


Figure 3
A Bonded Strain Gauge

gauge must be bonded to the stressed member in such a way that all the strain is transferred to and detected by the gauge. Strain gauge rosettes consisting of two or more strain gauges

with different orientations are used when stresses are expected in more than one direction. Hooke's law is used to calculate the stresses from the strains which are proportional to the applied loads.

Force-torque transducers based on strain gauge technology have been applied in the design of wrist force transducers. However, these tend to be expensive and complex requiring the part on which the strain gauge is mounted to be capable of deflection [Ref. 1:p. 15]. Also, such systems have a high susceptibility to noise since the small resistance changes require very high amplifier gains in order to produce a useful voltage signal. Hence, an alternative source of voltage output proportional to force input was sought which was low cost, robust and simple to construct, calibrate and use.

B. SENSOR DEVELOPMENT

1. Force Sensing Resistor

a. Description

(1) Construction

A Force Sensing ResistorTM is a device manufactured by Interlink Electronics of Santa Barbara, CA. Figure 4 shows the construction of a typical FSR. A sheet of polymer with a layer of semiconductive ink is faced with another sheet of polymer overlaid with a conducting pattern consisting of a set of interconnecting electrodes. These

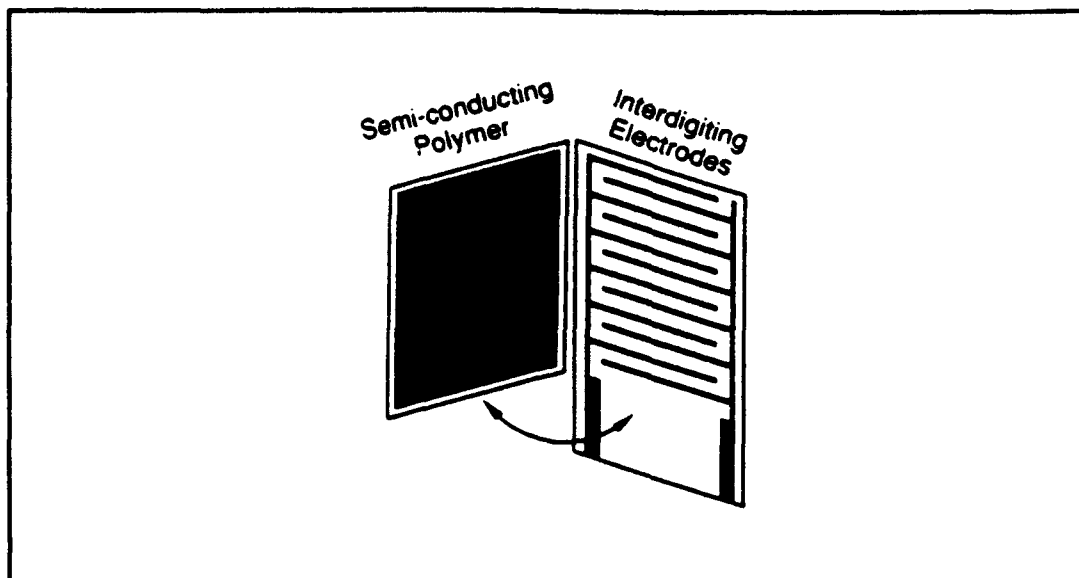


Figure 4
Typical Force Sensing Resistor [Ref. 4:p. 1]

electrodes are shunted by the semiconducting ink when the layers are brought together.[Ref. 4:pp. 1-2]

(2) Characteristics

The FSR has a very high no load resistance on the order of 1 Mohm or more. As the layered device is compressed the resistance drops proportionally. Figure 5 shows a typical plot of resistance verses force which is significantly more sensitive than the output of a strain gauge. Thus, the susceptibility to noise is immensely reduced.[Ref. 4:pp. 1-2]

Figure 6 displays the results of a longevity test conducted by the manufacturer demonstrating the durability of a typical FSR. Interlink Electronics also reports that the standard temperature range is up to about

170°C. Sensors capable of withstanding higher temperatures can be manufactured. FSRs are also relatively insensitive to humidity. [Ref. 4:p. 3]

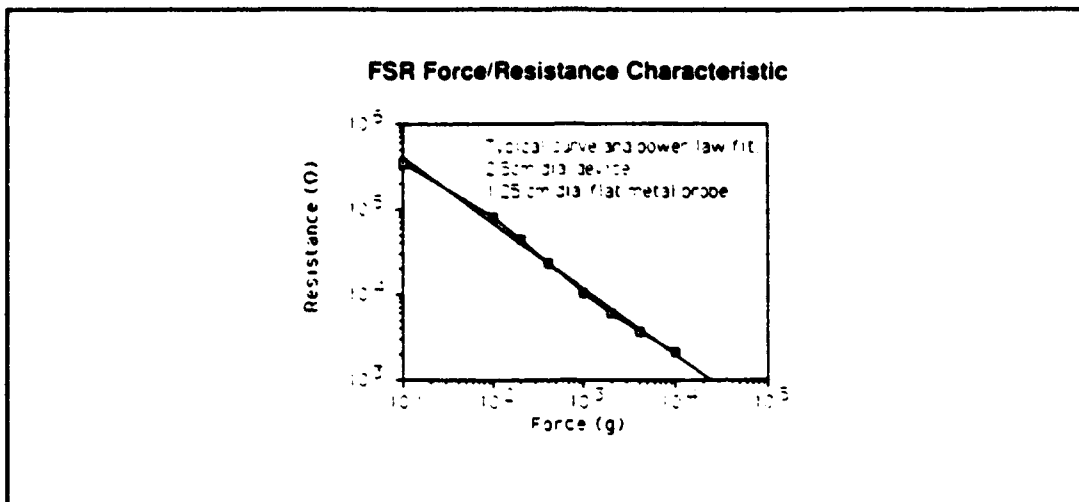


Figure 5
Typical FSR Force/Resistance Characteristic [Ref.4:p. 1]

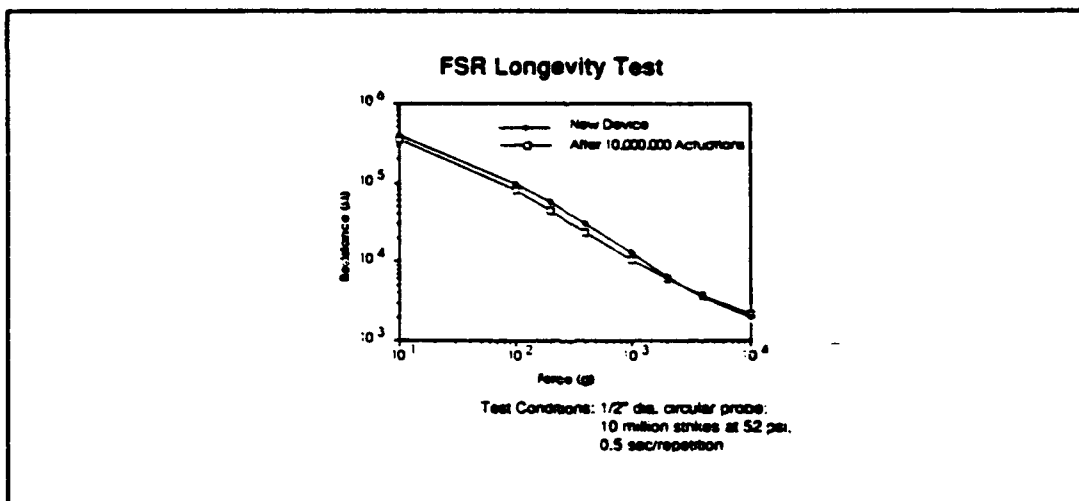


Figure 6
FSR Longevity Test [Ref.4:p. 3]

FSRs can be readily manufactured in various sizes as single sensors or arranged in arrays. It is also possible to vary the force range and the resistance range to meet specific requirements during fabrication. Interlink Electronics suggests that it is best to use the mechanical design to establish the force within a useable range.[Ref. 4:p. 2]

An FSR's performance is somewhere between a true force sensor and a pressure sensor. For a given force, a pressure sensor yields an output inversely proportional to the area of the applied force. Whereas a force sensor will yield a constant output regardless of the area and distribution over which the given force is applied. If the force distribution area is smaller than the FSR active area but large compared to the spacing between the interconnecting electrodes, then the resistance output will vary approximately as the reciprocal of the square root of the applied force area. However, when the area of the applied load is larger than the FSR active area the device can be used as a pressure sensor.[Ref. 4:p. 2]

Sensor electrical interfaces can be simple because typical resistance changes are relatively large; therefore, these circuits do not require a resistance bridge as do strain gauge circuits. Also, the impedance is almost entirely resistive. Depending on the circuit used, sensor

response signals are typically on the order of 0-10 volts.[Ref.4:p. 4]

Force sensing resistor technology offers many advantages over conventional strain gauge technology. In an attempt to develop the force override rate control system as a low cost, rugged and credible concept, a suitable force-torque transducer must be developed. Hence, the implementation of readily available FSRs is a logical choice for a simple, robust and inexpensive transducer design.

2. Transducer

a. Principle

The use of force sensing resistor technology was suggested to the project sponsor at NASA. Figure 7 shows the sponsor's suggested conceptual design for a suitable force-torque transducer using readily available FSRs [Ref. 1:p. 16]. Initially, it was proposed that the sensors be mounted on an inner cube which would be surrounded with a semi-compliant material like RTV and encased in a larger cube. When the joystick is moved, some of the FSRs will experience local normal forces and thus a change in resistance. When the appropriate electronic interface is used, a corresponding voltage change will be produced resulting in sensor signals which reflect the applied forces and moments. Ultimately, the sensors would be located in such a way that the applied forces

and moments could be detected and decoupled for use in a force
override rate control system. [Ref. 3:p. 11]

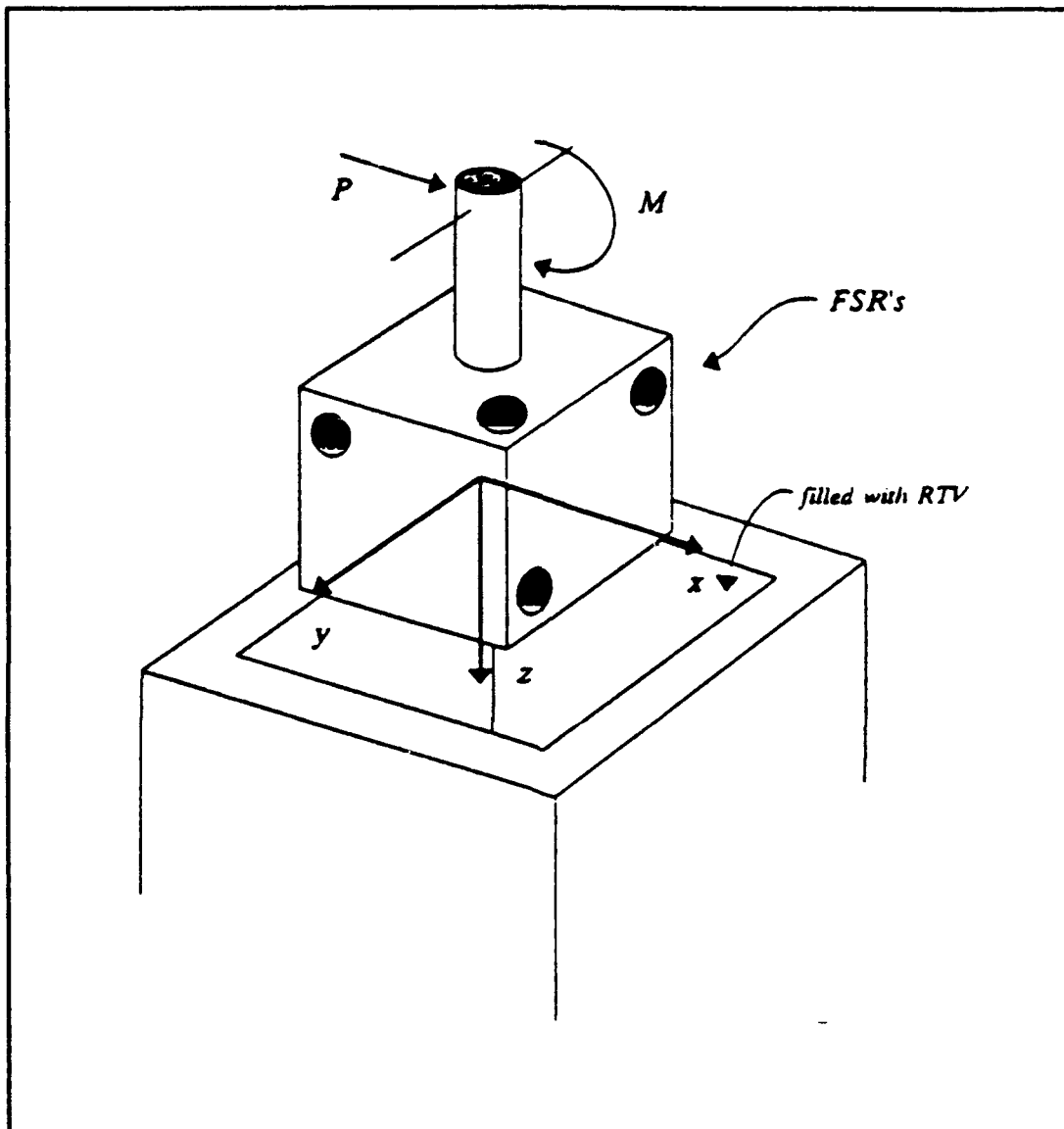


Figure 7
FSR-Based Transducer Conceptual Design [Ref. 1:p. 17]

b. Sensor Equations

The original mathematically generalized description of the problem was:

$$\begin{vmatrix} s_1 \\ s_2 \\ s_3 \\ \cdot \\ \cdot \\ s_n \end{vmatrix} = \begin{vmatrix} a_{1,1} & a_{1,2} & a_{1,3} & \cdot & \cdot & \cdot & a_{1,12} \\ a_{2,1} & \cdot & \cdot & \cdot & \cdot & \cdot & \cdot \\ \cdot & \cdot & \cdot & \cdot & \cdot & \cdot & \cdot \\ \cdot & \cdot & \cdot & \cdot & \cdot & \cdot & \cdot \\ \cdot & \cdot & \cdot & \cdot & \cdot & \cdot & \cdot \\ a_{n,1} & a_{n,2} & a_{n,3} & \cdot & \cdot & \cdot & a_{n,12} \end{vmatrix} \begin{vmatrix} F_x \\ F_{y+} \\ F_{y-} \\ F_{z+} \\ F_z \\ M_{x+} \\ M_x \\ M_{y+} \\ M_y \\ M_{z+} \\ M_z \end{vmatrix} \quad (2)$$

In this equation the sensor vector, \mathbf{s} , represents the voltage output for each sensor when the force and moment vector, \mathbf{F} , is applied, and n represents the number of sensors used which depends on the selected configuration. The positive and negative directions for each force and moment component had to be accounted for because the sensors were only used to detect applied compressive loads. Hence, the objective was to determine the right number and location of sensors and the associated \mathbf{A} matrix in order to resolve the 12x1 force and moment vector using:

$$\mathbf{F} = \mathbf{A}^{-1} \mathbf{s} \quad (3)$$

The elements of the A matrix would have to be determined using a calibration procedure which measured each sensor signal after applying known forces and moments individually. [Ref. 1:p. 18]

Since the number of sensors could be more than twelve, the A matrix may not be invertible. In which case the pseudoinverse must be utilized according to:

$$F = (A^T A)^{-1} A^T S \quad (4)$$

If the square matrix $A^T A$ is of full rank (i.e. a rank equal to the length of the force and moment vector), it may be inverted and used as shown in Equation 4 to identify the forces and moments. [Ref. 1:p. 19]

The initial model of a control device to detect the forces and moments was that of a planar joystick shown in Figure 8. An equation was developed for each sensor using the principle of superposition and modeling each FSR as a linear spring. The principle of superposition was used because the application of a force, P , at the top of the joystick would cause the device to translate and rotate. Hence, the following equations account for the contribution of both effects to the normal force on each spring:

$$F_1 = P/4 (1+d/a) \quad (5)$$

$$F_2 = P/4 (1-d/a) \quad (6)$$

$$F_3 = -P/4 (1+d/a) \quad (7)$$

$$F_4 = -P/4 (1-d/a) \quad (8)$$

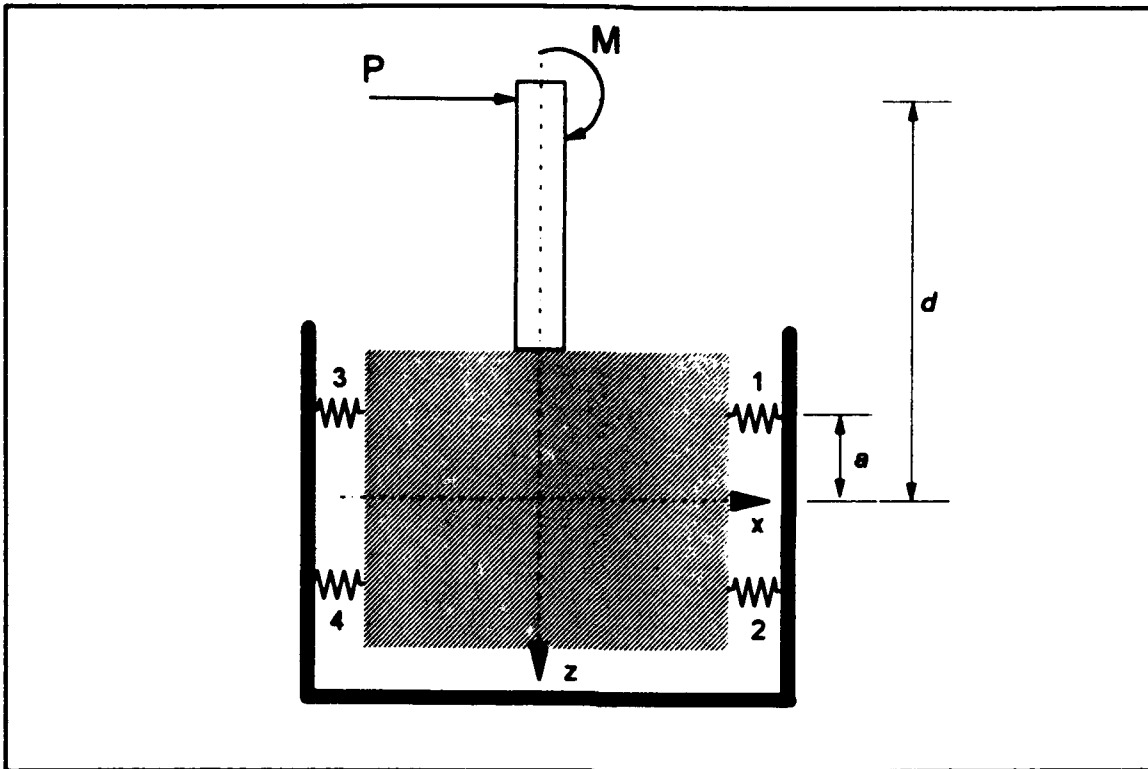


Figure 8
Planar Joystick [Ref. 3:p.20]

By applying a pure moment about the y axis the equations become:

$$F_1 = F_4 = M/4a \quad (9)$$

$$F_2 = F_3 = -M/4a \quad (10)$$

The sensor coefficient matrix **A** can be determined for a variety of three dimensional configurations by extending this methodology to a cube and determining the effects of each applied force and moment. [Ref. 1:pp.17-21]

c. Sensor Placement

Since the A matrix is dependent upon the location of the sensors on the cube, the first task in this iterative design process was to pick a number and distribution of FSRs on the cube. Then by applying the forces and moments of interest, the components of the A matrix were determined using the principle of superposition outlined earlier. The $A^T A$ matrix was then computed and its rank checked. If the results indicate a rank equal to the length of the force and moment vector, then that sensor configuration was considered capable of being used to resolve the forces and moments. If the rank was greater than the vector length, then too many sensors were being considered. If the rank was less than the vector length, then too few sensors were being considered. [Ref. 3:p. 14]

d. Early Results

The iterative process for determining the right number and location of sensors was carried out for a full order transducer consisting of 6 forces and 6 moments. This accounted for three dimensional forces and moments with sensors only capable of registering a compressive load. A possible placement pattern which resulted in an $A^T A$ matrix with a rank of 12 is shown in Figure 9. [Ref. 1:pp. 29-30]

The iterative process was then carried out in a similar fashion for a reduced order transducer capable of

resolving the three dimensional forces as before, but a moment only about the z axis. This was done because not all robotic

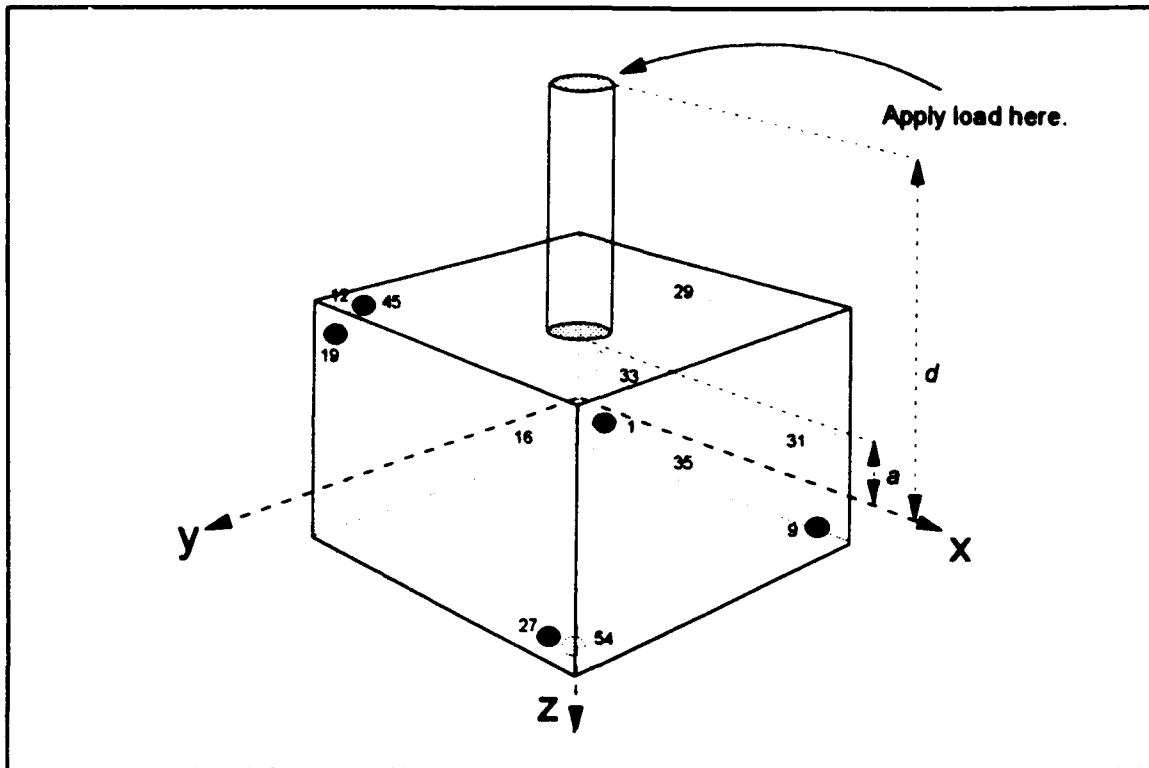


Figure 9
Arrangement for Full Order Transducer [Ref. 1:p. 30]

manipulator tasks require moments in all three directions. It is common to only require a torque about a single axis in addition to the forces along all three directions. Again, since the FSRs are only responsive to compressive loads, a separate sensor had to be allowed for the negative and positive directions of each of these components. The potential sensor layout with a rank of 8 is shown in Figure 10. [Ref. 1:pp. 31-33]

It is apparent that in order to reduce the number of sensors required, a design modification is necessary which addresses the response of FSRs only to compressive loads.

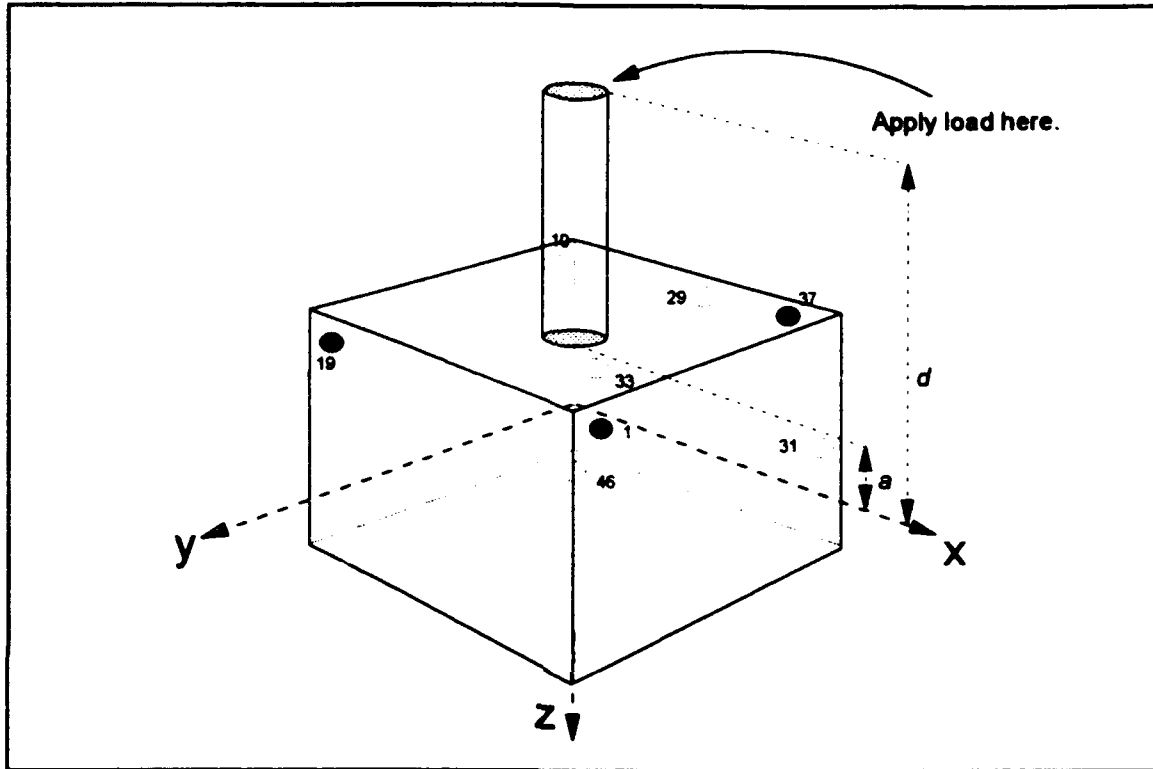


Figure 10
Arrangement for Reduced Order Transducer [Ref. 1:p.33]

This could, in effect, halve the force and moment vector length by not requiring sensors for negative direction forces and moments.

III. PRE-LOADED SENSOR TRANSDUCER DEVELOPMENT

A. SINGLE FSR PROTOTYPE

1. Objective

In an effort to resolve the problem of the FSR's inability to register a signal when a tensile load is applied, the concept of pre-loading the sensor was employed. This required the sensor to be loaded compressively with some initial force. The change in resistance caused by adding or removing normal force applied to the FSR is used to generate a proportional change in voltage. Provided that the initial pre-load is sufficient, a useable range is created in which a response is generated to both tensile and compressive force application.

2. Design and Construction

In order to test this concept a device had to be created which would show a reasonable range of resistance change for varying compressive and tensile- normal force application.

a. Mechanical Device

Figure 11 shows the prototype used to test the pre-load concept. The device was constructed using standard .25" aluminum plate. As shown .25" of neoprene material was used to transmit the applied load to the FSR which was mounted

using Scotch™ 467MP High Performance adhesive. The FSR was .25" square, product #30-301, readily available from Interlink Electronics™. A standard 1.5" 10/32 hex-head machine bolt with a locking nut was to apply the initial pre-load. A detailed drawing is provided in Appendix A.

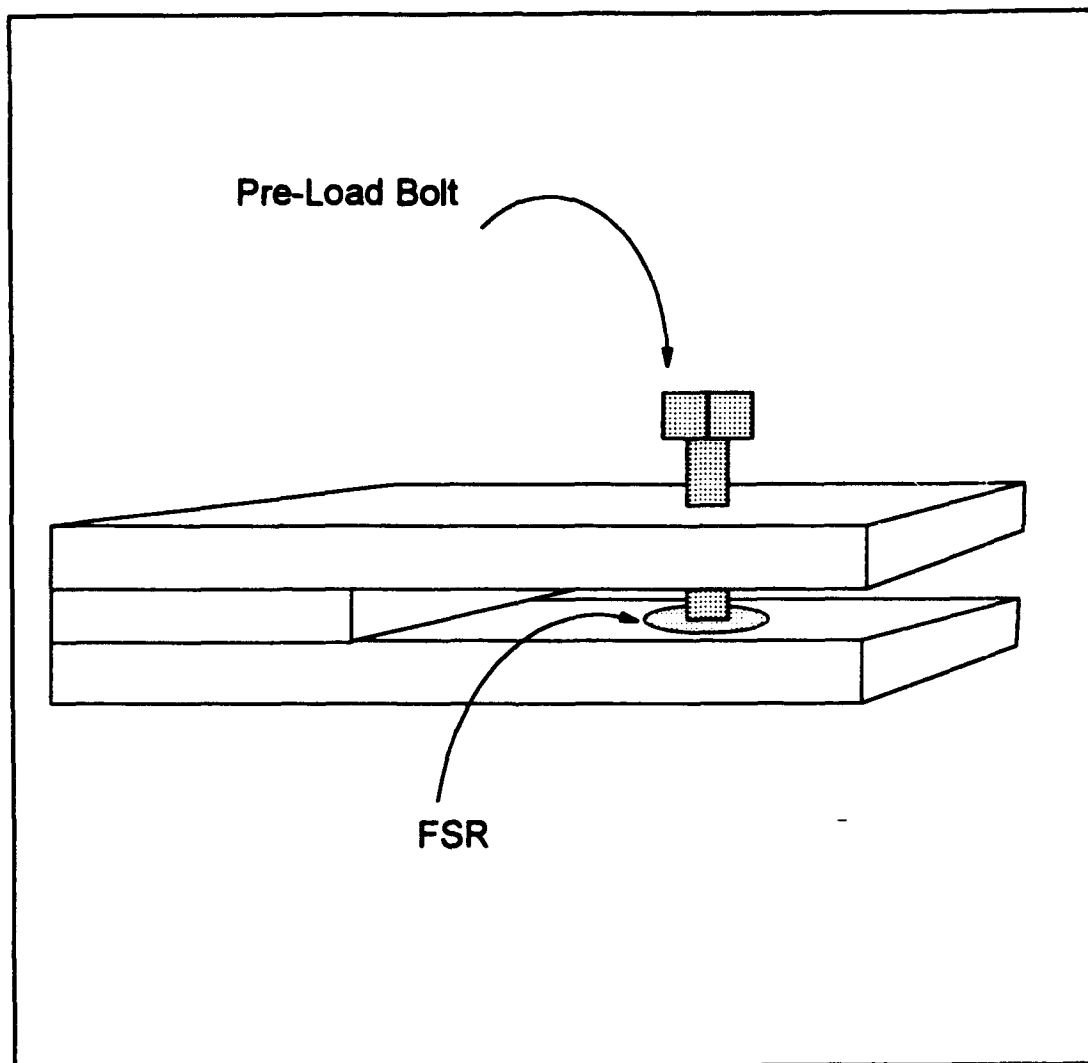


Figure 11
Single Pre-loaded FSR Prototype

b. Electronic Interface

In order to obtain a voltage change proportional to the applied load, the electronic interface pictured in Figure 12 was used. The circuit consisted of a +10 volt reference source, various values of R_O and an LM324 op-amp. The output voltage can be written as:

$$V_{OUT} = V_{REF}/2 \cdot [1 + R_O/R_{FSR}] \quad (11)$$

The expected voltage swing is from $V_{REF}/2$ to V_{REF} . [Ref. 5:p. 8]

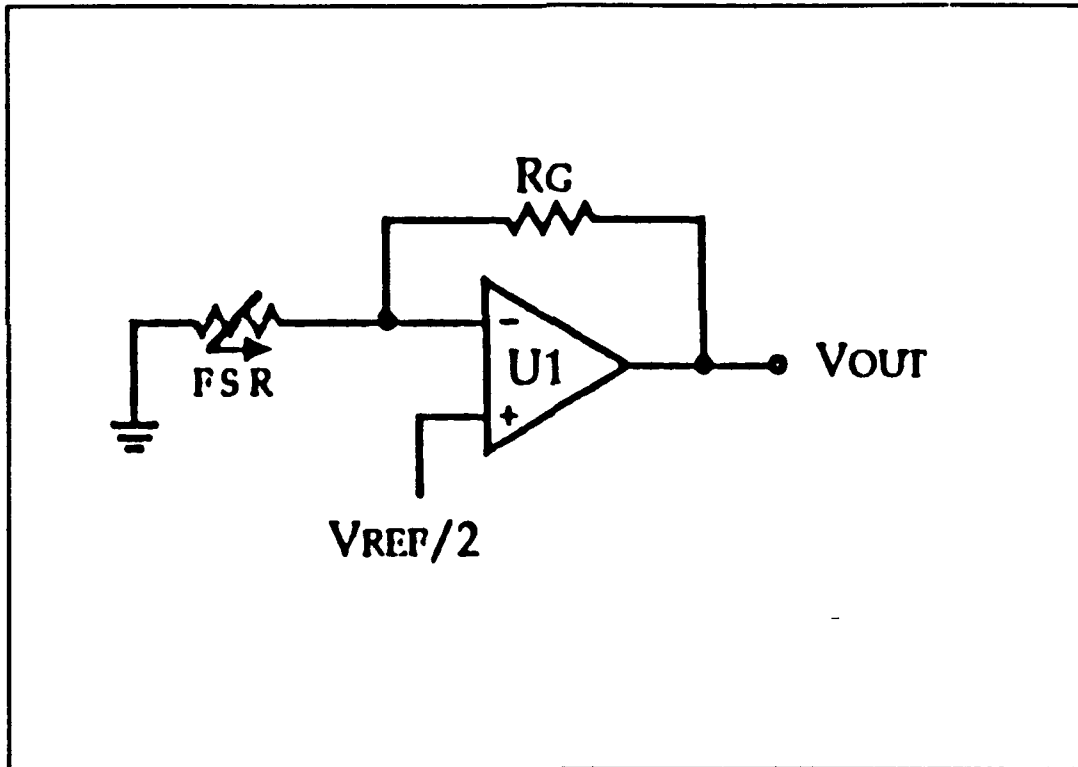


Figure 12
FSR Current-to-Voltage Converter [Ref. 5:p. 8]

3. Response Test

a. Data Collection

The prototype was configured to sit on a table top while a compressive load was applied by adding weights to a tray on top of the pre-load set bolt. Tensile loads were applied by turning the device over and suspending it by supporting the base on two cross members across a sufficient gap between two adjacent and parallel tables. The weights were then added to a tray suspended from the pre-load set bolt.

Initially, the masses, ranging from 4.17 to -1.97 lbm, were measured in English units and the corresponding voltages were read using the OMEGA BENCH™ data acquisition system and APPLE MACINTOSH™ microcomputer configured as a voltmeter. The first test used 4.7 kohms for the value of R_0 in an effort to produce a curve similar to that shown in Figure 13. This was the response for a standard FSR using a similar interface obtained by Interlink Electronics™. [Ref. 5:p. 7]

In order to more fully understand the nature of pre-loaded FSRs, similar tests were conducted using the following values for R_0 in kohms: 2.5, 5.0, 7.5, 10.0, 12.5. The masses used during these tests were measured in metric units for convenience.

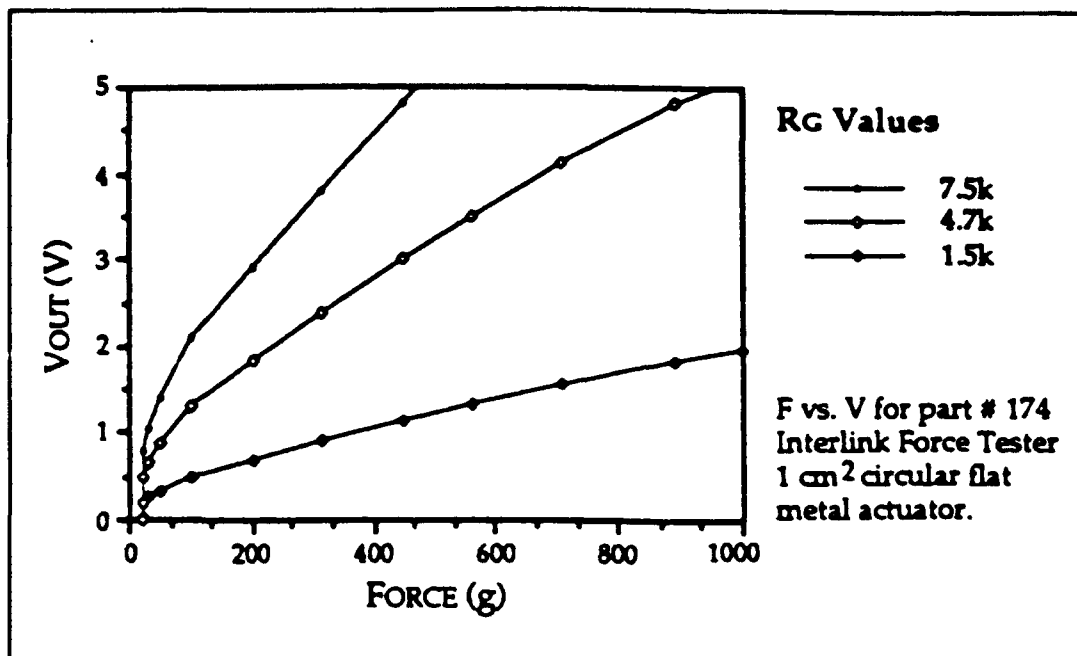


Figure 13
Force vs. V_{OUT} Curves [Ref. 5:p. 7]

b. Results

The data taken and the corresponding plots of applied force versus voltage response are provided in Appendix A. The plot resulting from the first test is shown in Figure 14. The curve resembles the expected results shown in Figure 13. The plot clearly shows two nearly linear regions separated by the initial no load set points. In subsequent tests the initial set point was physically unchanged. However, different values for R_0 resulted in curve shifts. This is seen in the variation of the no load voltage levels in accordance with the various values for R_0 . Also, depending on the value of the initial voltage, the useable range of the

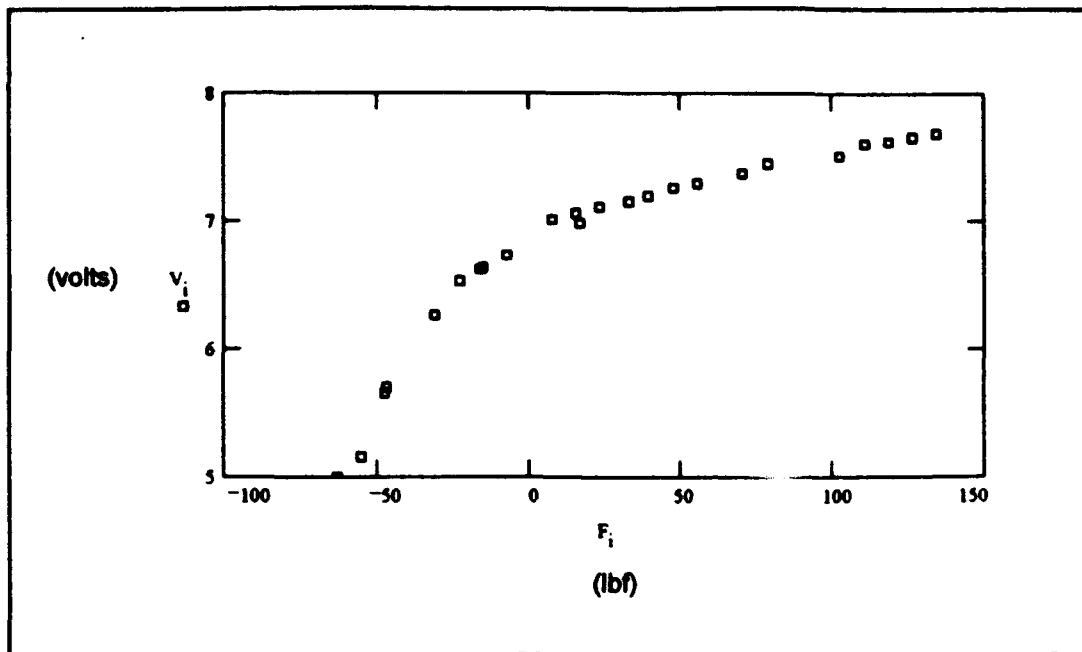


Figure 14
Pre-load FSR Test #1 Result

pre-loaded sensor was affected. Too high a value for R_0 caused positive saturation as in the 12.5 kohm case. The conclusion drawn from these tests was that the FSRs configured in a simple pre-loaded manner with a simple electronic interface are capable of registering a potentially useable voltage change which over limited regions varies almost linearly with applied loads in both the compressive and tensile directions.

B. INITIAL TRANSDUCER CONFIGURATION

1. Arrangement

Since each FSR can now be used to detect normal force loading in both the compressive direction and the tensile direction, the 12x1 force and moment vector in Equation 2 is

reduced to a 6x1 vector. The mathematically generalized description of the problem is now:

$$\begin{vmatrix} s_1 \\ s_2 \\ s_3 \\ \cdot \\ \cdot \\ s_n \end{vmatrix} = \begin{vmatrix} a_{1,1} & a_{1,2} & a_{1,3} & \cdot & \cdot & \cdot & a_{1,6} \\ a_{2,1} & \cdot & \cdot & \cdot & \cdot & \cdot & \cdot \\ \cdot & \cdot & \cdot & \cdot & \cdot & \cdot & \cdot \\ \cdot & \cdot & \cdot & \cdot & \cdot & \cdot & \cdot \\ \cdot & \cdot & \cdot & \cdot & \cdot & \cdot & \cdot \\ a_{n,1} & a_{n,2} & a_{n,3} & \cdot & \cdot & \cdot & a_{n,6} \end{vmatrix} \begin{vmatrix} F_x \\ F_y \\ F_z \\ M_x \\ M_y \\ M_z \end{vmatrix} \quad (12)$$

Where **S** represents the sensor voltage output and **F** is the force and moment column vector. The quest is still to determine a number and configuration of sensors such that the 6x1 force and moment vector can be resolved by inverting the **A** matrix according to:

$$\mathbf{F} = \mathbf{A}^{-1} \mathbf{S} \quad (13)$$

If the sensor configuration is such that only 6 sensors are used, then the **A** matrix will be square and the pseudoinverse will not be required as shown previously in Equation 4.

Figure 15 shows a three dimensional transducer built upon the planar joystick concept discussed in the previous chapter. The plan was to develop the equations necessary to determine the **A** matrix with all the sensors shown. Then, systematically cut out the signals from various groups of sensors and check the rank of the corresponding **A** matrix. If the rank was greater than or equal to six, then the

configuration was considered capable of resolving the 6 components of the force and moment vector. The goal was to determine a configuration which uses the minimum number of sensors and has a corresponding invertible \mathbf{A} matrix.

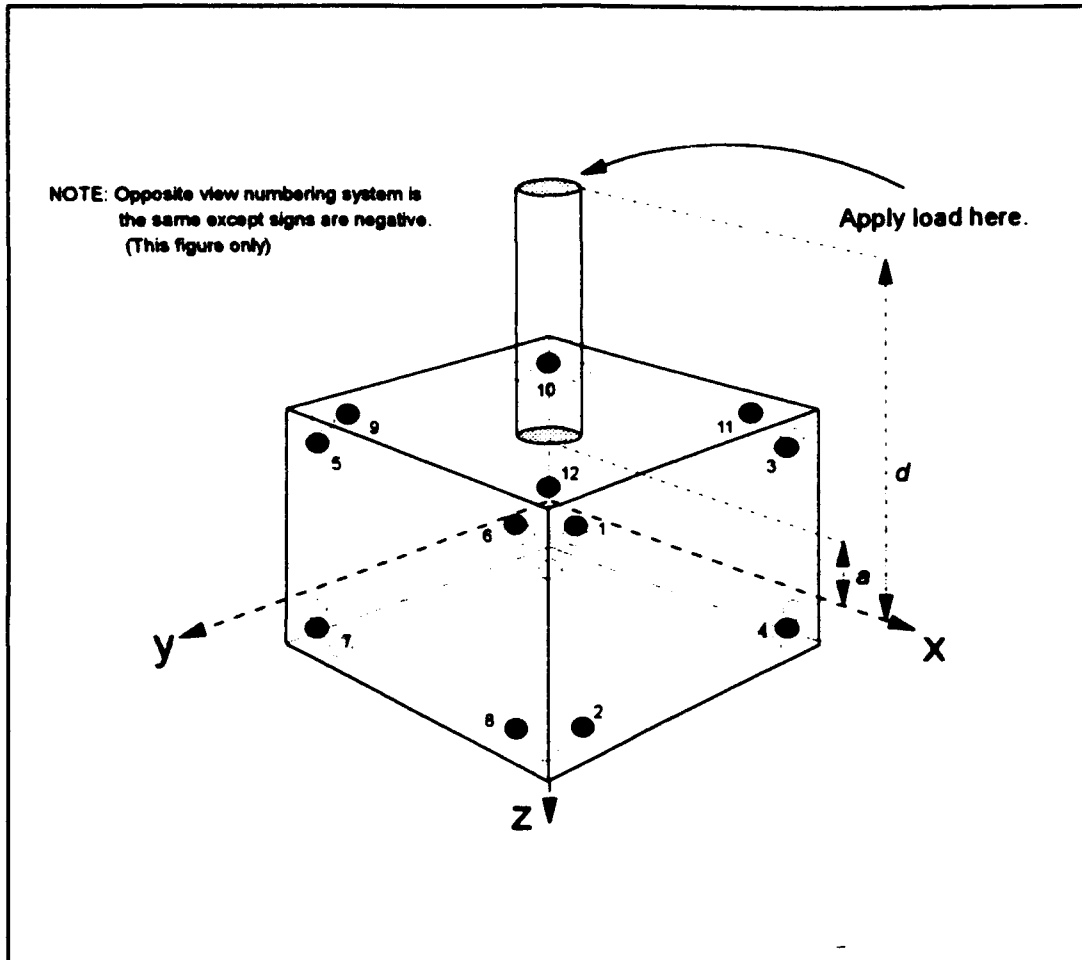


Figure 15
Initial Transducer Configuration

2. Sensor Equations

Using the principle of superposition mentioned earlier for the planar joystick, equations were developed for forces

applied in the x, y, and z directions as well as the moments about each axis. These forces and moments were considered to have been applied at the top of the joystick handle. First, a force applied in the positive x-direction, F_x , results in a translation of the inner cube as well as an incidental moment about the y axis. Since there are eight sensors on the x faces, the translation force contribution is simply:

$$F' = F_x / 8 \quad (14)$$

The sign of this force equation for each sensor depends on whether the sensor is on the positive or the negative x face. The incidental moment created by F_x causes activation of 16 sensors, eight on the x faces and eight on the z faces. Hence, the resulting applied load due to this incidental moment can be determined for each affected sensor according to:

$$16F''a = M \quad (15)$$

where,

$$M = F_x d \quad (16)$$

hence,

$$F'' = F_x d / 16a \quad (17)$$

Again, the sign of this force equation for each sensor depends on its location. Since this force is a result of the incidental moment, the location of the sensor with respect to the axis of rotation, the y axis in this case, determines the sign of F'' .

Finally, with the signs determined correctly for each activated sensor's force equations, the normal force experienced by each FSR resulting from the application of F_x is the sum of the translational force and the force from the incidental rotation:

$$F = F' + F'' \quad (18)$$

This rationale can be repeated for a force applied in the y direction, F_y . However, a force applied in the z direction, F_z , would not result in an a rotation of the inner cube. Therefore, the resulting normal forces on the affected sensors would only be from the translation of the inner cube with no incidental moment.

For a pure torque applied at the end of the joystick in the x direction, M_x , there would be sixteen sensors affected, 8 on the y face and 8 on the z face. The resulting force magnitude for each activated sensor is:

$$F = M_x / 16a \quad (19)$$

The sign for each of these activated sensor equations depends on its location with respect to the axis of rotation. Pure moments applied about the y axis and about the z axis, M_y and M_z respectively, result in similar force equations for each affected sensor.

The equations for each sensor activated as a result of the application of the individual components of the force and moment column vector make up the A matrix in Equation 12. The

complete equation for this configuration, showing the individual elements of the **A** matrix, is as follows:

$$\begin{array}{c}
 \begin{array}{c} V_1 \\ V_2 \\ V_3 \\ V_4 \\ V_5 \\ V_6 \\ V_7 \\ V_8 \\ V_9 \\ V_{10} \\ V_{11} \\ V_{12} \\ V_{13} \\ V_{14} \\ V_{15} \\ V_{16} \\ V_{17} \\ V_{18} \\ V_{19} \\ V_{20} \\ V_{21} \\ V_{22} \end{array}
 \end{array}
 =
 \begin{array}{ccccccc}
 1/8(1+d/2a) & 0 & 0 & 0 & -1/16a & -1/16a & \\
 1/8(1-d/2a) & 0 & 0 & 0 & 1/16a & -1/16a & \\
 1/8(1+d/2a) & 0 & 0 & 0 & -1/16a & 1/16a & \\
 1/8(1-d/2a) & 0 & 0 & 0 & 1/16a & 1/16a & \\
 0 & 1/8(1+d/2a) & 0 & 1/16a & 0 & -1/16a & \\
 0 & 1/8(1+d/2a) & 0 & 1/16a & 0 & 1/16a & \\
 0 & 1/8(1-d/2a) & 0 & -1/16a & 0 & -1/16a & \\
 0 & 1/8(1-d/2a) & 0 & -1/16a & 0 & 1/16a & \\
 d/16a & -d/16a & -1/8 & -1/16a & -1/16a & 0 & \\
 d/16a & d/16a & -1/8 & 1/16a & -1/16a & 0 & \\
 -d/16a & d/16a & -1/8 & 1/16a & 1/16a & 0 & \\
 -d/16a & -d/16a & -1/8 & -1/16a & 1/16a & 0 & \\
 -1/8(1+d/2a) & 0 & 0 & 0 & 1/16a & 1/16a & \\
 -1/8(1+d/2a) & 0 & 0 & 0 & -1/16a & 1/16a & \\
 -1/8(1+d/2a) & 0 & 0 & 0 & 1/16a & -1/16a & \\
 -1/8(1+d/2a) & 0 & 0 & 0 & -1/16a & -1/16a & \\
 0 & -1/8(1+d/2a) & 0 & -1/16a & 0 & 1/16a & \\
 0 & -1/8(1+d/2a) & 0 & -1/16a & 0 & -1/16a & \\
 0 & -1/8(1-d/2a) & 0 & 1/16a & 0 & 1/16a & \\
 0 & -1/8(1-d/2a) & 0 & 1/16a & 0 & -1/16a & \\
 -d/16a & d/16a & 1/8 & 1/16a & 1/16a & 0 & \\
 -d/16a & -d/16a & 1/8 & -1/16a & 1/16a & 0 & \\
 d/16a & -d/16a & 1/8 & -1/16a & -1/16a & 0 & \\
 d/16a & d/16a & 1/8 & 1/16a & -1/16a & 0 &
 \end{array}
 \begin{array}{c}
 P_1 \\ P_2 \\ P_3 \\ T_1 \\ T_2 \\ T_3
 \end{array}
 \quad (20)$$

3. Sensor Placement

This **A** matrix, resulting from the configuration shown in Figure 15, was entered into the software program MATLAB™ with the assumed values for *d* and *a* as 4.5 and 1.5,

respectively with units of length. The the rank of the full matrix was then determined to be six. This full rank meant that if all sensors were used, the pseudoinverse could be used to resolve the components of the force and moment vector, \mathbf{F} .

Next, the sensors on the negative x face were eliminated by setting the \mathbf{A} matrix elements in corresponding rows equal to zero. In this case, it was simulated that sensors labelled -1, -2, -3, and -4 had no output. Thus, the elements in rows 13 through 16 of matrix \mathbf{A} were set equal to zero. The resulting matrix had a rank of six. Hence, this configuration could be used to resolve the components of \mathbf{F} .

This process was repeated in a similar fashion by first eliminating additional sensors from the y face, and then from the z face. The result was a configuration with sensors only on the positive x, y, and z faces yielding an \mathbf{A} matrix with a rank of six. Since this would involve a total of 12 sensors, the \mathbf{A} matrix would not be square. However, the pseudoinverse could be used to resolve the forces and moments.

In an effort to reduce the number of sensors required even further, this iterative process of removing sensors from the configuration was continued. The next removal was that of the positive z face sensors. This resulted in an \mathbf{A} matrix rank of five which meant this sensor configuration could not be used. Hence, two sensors were added back to the positive z face. These were the diagonally arranged sensors numbered

10 and 12 in Figure 15. The resulting A matrix yielded a rank of six. This indicated a useable combination.

Using this rationale, two sensors were also removed in diagonal patterns from both of the positive x and y faces. The sensors numbered 2, 3, 5 and 8 were eliminated. The resulting rank was five indicating an unusable combination. Hence, the iterative process was continued to find a useable combination of only six sensors.

4. Results

Experimenting with diagonal combinations lead to the useable configuration shown in Figure 16 after only three more iterations. This is not the only possible combination, but it

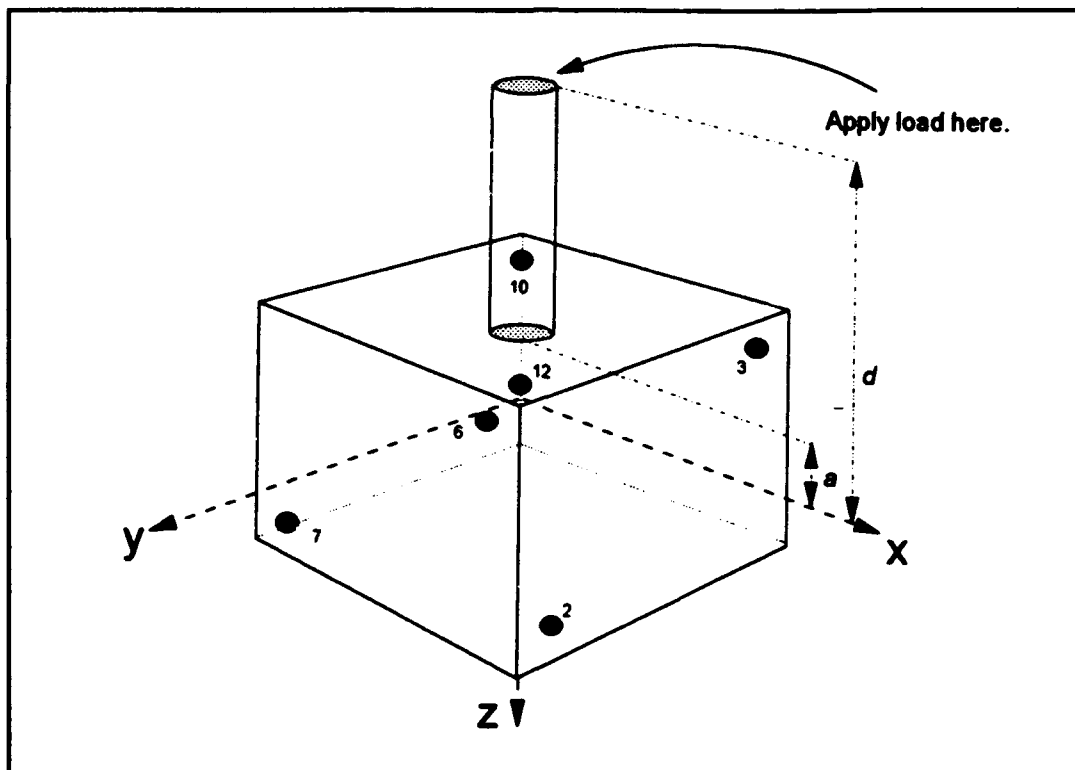


Figure 16
Initial Minimum Sensor Transducer Configuration

is one that yields a square A matrix which is directly invertible to determine the force and moment vector, F . For fewer than six sensors, the rules of matrix multiplication prohibit the formation of the pseudoinverse. Hence, no fewer than six sensors were considered in any configuration.

C. COMPARISON WITH PRELIMINARY WORK

1. Arrangement

For comparison purposes, an unsuccessful configuration analyzed in the preliminary work for a full order transducer without using the pre-loaded sensor concept was reexamined using pre-loaded sensors. This arrangement is shown in Figure 17 [Ref. 1:p. 25]. The goal was to determine what modifications, if any, had to be made to create a configuration using only six sensors which would produce an A matrix with a full rank.

2. Sensor Equations

Using this configuration and the fact that the individual FSRs are capable of measuring tensile and compressive loads, a new set of governing force equations were developed. These equations were determined using the principle of superposition analogous to the methods used in the previous section by individual application of each component of the force and moment vector, F .

Since only 12 sensors were considered in this initial configuration, in contrast to the 24 of the previous section,

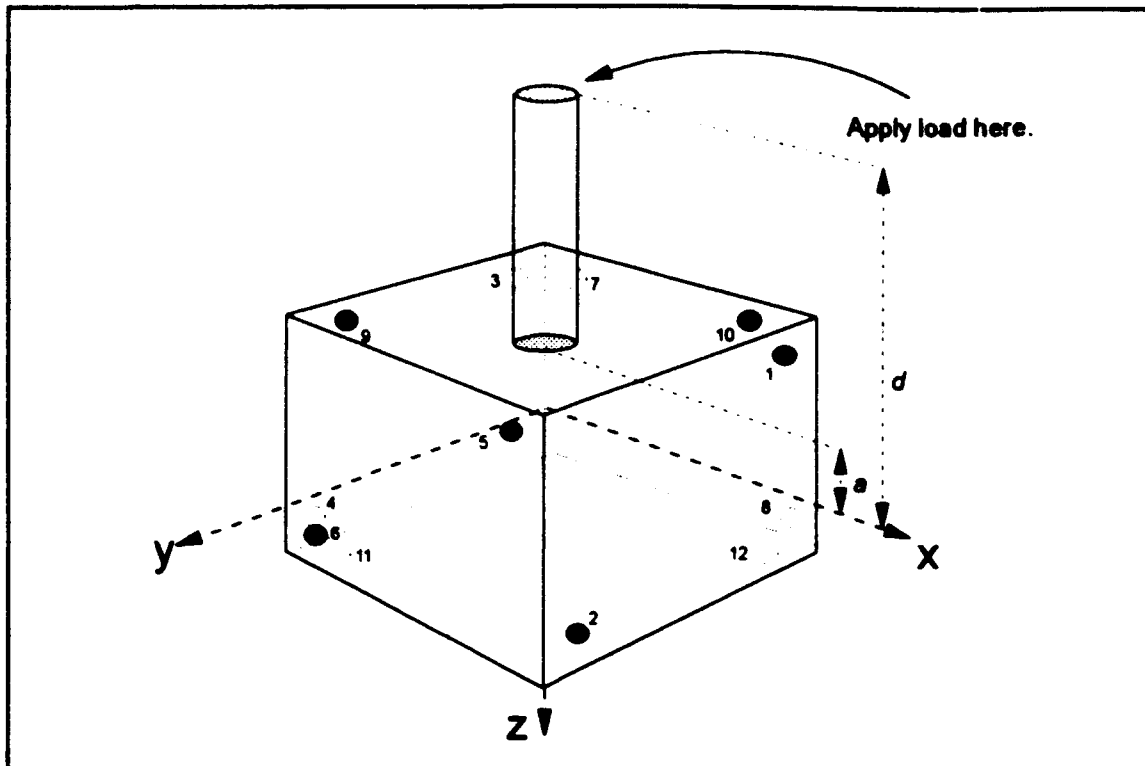


Figure 17
12 Sensor Preliminary Work Configuration [Ref. 1:p. 25]

the complete equation is as follows:

$$\begin{array}{c}
 \begin{array}{c} S_1 \\ S_2 \\ S_3 \\ S_4 \\ S_5 \\ S_6 \\ S_7 \\ S_8 \\ S_9 \\ S_{10} \\ S_{11} \\ S_{12} \end{array}
 \end{array}
 =
 \begin{array}{c}
 \begin{array}{ccccccc}
 1/4(1+d/2a) & 0 & 0 & 0 & -1/8a & 1/8a \\
 1/4(1-d/2a) & 0 & 0 & 0 & 1/8a & -1/8a \\
 -1/4(1+d/2a) & 0 & 0 & 0 & 1/8a & -1/8a \\
 -1/4(1-d/2a) & 0 & 0 & 0 & -1/8a & 1/8a \\
 0 & 1/4(1+d/2a) & 0 & 1/8a & 0 & 1/8a \\
 0 & 1/4(1-d/2a) & 0 & -1/8a & 0 & -1/8a \\
 0 & -1/4(1+d/2a) & 0 & -1/8a & 0 & 1/8a \\
 0 & -1/4(1-d/2a) & 0 & 1/8a & 0 & -1/8a \\
 d/8a & -d/8a & -1/4 & -1/8a & -1/8a & 0 \\
 -d/8a & d/8a & -1/4 & 1/8a & 1/8a & 0 \\
 -d/8a & d/8a & 1/4 & 1/8a & 1/8a & 0 \\
 d/8a & -d/8a & 1/4 & -1/8a & -1/8a & 0
 \end{array}
 \end{array}
 \begin{array}{c}
 X \\
 \begin{array}{c} F_x \\ F_y \\ F_z \\ M_x \\ M_y \\ M_z \end{array}
 \end{array}
 \quad (21)$$

Since there are half as many sensors over which the forces are distributed, the resulting elements of the A matrix are twice as large as in Equation 20. This has absolutely no effect since multiplying the A matrix by a scalar will not change its rank.

3. Sensor Placement

Using MATLABTM as before, the full A matrix was entered and its rank determined to be six. The length dimensions, d and a , were assumed to be 5.0 and 1.0, respectively. This full rank indicated that the configuration could be used to resolve the six components of the force and moment vector, F . In an attempt to optimize the number and placement of sensors, the sensors on the negative x , y , and z faces were eliminated, leaving active sensors numbered 1, 2, 5, 6, 11 and 12. The resulting configuration yielded an A matrix with a rank of only five. Since this is a rank deficient condition, another attempt was made by eliminating the sensors on only the negative x and y faces, and the sensors on the positive z face. This configuration left sensors numbered 1, 2, 5, 6, 9 and 10 active. The rank of the resulting matrix was five, again a deficient value, indicating an unusable combination.

4. Results

It was intuitively determined that in order to develop a combination utilizing the sensors on only the positive faces

or only the negative faces, this configuration may need a slight alteration. Hence, it was abandoned in search of a similar yet useable configuration.

D. MODIFIED PRELIMINARY CONFIGURATION

1. Arrangement

Considering the previous configuration, Figure 18 displays a similar arrangement. The only difference is the

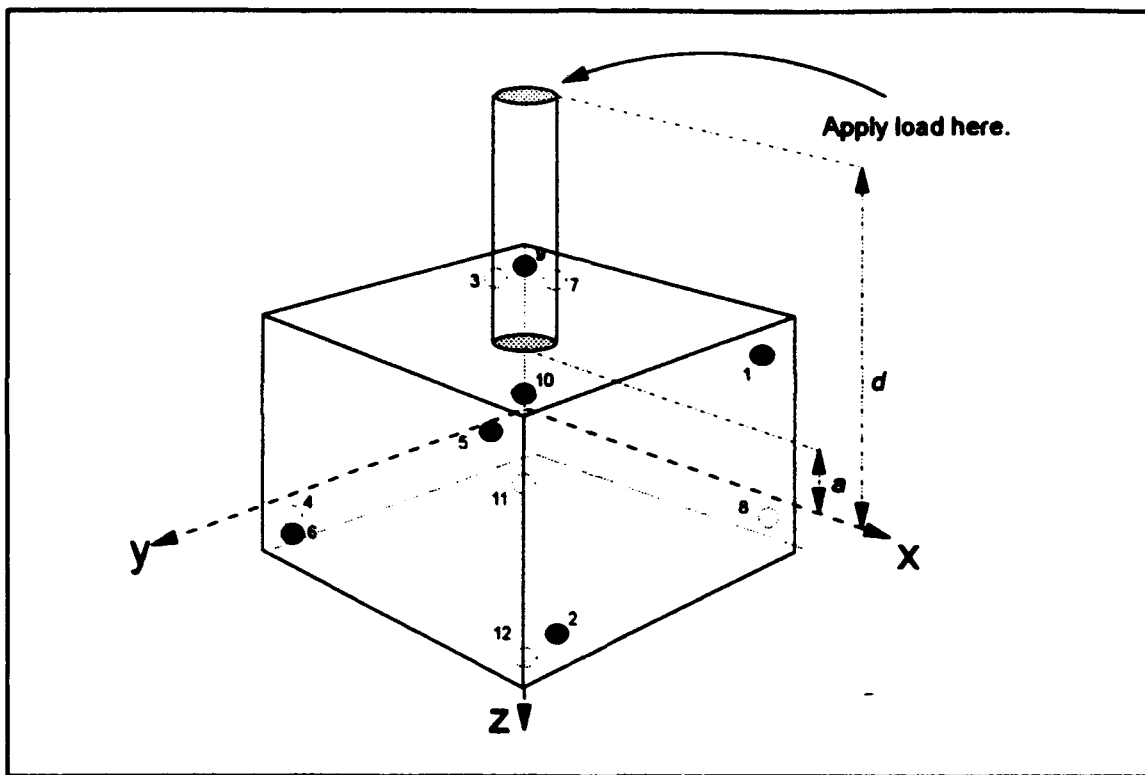


Figure 18
Modified 12 Sensor Preliminary Work Configuration

orientation of the z face sensors. Diagonally located sensors numbered 11 and 12, located on the positive z face, have been rotated 90° clockwise if viewed looking in the positive z

direction. Similarly, sensors numbered 9 and 10 have been shifted 90° clockwise if viewed in the positive z direction.

2. Sensor Equations

In this case the sensor equations which comprise the elements of the A matrix were very similar to those of the previous section. Since the number of sensors was the same, the only change was in the signs of the various force contributions as a result of the changed sensor orientation. The complete equation describing the new situation is:

$$\begin{array}{c|c|c|c|c|c|c|c}
 S_1 & & 1/4(1+d/2a) & 0 & 0 & 0 & -1/8a & 1/8a \\
 S_2 & & 1/4(1-d/2a) & 0 & 0 & 0 & 1/8a & -1/8a \\
 S_3 & & -1/4(1+d/2a) & 0 & 0 & 0 & 1/8a & -1/8a \\
 S_4 & & -1/4(1-d/2a) & 0 & 0 & 0 & -1/8a & 1/8a \\
 S_5 & & 0 & 1/4(1+d/2a) & 0 & 1/8a & 0 & 1/8a \\
 S_6 & = & 0 & 1/4(1-d/2a) & 0 & -1/8a & 0 & -1/8a \\
 S_7 & & 0 & -1/4(1+d/2a) & 0 & -1/8a & 0 & 1/8a \\
 S_8 & & 0 & -1/4(1-d/2a) & 0 & 1/8a & 0 & -1/8a \\
 S_9 & & d/8a & d/8a & -1/4 & 1/8a & -1/8a & 0 \\
 S_{10} & & -d/8a & -d/8a & -1/4 & -1/8a & 1/8a & 0 \\
 S_{11} & & -d/8a & -d/8a & 1/4 & -1/8a & 1/8a & 0 \\
 S_{12} & & d/8a & d/8a & 1/4 & 1/8a & -1/8a & 0
 \end{array}
 \times
 \begin{array}{c}
 F_x \\
 F_y \\
 F_z \\
 M_x \\
 M_y \\
 M_z
 \end{array}
 \quad (22)$$

As expected the only changes were the signs of the elements corresponding to the application of F_y and M_x on sensors numbered 9, 10, 11, and 12.

3. Sensor Placement

MATLAB™ was used to first check the rank of the **A** matrix with all 12 sensors activated. This value was six, again indicating a useable configuration. Next, the sensors located on the negative **x**, **y**, and **z** faces were again eliminated. The rank of the associated matrix was determined to be six. With this rank, the configuration is useable.

4. Results

A rank of six indicates a full rank allowing the **A** matrix to be directly inverted to determine the forces and moments according to Equation 3. Since the minimum number of sensors possible is six, this configuration was determined to be one of many acceptable choices. Using the trial and error methodology it is possible to determine other configurations using only six sensors which yield an **A** matrix capable of direct inversion.

IV. REDUNDANCY ANALYSIS

A. GOAL

Given a transducer with four sensors mounted on each face of the inner cube, there is more than one combination of the minimum number of sensors, six, which will provide an A matrix with a full rank used to resolve the six components of the force and moment column vector, F . It would be advantageous to develop a system that would automatically find another useable combination of remaining sensors necessary to continue operation in the event of a sensor failure while in use. Hence, the aim was to develop an algorithm which would search for and identify various combinations of six sensors that could be used to identify the force vector, F . This was to be done with a 24 sensor transducer utilizing some initial useable configuration of six sensors subject to random FSR failures which would drive the system to search for an alternate configuration. The number of possible combinations would be described by the following equation:

$$C(n,r) = n! / (n-r)!r! \quad (23)$$

Where n represents the total number of sensors and r represents the number of sensors in each group necessary to resolve the force and moment vector. [Ref. 6:p. 1-8]

In this case, n equals 24 and r equals 6. After doing the calculation, the resulting number of combinations is 134,596. Potentially, this many combinations would have to be analyzed to find another configuration which would yield a full rank \mathbf{A} matrix. However, as sensors fail the number of possible combinations decreases. It was decided that with this finite limit to the number of possible search iterations, a FORTRAN code would be developed to mimic the methodology of the previous chapter in finding a useable combination.

B. THEORY

1. Sensor Configuration

As a prelude to developing this FORTRAN code, a 24 sensor configuration had to be developed with a convenient numbering system. Also, it was decided to use a configuration that could be initially broken into four separate, six sensor configurations which were symmetrical and individually capable of resolving the three components of force and three components of moment. The purpose of these subsystems was to initially provide four layers of redundancy. In the event of a sensor failure, a quick switch to another subsystem would allow continued use of the joystick without the delay of randomly searching for other possible combinations of six working sensors from the remaining sensors. This could be repeated until no intact subsystems remained.

To do this, a 24 sensor transducer, similar to that shown in Figure 15, was used. The initial numbering system thought to be best was a simple numbering of the sensors from #1 through #24. This is shown on the inner cube faces in Figure 19. Since it was shown in the previous chapter that

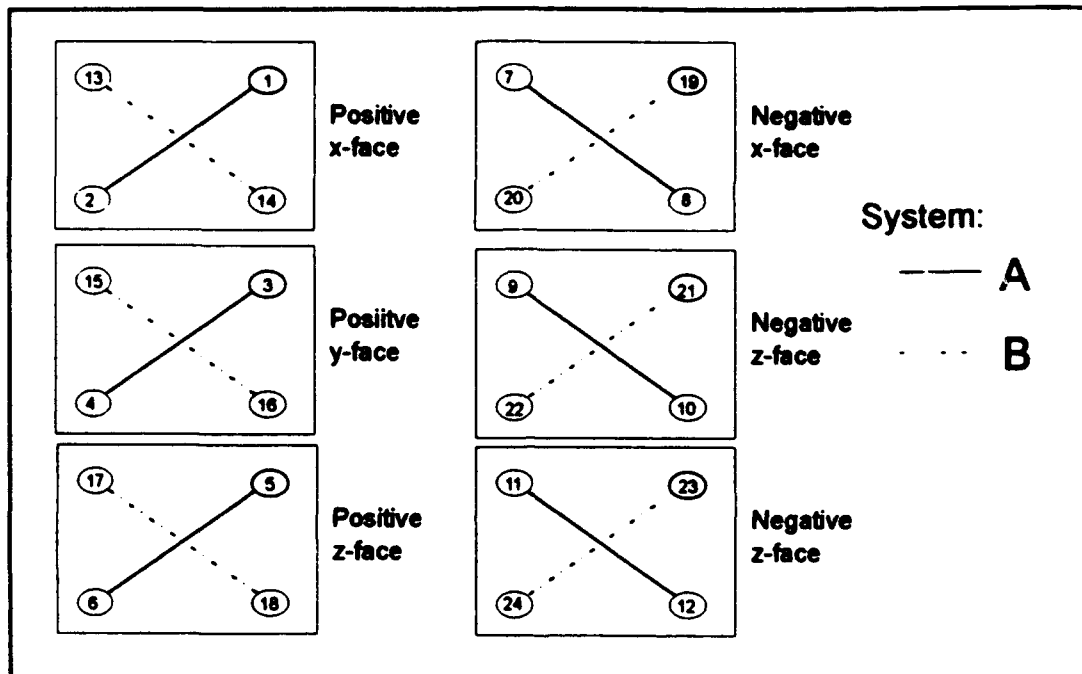


Figure 19
First Sequential Cube Face Numbering Scheme

only half the sensors on the positive cube faces were required to develop a useable configuration, the symmetrically analogous configurations were obvious choices for other possible configurations. Hence, the four separate configurations were comprised of two positive face systems and two negative face systems. As shown in Figure 19, these

systems were respectively labeled: A-positive, B-positive, A-negative and B-negative.

To develop a numbering system such that the complete 24x6 A matrix could be conveniently broken into the four separate 6x6 smaller matrices each with a rank of six as a result of the four separate six sensor configurations, a trial and error procedure was necessary. First, the numbers of the sensors were arranged such that A-positive system had sensors #1-#6; the A-negative system had sensors #7-#12; the B-positive system had sensors #13-#18; and the B-negative system had sensors #19-#24 as shown in Figure 19. Then, in a manner similar to that in the previous chapter, the equations representing the normal forces on each sensor were developed as a result of the individual application to the components of F . As in the previous chapter, these equations were placed in the A matrix and values for the length dimensions d and a were assumed to be 4.5 and 1.5, respectively. The matrix rank was determined using MATLAB™ to be six. Next, the four subsystems were formed into smaller 6x6 matrices and checked for ranks of six. However, the B-positive and the B-negative subsystem matrices each had ranks of only five. Hence, this configuration was not capable of providing the four levels of redundancy initially sought.

To find a configuration that would yield four useable subsystems, the sensor numbering scheme had to be changed. As

shown in Figure 20, the first such change was to swap #5 with #17, #6 with #18, #11 with #23 and #12 with #24. This scheme failed to produce the four matrices with ranks of six. In this

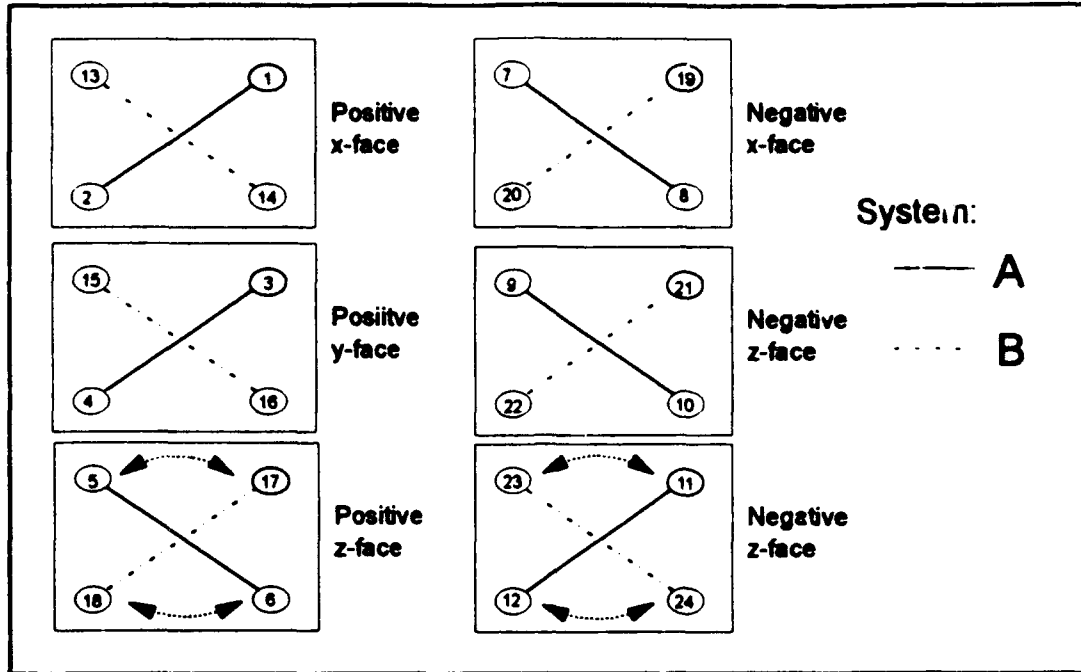


Figure 20
Second Sequential Cube Face Numbering Scheme

case the A-positive and the A-negative subsystems were rank deficient. In an effort to find other arrangements which consisted of four useable subsystems sequentially numbered, this iterative procedure was continued. Table 1 summarizes the results of all the sensor number switches.

The third scheme, shown in Figure 21, was similar to the first scheme except that the switch of #6 with #17 and #12 with #23 was made. The resulting matrices were of full rank. Hence, this was the numbering scheme chosen for the FORTRAN code development.

TABLE 1
SENSOR NUMBER ARRANGEMENT ITERATIONS

Sensors Switched	A-Positive Subsystem	A-Negative Subsystem	B-Positive Subsystem	B-Negative Subsystem	Comments
Figure 19 Arrangement	rank=6	rank=6	rank=5	rank=5	NOT USEABLE
5&17, 6&18, 11&23, 12&24	rank=5	rank=5	rank=6	rank=6	NOT USEABLE
6&17, 12&23	rank=6	rank=6	rank=6	rank=6	USEABLE
18&5, 24&11	rank=6	rank=6	rank=6	rank=6	USEABLE
6&17, 11&24	rank=5	rank=5	rank=5	rank=5	NOT USEABLE
5&17, 11&23	rank=5	rank=5	rank=5	rank=5	NOT USEABLE
6&18, 12&24	rank=5	rank=5	rank=5	rank=5	NOT USEABLE
5&18, 12&23	rank=5	rank=5	rank=5	rank=5	NOT USEABLE

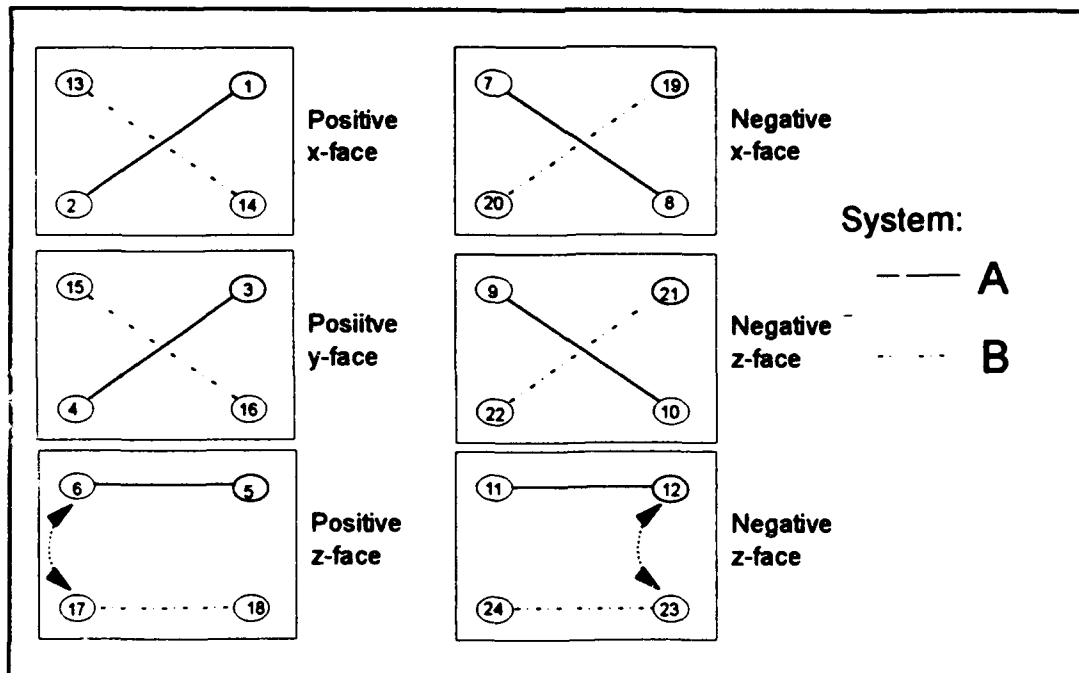


Figure 21
Successful Sequential Cube Face Numbering Scheme

2. Algorithm

The general procedure followed to provide multiple layers of redundancy for a force-torque transducer is now summarized. It began with a 24 sensor transducer consisting of a 2x2 array of FSRs on each of the six inner cube faces. The procedures of the previous chapter were utilized to determine the normal forces on each sensor resulting from the individual application of the three dimensional forces and moments. Nominal length dimensions were assumed for d and a and the resulting 24x6 matrix was multiplied by a scalar value of 24 to produce convenient elements for display purposes.

The rows of this large matrix were sectioned into four invertible 6x6 matrices, arranged sequentially, representing individual subsystems capable of being used to resolve the force and moment column vector, P , according to Equation 3. Each row represented a single sensor, and these subsystems were arranged sequentially for FORTRAN programming convenience. The ranks of these resulting 6x6 matrices were determined to ensure invertibility.

A sensor was then randomly selected for failure. The algorithm had to then determine which subsystem this FSR was in and switch to another intact subsystem. This step was repeated until no intact subsystems remained. A determination was then made as to whether or not there remained enough active sensors to conduct a random search for a combination of 6 remaining sensors to provide a 6x6 invertible matrix for use

in resolving \mathbf{F} as discussed. If there were at least 6 remaining sensors, comprised of at least one sensor remaining in each the x, y, and z directions, the random search was commenced. This search consisted of randomly picking 6 of the remaining sensors, again with at least one in each direction. The matrix rows associated with these FSRs were then sequentially arranged into a 6x6 matrix. The rank of this matrix was calculated in order to determine invertibility. If the rank was six, then the algorithm requested to fail another FSR and conduct another search. If the rank was less than six, then a different combination of six of the remaining sensors was chosen and the rank was checked. This was repeated until a successful 6x6 matrix was produced or a sufficient number of iterations had occurred in which case the algorithm could be terminated.

C. FORTRAN PROGRAM

The flow chart for this algorithm is presented in Figure 22. The resulting FORTRAN code was written and is presented in Appendix B. It was based on the numbering arrangement displayed in Figure 21. The values assumed for the length dimensions shown Figure 15, d and a , were 4.5 and 1.5, respectively. The resulting 24x6 \mathbf{A} matrix was multiplied by the scalar value 24 in order to produce a simple numerical format.

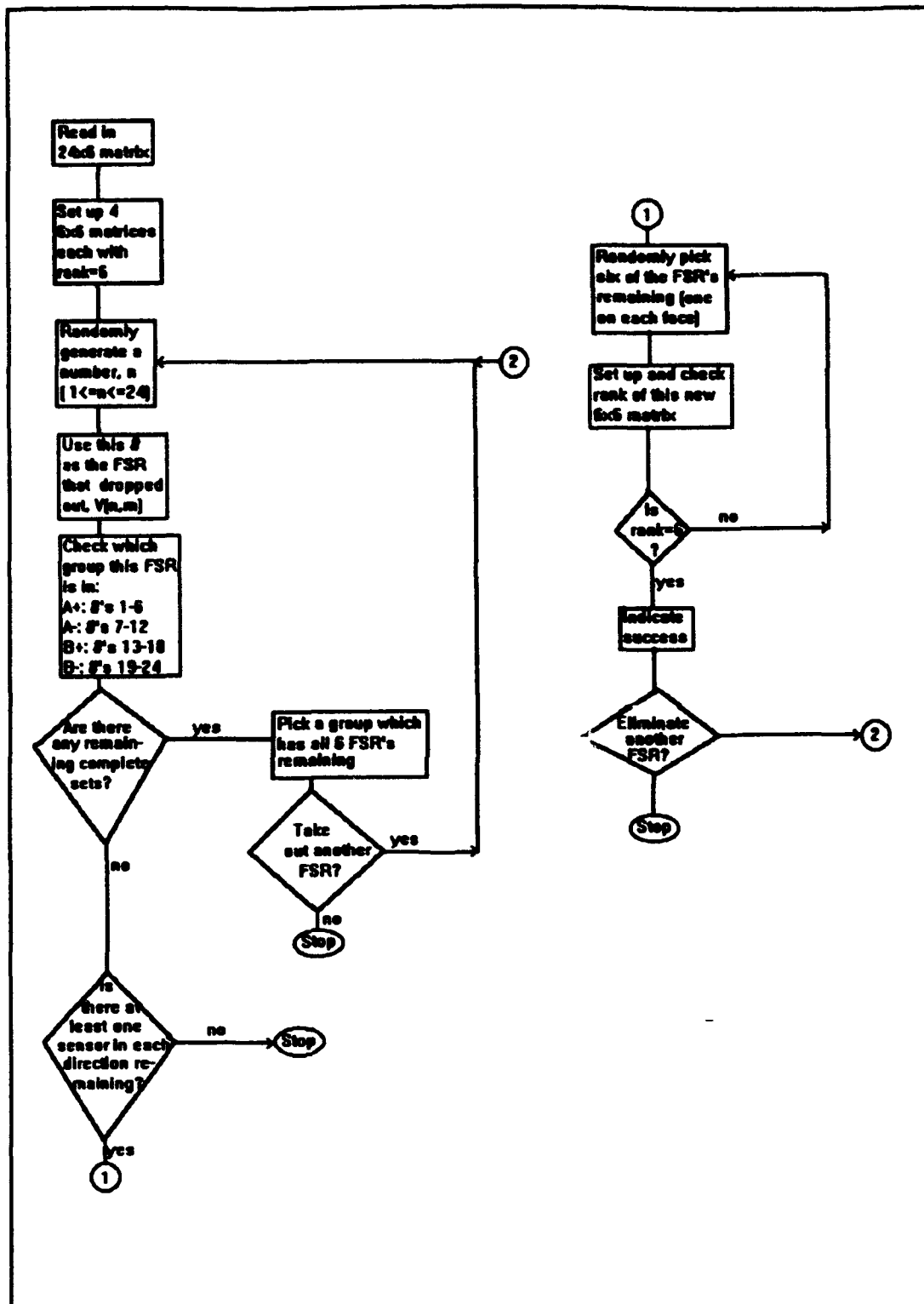


Figure 22
Redundancy Analysis Flowchart

D. RESULTS

The resulting FORTRAN program ran successfully. In most cases, many combinations were generated in a matter of seconds. The slowest part to the process was operator interaction and screen display. A sample output is provided after the code listing in Appendix B.

The output shows a listing of the original 24x6 A matrix with the option to correct or change any elements. Next the sequentially ordered subsystems and their corresponding ranks are shown. The program then randomly picks and eliminates a sensor. The display shows the sensor chosen and its corresponding subsystem. The output then shows which subsystems have not yet been disturbed. This is repeated at the operators discretion until no more undisturbed subsystems remain. At that point the display shows the program shifting to the mode of randomly picking six of the remaining FSRs and generating a new 6x6 subsystem matrix with a rank of six. The number of iterations required to generate this subsystem, which must meet specific requirements, is also shown. The operator is given the opportunity to allow the program to eliminate another FSR and repeat this random generation of a useable 6x6 matrix from the remaining FSRs. This process continues provided there are at least six sensors remaining with at least one in each direction.

V. REDUCED ORDER TRANSDUCER THEORY

A. MOTIVATION

Many robotic manipulator tasks require only single axis moments. An example would be the act of inserting and tightening a threaded screw or bolt. The transducer configurations considered thus far have been for three forces and three moments about each of the x, y, and z axes. In order to simplify the transducer design and construction, an analogous configuration was developed for a reduced order transducer requiring torques about only the z axis and the three dimensional forces.

B. SENSOR CONFIGURATION

1. Arrangement

The concept of a reduced order transducer was investigated in the preliminary work which considered each FSR capable of detecting only compressive loads [Ref.1:pp. 31-31]. However, when the concept of the pre-loaded sensor is utilized, the analysis is similar to that used for the full order transducer configuration discussed in Chapter III.

Since it is desired to detect and resolve three forces and only one moment, the force and moment column vector, \mathbf{F} , has only four elements. The reduced order mathematical generalization of the problem is therefore:

$$\begin{vmatrix} s_1 \\ s_2 \\ s_3 \\ s_n \end{vmatrix} = \begin{vmatrix} a_{1,1} & a_{1,2} & a_{1,3} & a_{1,4} \\ a_{2,1} & \cdot & \cdot & \cdot \\ \cdot & \cdot & \cdot & \cdot \\ a_{n,1} & a_{n,2} & a_{n,3} & a_{n,4} \end{vmatrix} \mathbf{x} \begin{vmatrix} F_x \\ F_y \\ F_z \\ M_z \end{vmatrix} \quad (23)$$

As before, \mathbf{S} represents the sensor voltage output and \mathbf{F} is the force and moment column vector. Also, since it is desired to minimize the number of sensors required to resolve the components of the 4×1 \mathbf{F} vector, n will be four. The goal was to choose a configuration which will yield an invertible square \mathbf{A} matrix.

Figure 18 showed the modified preliminary transducer configuration which was successful in providing an \mathbf{A} matrix with a full rank. Hence, in order to obtain a reduced order transducer, the iterative process of removing sensors and their corresponding \mathbf{A} matrix rows began with this layout.

2. Equations

As described in Chapter III, the principle of superposition was employed to develop the equations describing the normal forces on each sensor as a result of the application of the three dimensional forces. Also, equations were developed to reflect the application of moment about only the z axis. The resulting complete equation is similar to Equation 22. The only difference is that the two \mathbf{A} matrix

columns which were a result of the application of M_x and M_y , are now gone. The new equation is as follows:

$$\begin{array}{c|cccc|}
 S_1 & 1/4(1+d/2a) & 0 & 0 & 1/8a \\
 S_2 & 1/4(1-d/2a) & 0 & 0 & -1/8a \\
 S_3 & -1/4(1+d/2a) & 0 & 0 & -1/8a \\
 S_4 & -1/4(1-d/2a) & 0 & 0 & 1/8a \\
 S_5 & 0 & 1/4(1+d/2a) & 0 & 1/8a \\
 S_6 & 0 & 1/4(1-d/2a) & 0 & -1/8a \\
 S_7 & 0 & -1/4(1+d/2a) & 0 & 1/8a \\
 S_8 & 0 & -1/4(1-d/2a) & 0 & -1/8a \\
 S_9 & d/8a & d/8a & -1/4 & 0 \\
 S_{10} & -d/8a & -d/8a & -1/4 & 0 \\
 S_{11} & -d/8a & -d/8a & 1/4 & 0 \\
 S_{12} & d/8a & d/8a & 1/4 & 0
 \end{array}
 =
 \begin{array}{cccc}
 1/4(1+d/2a) & 0 & 0 & 1/8a \\
 1/4(1-d/2a) & 0 & 0 & -1/8a \\
 -1/4(1+d/2a) & 0 & 0 & -1/8a \\
 -1/4(1-d/2a) & 0 & 0 & 1/8a \\
 0 & 1/4(1+d/2a) & 0 & 1/8a \\
 0 & 1/4(1-d/2a) & 0 & -1/8a \\
 0 & -1/4(1+d/2a) & 0 & 1/8a \\
 0 & -1/4(1-d/2a) & 0 & -1/8a \\
 d/8a & d/8a & -1/4 & 0 \\
 -d/8a & -d/8a & -1/4 & 0 \\
 -d/8a & -d/8a & 1/4 & 0 \\
 d/8a & d/8a & 1/4 & 0
 \end{array}
 \times
 \begin{array}{c}
 F_x \\
 F_y \\
 F_z \\
 M_x
 \end{array}
 \quad (24)$$

3. Sensor Placement

First, the values for d and a were assumed to be 5 and 1, respectively. Then the complete A matrix was put into MATLABTM and the rank was calculated to be four. As expected, this indicated a sufficient configuration to resolve the components of F . In an effort to reduce the number of sensors in the layout, all the sensors on the negative faces of the cube were eliminated by setting their associated rows in the A matrix to zero. This resulted in a configuration with six sensors on the positive face of the cube which yielded an A matrix with a rank of four.

The layout was then reduced to five sensors by next removing one of the two remaining sensors on the positive z face. The choice was sensor #11. The associated A matrix yielded a full rank of four. Next, sensor #12, the last remaining z face sensor, was removed. The resulting A matrix was rank deficient indicating a combination incapable of resolving F . Hence, this sensor was returned to the configuration.

Sensor #5, a y face FSR, was the next choice. The resulting configuration generated an A matrix with a rank of four capable of being used to resolve the components of the force and moment column vector. For continuity, this sensor was returned and sensor #1, a positive x face sensor, was removed. This also yielded an A matrix with a rank of four indicating another successful combination. Finally, a configuration which was nearly a mirror image to the layout missing sensor #5 was used generate an A matrix of full rank.

4. Results

After the eight iterations discussed above, two useable sensor configuration were determined. These layouts consist of the minimum number of pre-loaded sensors, four, necessary to resolve the elements of the 4×1 force and moment column vector using Equation 13. Figures 23 and 24 display the resulting transducer configurations.

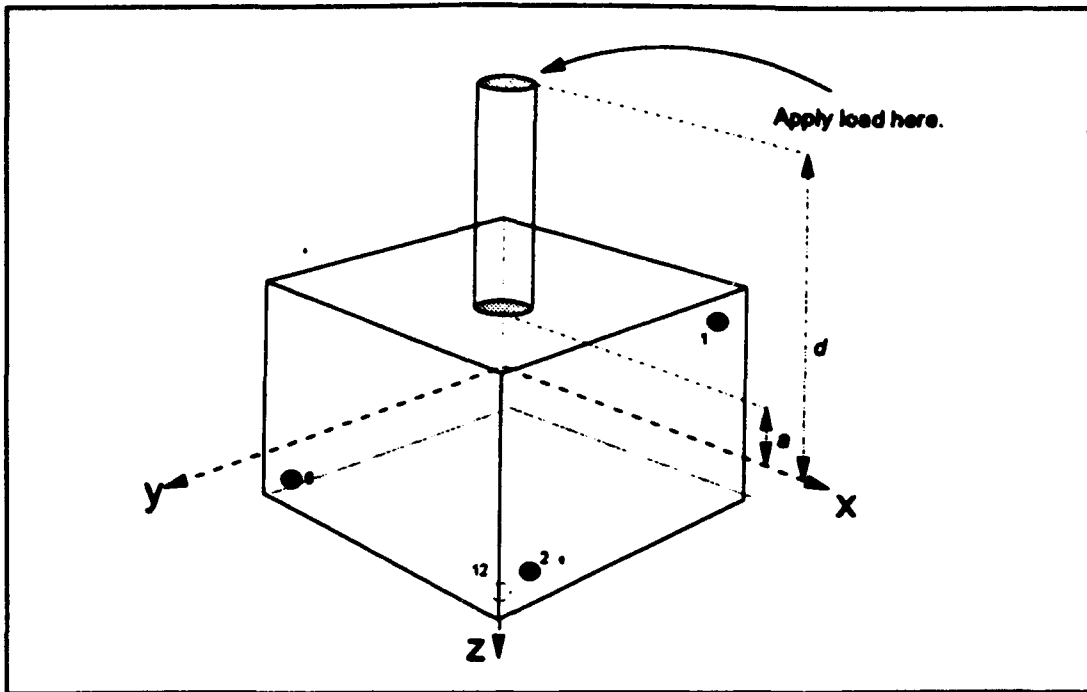


Figure 23
Positive Face Pre-Loaded Sensor Reduced Order Transducer

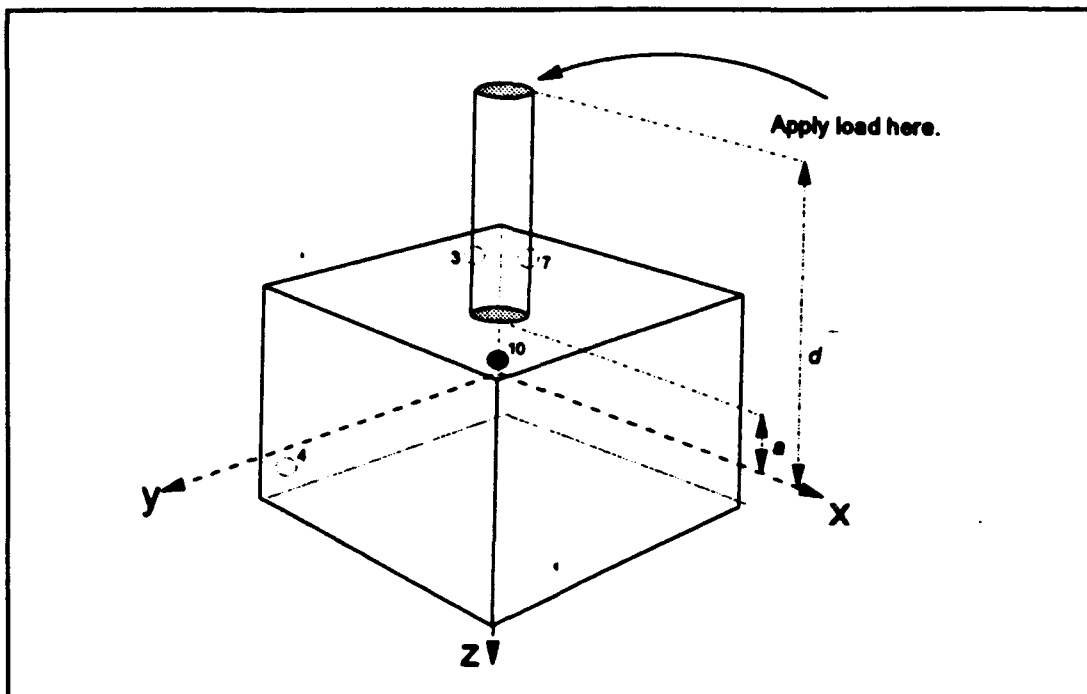


Figure 24
Negative Face Pre-Loaded Sensor Reduced Order Transducer

VI. PROTOTYPE TRANSDUCER

A. 4 INCH REDUCED ORDER VERSION

1. Objective

It was decided to build a suitable prototype force-torque transducer for the reduced order sensor configuration. The layout to be used is pictured in Figure 23 and was shown theoretically capable of being used to resolve forces in three directions and moments about a single axis. After calibration, a physical model could be used to qualitatively demonstrate the capability of resolving the associated force and moment column vector given some arbitrary applied loads to the joystick handle.

2. Design and Construction

a. Mechanical Design

Appendix C consists of the detailed machine drawings of a 4" force-torque transducer. Figure 25 shows a general view of the prototype design. The outer cube was constructed using .25" aluminum plate surrounding a plexiglass, smaller solid cube with an attached plexiglass joystick handle. The handle was fastened using a pin and epoxy. Phillips head 4x1/2" tapping screws were used to secure the walls of the outer cube.

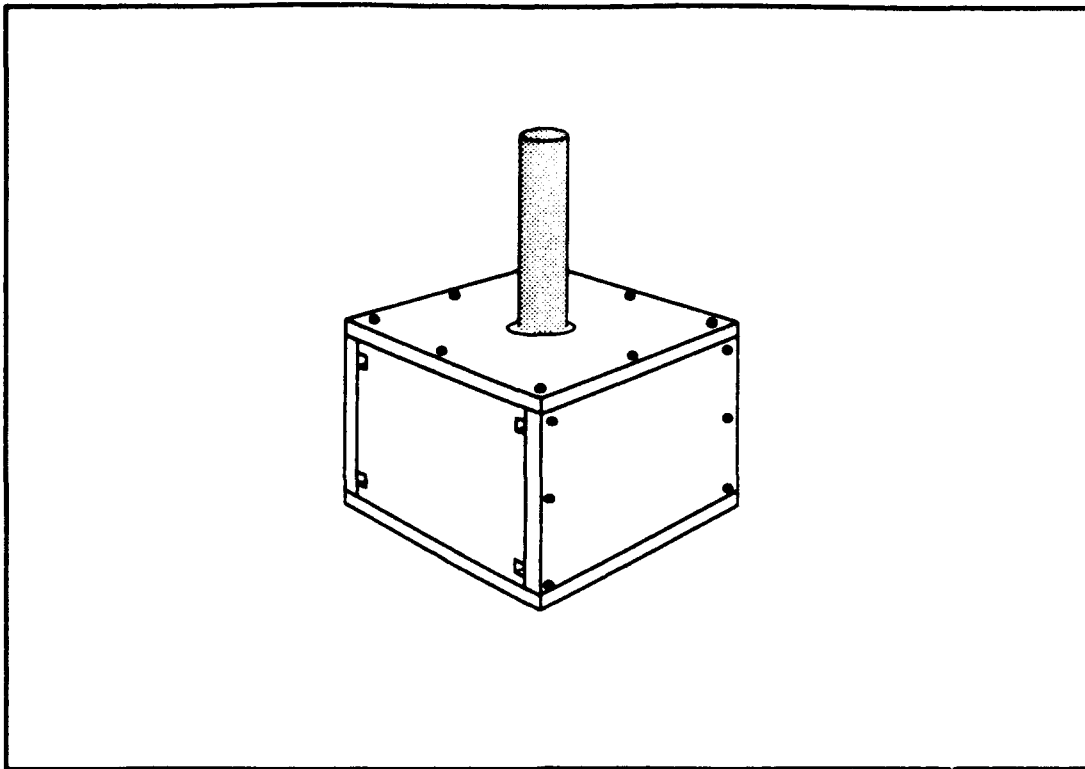


Figure 25
Generic Prototype Transducer

The 4" outside dimension was chosen in order to allow for a 3" inner cube using .25" aluminum plate and a .25" space between cubes. The need for the 3" inner cube was established by the size of the readily available .25" square FSR, Interlink Electronics™ product #30-301. Each sensor had an overall length of 2". In order to mount these on the inner cube and allow enough room for sensor protective padding and sensor wiring, the 3" dimension was chosen.

The four FSRs were configured as shown in Figure 23, allowing for the detection and resolution of the four elements of the force and moment vector according to Equation

3. The sensors were mounted to the faces of the inner plexiglass cube using Scotch™ 467MP High Performance adhesive. A 10/32 threaded set bolt was inserted above each sensor site to allow for the application of an initial compressive force as a pre-load.

To protect the sensing surface of each FSR, a .5"x1.75" steel shim was fastened to the inside face of the outer cube. The sensor side of this shim was initially lined with .25" neoprene padding material. This padding was later changed to a .30" polyurethane bumpon^R to better protect and transmit normal forces to the FSR. This alteration provided enough padding in the gap between cubes to exert a sufficient pre-compressive load to eliminate the set bolts except as a method for manually controlling or refining the set point.

b. Electronic Interface

The electronic interface shown in Figure 12 was used to convert the change in resistance provided by each sensor to a suitable voltage change. The sensors were wired such that FSR #1 used orange/yellow colored wires, FSR #2 used brown/red colored wires, FSR #6 used blue/green colored wires, and FSR #12 used gray/violet colored wires. These were multi-strand, 24 gauge wires separated from 16 wire ribbon cable. Various feedback resistance values were used in conjunction with an LM324 op-amp. This circuit was essentially four of the circuits used in the pre-load sensor test apparatus.

3. Calibration and Testing

a. Apparatus

A general sketch of the calibration and test apparatus is shown in Figure 26. The device was constructed using readily available pine 1"x10" material with .125" press

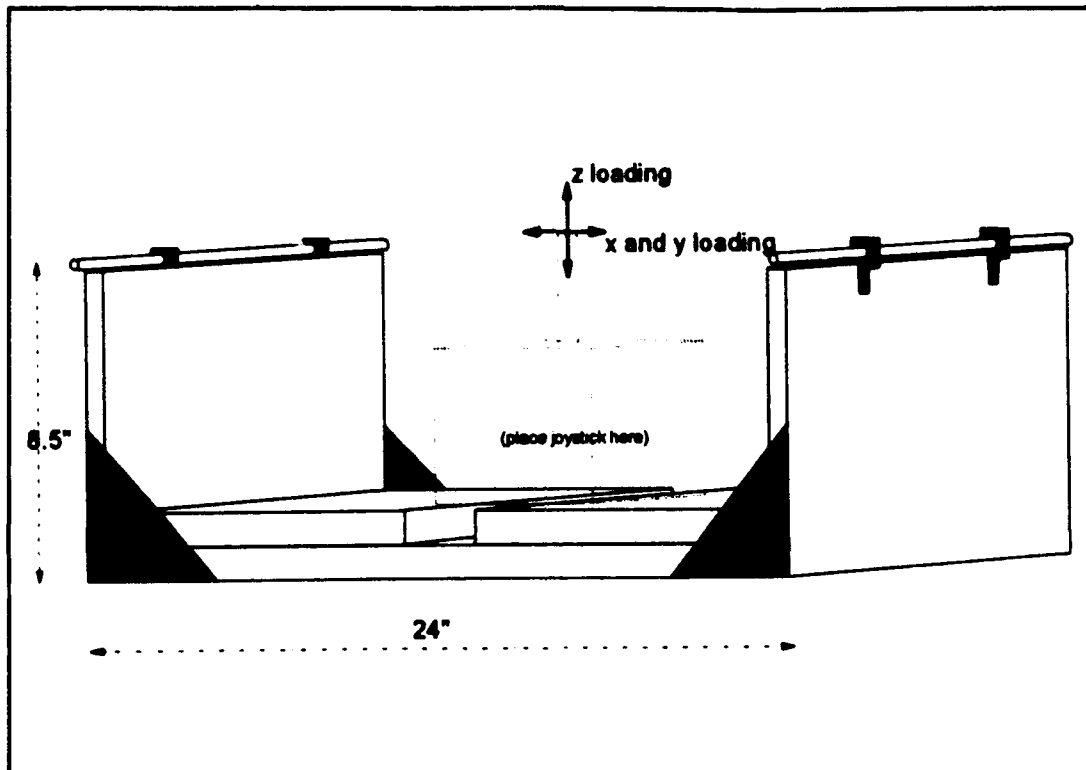


Figure 26
Transducer Test and Calibration Apparatus

board used to reinforce the corners as shown. The uprights were 8.5" high and the device was 24" wide. The force-torque transducer was mounted as shown enabling individual loading in each direction of interest. A system consisting of two aluminum shafts mounted through ball bearing supports was

added to reduce friction between the uprights and load supporting strings which pass over the ends.

b. Technique

Incremental masses hung from strings laid over the upright ends and attached to the joystick handle served to load the system in the x and y directions. The joystick cube had be rotated 90° for measuring the positive and negative y forces after the positive and negative x direction forces were applied and measured.

To measure forces in the positive z direction incremental masses were placed in a tray which was mounted to the top of the joystick handle. To measure forces in the negative z direction, the apparatus was designed to be turned over across a gap between two adjacent parallel tables. The loads were applied by incrementally placing masses in a tray hanging from the joystick handle.

A bar was bolted to the top of the joystick handle parallel to the upright ends in order to measure moments about the z axis. Masses were hung in opposite directions from each end of this bar using strings passed over the rollers on the uprights providing a couple with the bar length as the moment arm. The right hand rule was used to determine the directions in which to load the bar for the respective positive and negative z axis moments.

c. Data Acquisition

Masses ranging from -2.762 kg to +2.762 kg in increments of .25 kg were used to calibrate the transducer. The moment arm provided by the bar bolted to the top of the joystick handle was .0984 meters. The masses were carefully used to apply isolated forces in x, y, and z directions as well as isolated moments about the z axis. For calibration, the OMEGA BENCH™ data acquisition system and APPLE MACINTOSH™ microcomputer were configured as a voltmeter to detect the voltage response for each sensor as each load in each direction of interest was applied. The changes in voltage for each change in load were plotted as 16 separate curves. The slopes of these curves were used to relate the force and moment column vector to the sensor output according to Equation 24 as the 16 elements of the 4x4 **A** matrix.

With the elements of the **A** matrix determined, Equation 13 could be used to resolve arbitrary applied reduced order forces and moments. The OMEGA BENCH™ data acquisition icon system was configured as shown in Figure 27 in order to perform the matrix multiplication in real time. The first column of icons represents the incoming analog signals provided by the sensor outputs in response to an applied load on the joystick handle. The second column of icons shows calculation boxes in which the sensor voltage signals were summed with the initial pre-load voltages. This resulted in

a change in voltage response to the applied load which could be multiplied by the elements of the inverted A matrix. The multiplication was done in the third and fourth columns of icons by first multiplying each change in sensor voltage signal by the inverted A matrix element in the corresponding matrix column. Then adding each matrix row of products provided each of the four outputs. Each force or moment output was displayed in real time using a meter and a chart icon.

d. Results

Two calibration tests were conducted. The first used a feedback resistor, R_0 , with a value of 20 kohms and the second used 10 kohms for feedback resistance. In both tests, it was possible to obtain very linear force and moment versus voltage curves, although the curves appeared to be somewhat discontinuous at the zero points. This was due to the physical variations in first measuring the response to applied loads in the positive directions and then unloading the axis under consideration and applying the loads in the negative direction in order to measure the response. This discontinuity was accounted for by determining the slopes using four different techniques. The first was slopes determined using a least-squares regression line over the entire range. The second and third were using the slopes from just the positive and negative portions of the curves,

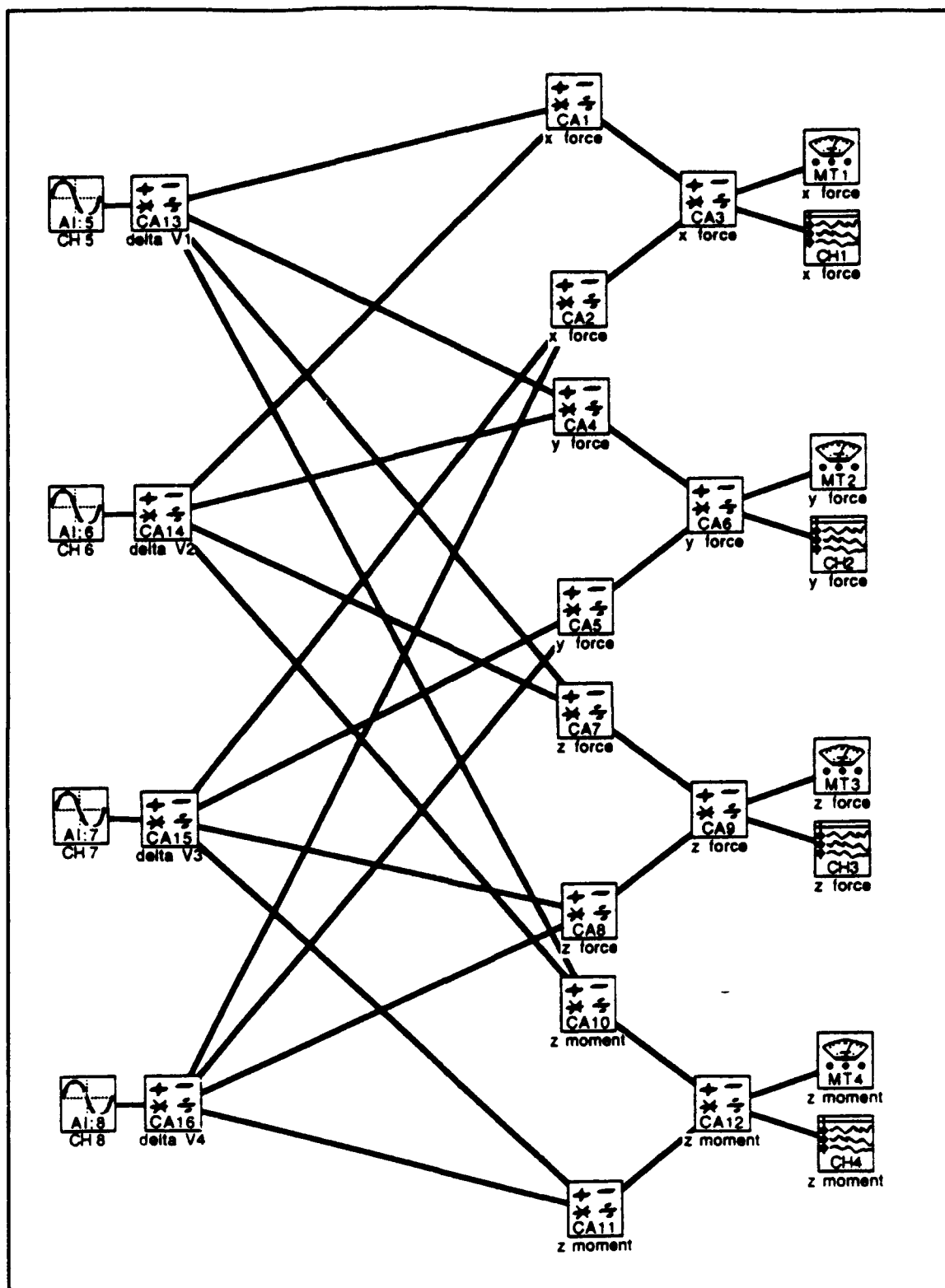


Figure 27
Icon Arrangement for Real Time Matrix Multiplication

respectively. The fourth was taking the average of the two slopes determined for each curve using the second and third technique of isolating the respective positive and negative ranges.

Once calibrated using the 20 kohm feedback resistance, the procedure discussed in the previous section, and the slopes resulting from the least-squares regression line, the system was tested by applying a known force of 10 N in the positive x direction. The first time this load was applied the response was good. That is the display of forces in the y and z directions remained less than about 2 N and the moment display registered very little change while the x direction force display was about 8.5 N indicating successful decoupling of the forces and moments. However, the system did not prove to be repeatable. When a force of 10 N was applied in the negative x direction the force and moment displays in the y and z directions began to show a substantial response indicating poor force and moment resolution. The inverted A matrix elements resulting from the various slope determination techniques were all tried in the data acquisition system in an attempt to produce a more repeatable arrangement. None seemed to provide a satisfactory result. The matrix elements from the technique of determining the slope from only the positive load application outputs seemed to qualitatively provide the best force and moment resolution.

The calibration procedure was repeated using the 10 kohm feedback resistance with no pre-load set bolts in an attempt to refine the data taking technique and overcome this non-repeatability. The results were virtually the same.

B. 2 INCH REDUCED ORDER VERSION

1. Objective

In parallel to building a 4" reduced order force-torque transducer, it was desired to design a smaller reduced order force-torque transducer to meet the specific payload requirements of the PUMA 560 robotic manipulator. This required a device with a 2" outside dimension weighing less than 5 lbs. In order to do this, a shorter force sensing resistor was needed.

2. Shortened FSR

a. Methods

The smallest FSRs available measured about 1.5" in length overall. It was desired to use the same type of FSR used in the 4" transducer design in the smaller transducer since these provided a good response for a given force application. Since the outside dimensions of the transducer had to be approximately 2", the inside cube could only be about 1.25" to allow a .1875" gap using .1875" aluminum plate. Hence, the FSR resistor used could not be any longer than 1" to allow enough clearance for wire attached to the terminals. Also, the FSRs could be no wider than .5".

The .25" square FSRs used in the 4" transducer had an overall length of 2". In order to reduce this length, two methods were tried which did not use soldering due to the low melting temperatures of the materials used to manufacture the FSRs. Both methods attempted to leave the sensing pad of the device undisturbed and only shorten the tail portion which was used to connect to the circuit wiring. The first method consisted of separating the outside polymer layers on the tail portion of the device. With the silver electrode terminals exposed, a 1" section was removed. The remaining .25" portion crimped with the wire terminals was inverted and attached to the exposed electrodes near the sensing portion with an electrically conductive epoxy. After several attempts an adequate bond between the shortened pieces was not achieved.

The second technique again required splitting the polymer covering layers on the tail portion of the FSR. The device was trimmed such that only .125" of exposed electrode remained as the tail piece. A small, .0625"x.125" piece of the polymer was trimmed away from each side of each exposed silver electrode. Small metal terminal pin connectors with 24 gauge multi-strand wires pre-soldered in position were then spread with conductive epoxy and crimped onto the exposed electrodes. This provided a strong bond and wire attachment for the shortened FSRs.

b. Test and Comparison

To determine the effects of this shortening process, a shortened FSR was placed in the pre-load sensor test apparatus shown in Figure 11 using the electronic interface shown in Figure 12. The test conducted was similar to the previous test conducted to prove the pre-load concept. A plot of the results is provided in Figure 28. The results showed a very linear relationship between the applied force and the voltage response when compared to the earlier pre-load concept test results shown in Figure 14.

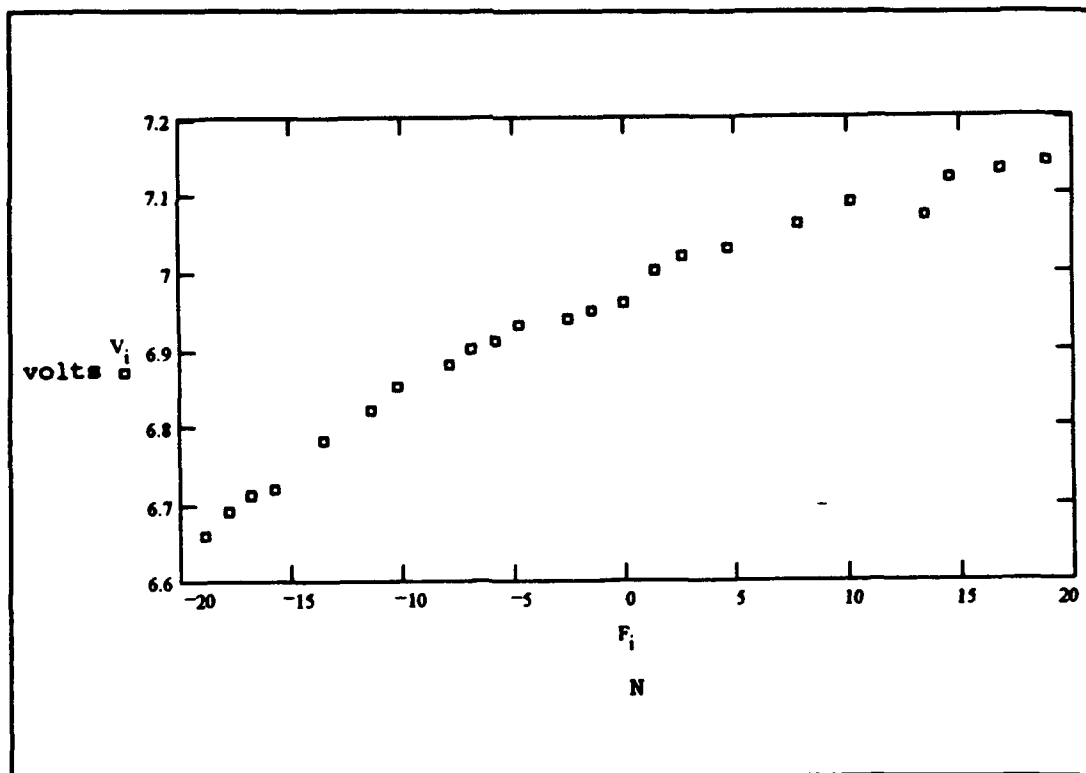


Figure 28
Shortened FSR Performance Test Results

It was observed that for the shortened test the time between incremental loadings was relatively short and consistent. During the pre-load concept test, no specific care was taken to provide a consistent time interval between load applications. This was thought to be important since at this point it was noticed that the output slowly crept higher as the device was loaded and left undisturbed.

The test was repeated using a feedback resistance of 10 kohms for three different initial pre-load set points. A plot of the results is provided in Figure 29. Run #2 and

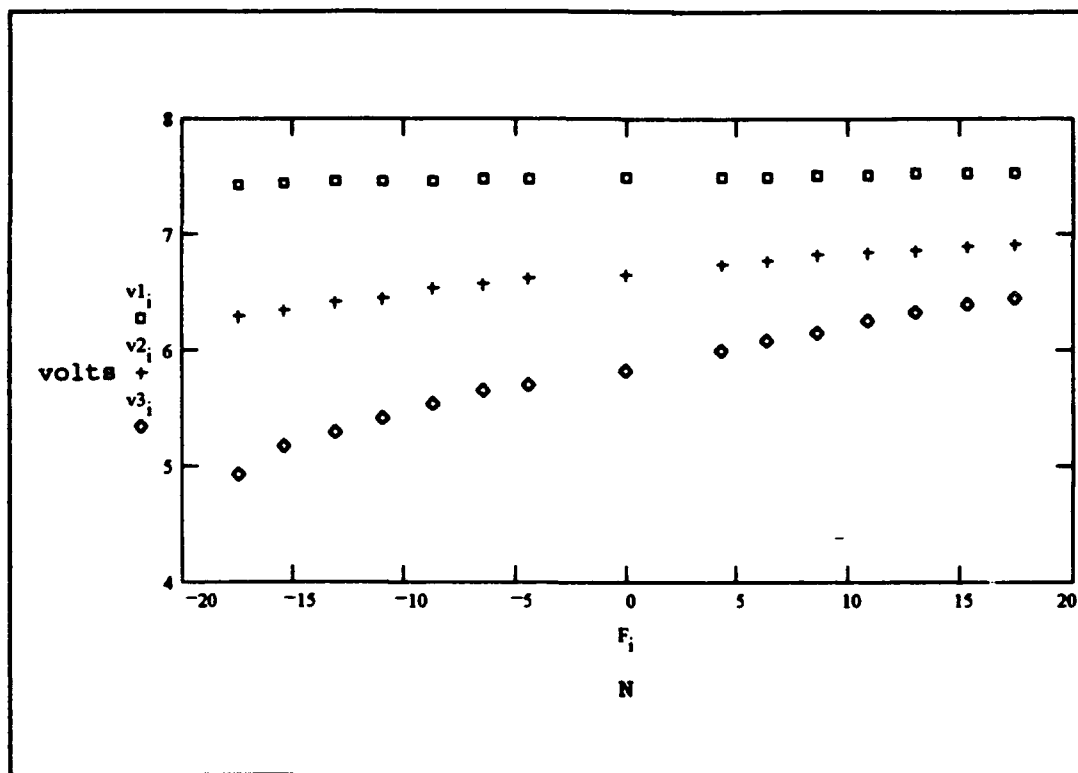


Figure 29
Shortened FSR Performance Tests at Various Pre-Loads

run #3 appear to provide the best set point since they offer

the largest change in voltage for a given change in load and remain roughly linear. At this point, the shorter FSR appears to provide a more linear output than the unaltered sensor. This was initially thought to be the result of consciously applying the incremental loads and recording the voltage response data in a quick consistent fashion in order to compensate for the drift phenomenon noticed earlier.

To test the effects of this data taking technique, an unaltered FSR was placed in the apparatus and loaded to attain three set points similar to the previous test on the shortened FSR. Figure 30 shows the results of this test. The response curves are nearly linear indicating that the speed and consistency of the data taking technique was important due to the drift tendency. The important difference was that the pre-load set points used in the shortened FSR test were not repeatable in the unaltered FSR test using a feedback resistance of 10 kohms. The higher set point was attained using a feedback resistance of 30 kohms while the lower two set points were made using a 20 kohm feedback resistance. This indicated that the shortening process added about 10 to 20 kohms of resistance in series with the shortened FSR since the unaltered sensor required additional resistance to attain the same three set points used earlier and shown in Figure 29. The resistance added to the altered FSR is thought to be the result of the conductive epoxy used in the fastening process of the wire terminals.

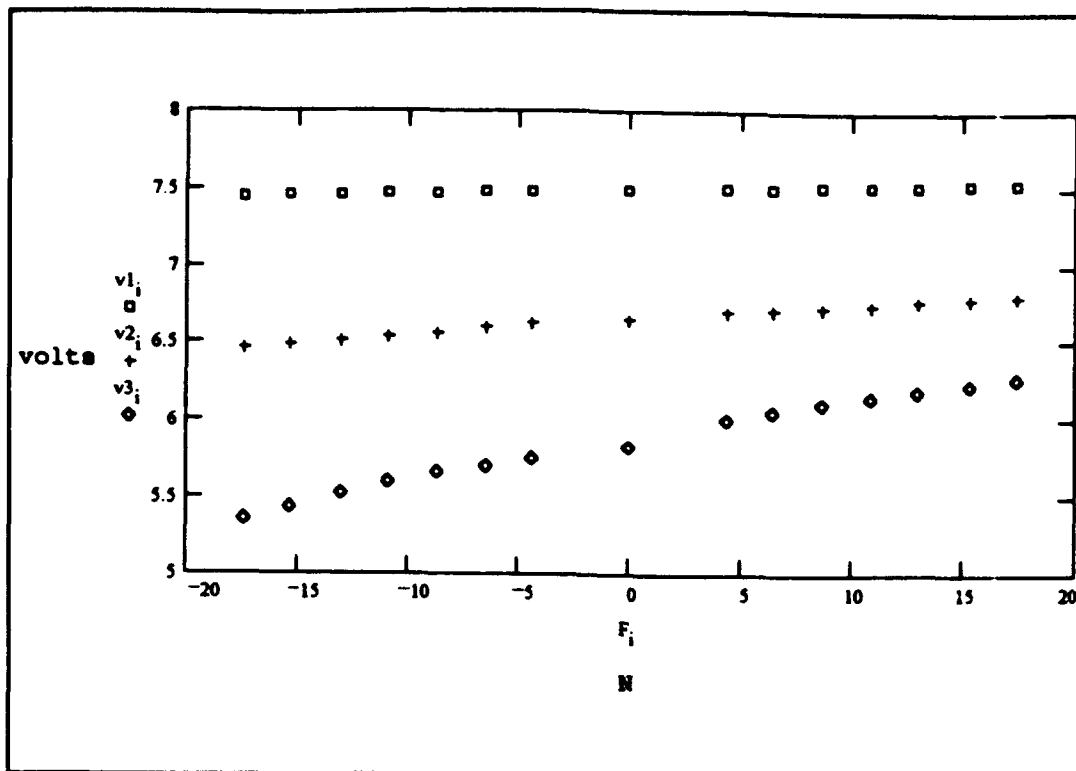


Figure 30
Unaltered FSR Test at Three Different Pre-Loads

c. Drift Analysis

(1) Description

As discussed in the previous section, the drift phenomenon was noticed while applying loads and recording the voltage response during testing of the shortened FSR. The presence of voltage response drift was confirmed by leaving the apparatus loaded and undisturbed for a period of about 3 hours. In this time the voltage output ranged from 5.988 volts to 6.290 volts. However, when an arbitrary compressive force was suddenly applied and released, the voltage output dropped back to approximately 5.9 volts. Therefore, this

indicates that the effects of drift do affect the output and the response curves whose slopes are used to determine the elements of the \mathbf{A} matrix.

(2) Test Conducted

To more fully understand the effects of drift, an arrangement consisting of the four sensors of the 4" prototype transducer with a feedback resistance of 10 kohms, an unaltered FSR in the pre-load test apparatus with a feedback resistance of 30 kohms, an unaltered FSR with no load with a feedback resistance of 1 Mohms, a shortened FSR loaded with vice grips using minimal padding with a feedback resistance of 1 Mohms, and an open channel with 5 volts directly applied using no FSR with a feedback resistance of 1 Mohms was developed. Therefore, this arrangement consisted of eight channels, numbered channel 1 to channel 8, representing the eight respective sensor setups just delineated. The voltage output was plotted over a specific period of time at various intervals.

Two tests were conducted using this eight sensor arrangement. The first test was over a period of almost 65 hours with 17 output recordings at various time intervals for all eight channels with little delay between channels. During this test a sudden compressive load was applied and released twice and a facility power outage occurred. The second test covered a 175 minute period with

the output data taken regularly every 10 minutes for each of the respective eight channels.

Another test was conducted using a single unaltered .25" square FSR in order to further study the effects of the padding used between the load application and the FSR active surface. This test consisted of placing the FSR between two smooth rigid metal surfaces. One was aluminum plate and the other was steel plate material. The data was taken first over a period of 276 minutes in 13 intervals. These were every 3 minutes for the first 27 minutes and then at the 246, 261 and 276 minute points. A second set of readings was taken over a 70 minute period in 23 interval. These intervals were every minute for the first 10 minutes and increased to every 5 minutes for the remainder of the time.

(3) Results

The results of the four tests discussed in the previous section are provided in Appendix D. The first test was conducted over the longest interval. The general conclusions from the data plots is that the drift is apparent in all channels except channels #6 and #8 which were the channels with the unloaded FSR and no FSR, respectively. It was also apparent that as the load condition was disturbed, by applying a sudden change and quickly returning the original loading condition, the voltage value would drop back to the initial value and resume drifting upward. This load change

was experienced by the apparatus at elapsed times of 10.37 hours and 57.11 hours. Also, at 59.46 elapsed hours the facility experienced a power outage which caused the voltage value to drop and resume the upward drift. Throughout all these disturbances, the outputs of channels #6 and #8 remained nearly constant.

The second test conducted was similar to the first except that the overall time period was shorter and the interval between voltage readings was more regular at 10 minutes each except toward the end of the test. The results were as expected, demonstrating the drift in all but channels #6 and #8. The only disturbance experienced was an intentional system power outage after 155 minutes had elapsed. It was at this point that the data acquisition interval was decreased to 5 minutes. Except for channels #6 and #8 the voltage outputs show the drift upward both after initial load application and after the power disturbance. In the resulting plots the approach of the effected output curves can be seen to approach some apparent asymptotic voltage level.

In order to understand the effects of the padding between the applied load and the FSR sensing surface, the last two tests were conducted as discussed in the previous section. The results of the tests clearly indicate a voltage output gradually rising toward some asymptotic value. No disturbances were caused or occurred during these two tests. The conclusion was therefore drawn that the type of padding

between the load and the FSR sensing surface had no effect on the upward drift experienced by the voltage output.

In the eight channel test, Channel #8 was used to show that this drift phenomenon was not caused by the circuitry used since no drift was experienced when no FSR was used. The conclusion drawn from the results of the Channel #6 test is that an unloaded FSR does not experience a drift in response. Hence, it was shown that only FSRs with applied loads experience a circuit output drift upward toward some final steady state voltage value. This drift can be stopped and started again from an initial voltage output value by suddenly disturbing the loading or interrupting the system power.

3. Design and Construction

a. Mechanical Device

The design of the 2" force-torque transducer was very similar to that of the 4" force-torque transducer. The detailed mechanical drawings are provided in Appendix E. The primary difference other than the size was the round top and bottom to allow enclosure of the device in a cylindrical tube. Also, the inner cube was made from aluminum with an aluminum joystick handle threaded and inserted into a threaded hole in the top. The top of the handle was threaded to allow for fastening the bar used to measure the moments about the z axis. The size of the inner cube allowed installation of the

shortened FSRs exactly on the edges in accordance with the reduced order configuration shown in Figure 24. This layout was chosen so that pre-load set bolts could be applied to the sensor in the z direction at the top of the cube, which is the negative z face, in order to allow mounting the transducer on the end effector of the PUMA 560 robotic manipulator. Polyurethane bumpons^R which were .44"x.20" were used between cubes in order to apply normal forces to the sensors. Since these were slightly larger than the .1875" gap, they provided enough pre-compressive load after completely assembling the device to eliminate the need for the set bolts. The set bolts were therefore only necessary as a means of fine tuning the initial set points by adjusting the individual pre-loads on each sensor.

b. Electronic Interface

The current-to-voltage circuit shown in Figure 12 was again used for this smaller design. Feedback resistance values of 10 and 20 kohms were used. The circuit design was essentially identical to that used for the 4" prototype transducer discussed earlier in this chapter. The only difference was the wiring color scheme used. FSR #3 used the gray/violet colored wires, FSR #4 used the white/black colored wires, FSR #7 used the brown/red colored wires, and FSR #10 used the orange/yellow colored wires. The wires were the same

type of 24 gauge multi-strand insulated wires cut from 16 wire ribbon cable.

4. Calibration and Testing

The technique of calibrating the 2" transducer was virtually the same as that of the 4" transducer. The apparatus shown in Figure 26 and the OMEGA BENCH™ icon arrangement shown in Figure 27 were designed to be used with both the 2" and 4" devices in a manner similar to that described for the 4" version earlier. Four calibration and testing attempts were made.

The first two calibration tests were conducted using a feedback resistance value of 10 kohms. The slopes of the resulting 16 least-squared regression lines were calculated for each of the two test runs. The respective sets of 16 slopes were used as the elements of two A matrices. These matrices were inverted and used in the calculation icon boxes to perform the real time matrix multiplication in accordance with Equation 13. The resulting output was similar to that of the 4" transducer when an arbitrary load in the x , y or z direction was applied. The force was not consistently resolvable. As the joystick was manipulated, force resolution, if attained, was not repeatable. As arbitrary moments about the z axis were applied, the same effects were observed. The third calibration test was conducted using a

feedback resistance of 20 kohms. The results were also not repeatable with no clear resolution of forces or moments.

The fourth test was conducted using no pre-load set bolts which had been used earlier to adjust the initial pre-load voltage to the nominal starting value used during calibration. This test showed very good resolution of arbitrarily applied forces in the negative direction, but still no repeatable results were attained.

VII. DISCUSSION OF RESULTS

A. DRIFT PHENOMENON

The presence of drift in output voltage over time was demonstrated in the previous chapter. This phenomenon was discovered while attempting to calibrate the 2" FSR force-torque prototype transducer. The drift in voltage output was noticed while loading the device. The output crept upward as the load was left undisturbed. The output would drop and resume the upward drift from a voltage very near the starting voltage as a result of disturbing the load. The load disturbances during the tests consisted of suddenly applying and removing a larger load. Also, an interruption in power would cause the drift to repeat. In all cases the drift in voltage appeared to approach some asymptotic value.

The effects of this drift were not accounted for in the initial test of the pre-load concept. The output is shown in Figure 14 and does not appear as linear as the output shown in Figure 28. The output shown in this later figure was produced by attempting to compensate for the drift by using equal increments of mass additions over roughly equal intervals of time. In an effort to remain consistent, the emphasis was on preventing any disturbance which would disrupt the drift while taking data. The artificiality imposed by this rigid data

taking technique was duplicated during the calibration procedures conducted on the prototype transducers. However, in actual use of the transducers, it would not be possible to accurately account for the drift phenomenon. Sudden changes in loading are inherent in the operation of force-torque transducers.

Therefore, it was determined to disregard the effects of the drift phenomenon while developing physical models of the force-torque transducers based on force sensing resistor technology. When a prototype is built which is capable of repeatedly resolving the desired forces and moments, the error resulting from the drift could be determined. Not only would drift effects have been difficult to quantify, during the design of the prototypes it was considered superfluous since the drift appeared to be less than 10% of the pre-load voltage set points. The accuracy of the FSRs used in this application were unknown and hence the overall uncertainty of the transducer output was not known. At this point in the design, accuracy was not the primary concern. The goal was to show actual decoupling of the elements of the force and moment column vector, F , according to Equation 13.

B. PROTOTYPE PERFORMANCE

1. Single FSR Prototype

The single FSR prototype displayed in Figure 11 using the electronic interface shown in Figure 12 was used as a test

platform for the pre-load concept discussed in Chapter III and for the shortened FSR discussed in Chapter VI. As mentioned previously, during the testing for the single pre-loaded FSR care was not taken to consistently load the device without disturbing the drift inherent in the voltage output. However, the device was used to successfully show the ability of the pre-loaded FSRs to be used for a voltage signal change, for not only compressive loads but also tensile loads. This result was significant because it allowed the required number of sensors in the transducer design to be halved. This was because one pre-loaded sensor was now used to measure forces in both the positive and negative directions of the axis on which it was mounted.

The second use of the single FSR prototype was that of proving the successful FSR shortening process. A total of 10 .25" FSRs, Interlink Electronics™ product # 30-301, were shortened as discussed in the previous chapter. After each FSR was altered, it was mounted in the single FSR pre-load device and tested to ensure a adequate response.

2. Transducer Prototypes

The results of the single FSR test device were applied to the three dimensional theoretical and physical force-torque transducer models. The impact of the successful demonstrations of the pre-load concept and the FSR shortening process were significant. Also, the effects of the interface

between the force application and the FSR sensing surface proved to be important.

First, the pre-load concept was extended to the theoretical model of the three dimensional transducer allowing the associated A matrix, originally introduced in Equation 2, to be square. This was a direct result of halving the number of sensors required to detect forces in each direction. It was shown for the full order case, which sought the forces in each of the x , y , and z directions as well as the moments about these three axes that the force and moment column vector, F , would have six elements. The elements could be resolved using a transducer configuration of only six sensors. A similar demonstration was made for the reduced order case which sought the forces in the three directions but only the moment about a single axis. This simplified the problem, as shown in Equation 13, by allowing a square A matrix which, if constructed so as to provide a full rank, could be inverted and use to solve for F directly.

Second, the ability to shorten the individual FSRs provided the means of building a force-torque transducer of smaller dimensions to meet specific robotic manipulator payload requirements. The smaller design was analogous to the first larger physical three dimensional design except that it used the altered FSRs whose performance had been proven on the single FSR test device. The FSRs altered in the manner discussed in Chapter VI gave the ability to proceed with the

design of an adequate force-torque transducer to be used with the PUMA 560 robotic manipulator without the time and expense of ordering custom FSRs manufactured to meet the specific size requirements.

Finally, in the actual construction, calibration and testing of the 2" and 4" prototype transducers, output repeatability was a problem. Both prototype devices provided an initial response which showed definite decoupling of the forces and moments of the F vector according to the reduced order theory. However, a consistently repeatable response was not obtained regardless of many attempts to accurately determine the elements of the A matrix during calibration procedures. Ultimately, this lack of repeatability was attributed to the tendency of the inner cube to become skewed in an orientation with respect to the outer cube which was somewhat different than the original orientation. The padding used to transfer the load to the sensor was a set of polyurethane hemispherical devices which theoretically provided a single point of contact on the FSRs sensing surface. In actuality, each pad was compressed a small amount providing a relatively small flat spot that remained in contact with the sensing surface. In either case, the load across the FSR was applied in a relatively small local pattern which was free to move across the FSR as the joystick handle was moved. Moving the joystick caused the inner cube to move with respect to the outer cube. The padding was firmly

attached to the outer cube while the FSR sensing surface was securely attached to the inner cube. The result was a situation in which the application point of the load was free to change; therefore, the output of the FSR response was reflecting a change in the force application footprint. This force application footprint was different than experienced in calibration of the device requiring a different A matrix to resolve the force and moment vector, F .

This effect could be proven by utilizing a different polyurethane pad above each FSR. These pads should not be hemispherical, but cylindrical in shape so that the force application footprint on each FSR surface remains constant over the relatively small range of motion between the inner and outer cubes of the transducer. After eliminating the force application footprint as a variable, the device should be calibrated as discussed earlier and retested. Upon successful and repeatable resolution to the force and moment vector, the force-torque transducer accuracy could be quantified. The device would then be ready to be placed in a force override rate control system as discussed in the preliminary work.

C. REDUNDANCY ALGORITHM

The FORTRAN code developed in Chapter IV demonstrates the ability of a full order force-torque transducer to be built with multiple levels of redundancy. The theoretical

development of the redundancy algorithm could also be applied to a reduced order transducer requiring moments only about a single axis as modelled in Chapter VI. Once proven, the physical device could be built with multiple levels of redundancy by simply adding more FSRs and a computer interface which would conduct the search for useable combinations as the need arose. The only limit to the levels of redundancy would be imposed by the space limitations dictating the possible number of sensors in the physical transducer.

The full order design used to develop the algorithm allows, at a minimum, four layers of redundancy simply by using all the available corners of the cube. In the sample output in Appendix B, it took 11 sensor failures to exhaust the four initial subsystems set up by using 24 FSRs and requiring six sensors for each subsystem. This left 13 sensors in an arbitrary configuration from which the search for subsequent sets of six sensors would be conducted to find useable configurations. In the example output, seven such useable systems were found in less than one minute after eliminating a sensor each time another set was discovered. This example provided for 18 sensor failures out of 24 possible sensors. The maximum levels of redundancy for this configuration is 18 since at least six sensors are required to resolve the six elements of the force and moment vector, F .

VIII. CONCLUSIONS AND RECOMMENDATIONS

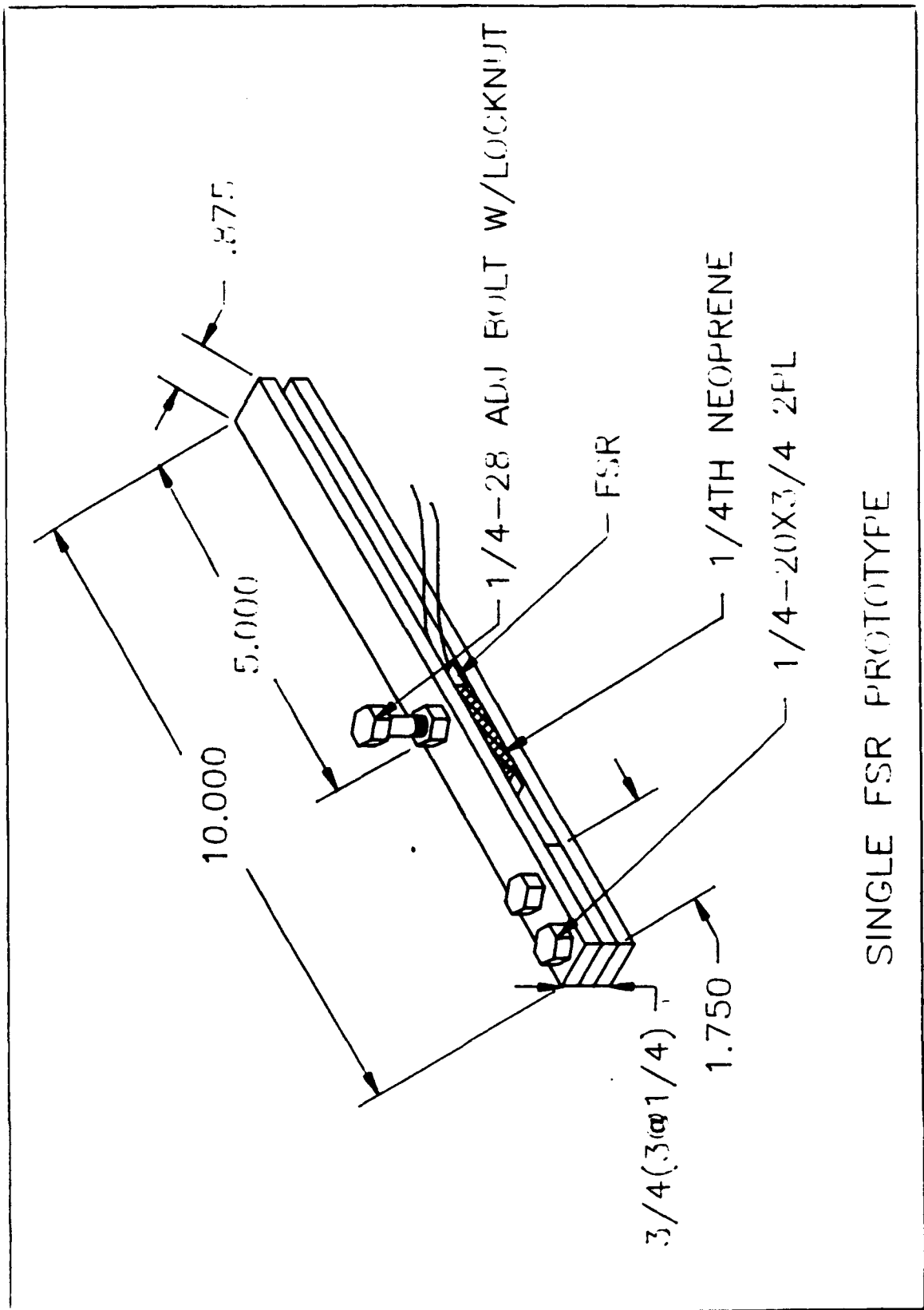
A. CONCLUSIONS

- Force Sensing Resistors offer a practical, robust and inexpensive alternative to strain gauge technology for use in force-torque transducers.
- Two, three dimensional reduced order force-torque transducers were successfully designed, constructed and used to qualitatively demonstrate the ability to resolve forces and moments.
- Three dimensional force-torque transducers are capable of multiple levels of redundancy using a simple algorithm to search for acceptable configurations given an adequate remaining layout of sensors after a sensor fails.
- The effects of voltage output drift over time will effect the overall accuracy of resolving forces and moments using FSR based force-torque transducers.
- Effects of the interface between the force application surface and force sensing resistor significantly impact the repeatability of the force and moment resolution for the force-torque transducer due to position instability preventing a consistent force application footprint on individual sensors.

B. RECOMMENDATIONS

- Conduct a study of different force application surfaces and quantify the effects of their footprints on FSR based force-torque transducer output repeatability.
- Use adequate force application surface in existing force-torque transducer design to obtain a repeatable resolution of the element of the force and moments column vector of interest.
- Develop application software to utilize the resolved forces and moments from the FSR based force-torque transducer in the force override rate control system.

APPENDIX A



SINGLE FSR PROTOTYPE

TEST #1 OF SINGLE PRE-LOADED FSR:

RESISTANCE: 4.7 (kohms) $i = 1.25$

DATA:

MASS (lbm) VOLTAGE (v)

$m_i =$

$V_i =$

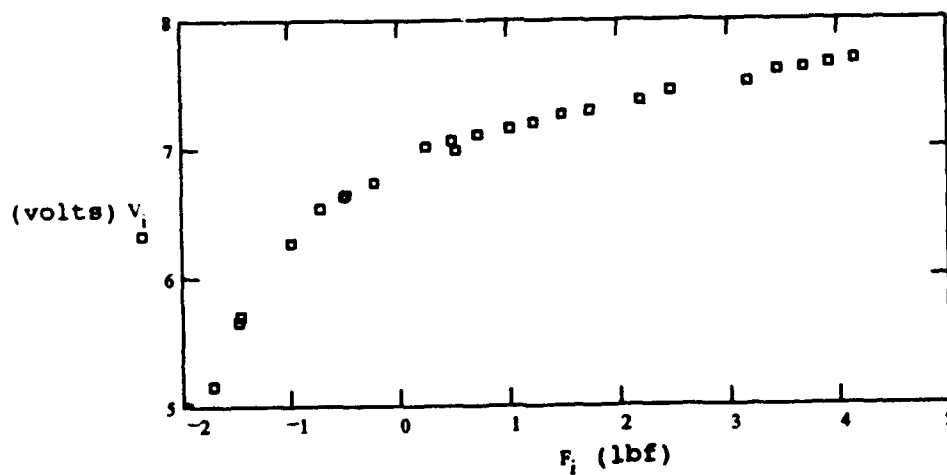
-1.97
-1.49
-1.73
-1.47
-.99
-.72
-.51
-.50
-.48
-.24
.24
.48
.51
.72
1.01
1.23
1.48
1.73
2.20
2.46
3.18
3.45
3.69
3.93
4.17

5.0
5.65
5.15
5.71
6.26
6.53
6.62
6.63
6.64
6.74
7.01
7.06
6.99
7.11
7.16
7.20
7.26
7.29
7.38
7.45
7.52
7.61
7.62
7.65
7.69

FORCE (lbf):

$$F_i = \frac{m_i \cdot g}{32.174} (\text{lbf})$$

Response Graph:



TEST #2-#6 OF SINGLE PRE-LOADED FSR USING VARIOUS FEEDBACK RESISTANCES:

RESISTANCE: various (kohms) $i = 1..14$

DATA:

MASS (g) VOLTAGE (v)
 $m_i = V1_i = V2_i = V3_i = V4_i = V5_i =$

-1149.8	5.33	5.6	5.87	6.15	6.39
-1043.1	5.36	5.66	5.97	6.27	6.58
-936.2	5.41	5.76	6.11	6.46	6.80
-724.1	5.50	5.95	6.40	6.85	7.31
-494.2	5.56	6.06	6.56	7.06	7.56
-49.5	5.61	6.17	6.73	7.30	7.86
-.01	5.86	6.26	6.87	7.46	8.05
.01	5.81	6.56	7.31	8.07	8.77
49.5	5.84	6.62	7.43	8.21	8.77
494.2	5.89	6.74	7.59	8.43	8.77
724.1	5.90	6.75	7.61	8.44	8.77
936.2	5.90	6.74	7.59	8.44	8.77
1043.1	5.91	6.75	7.59	8.44	8.77
1149.8	5.92	6.80	7.69	8.59	8.77

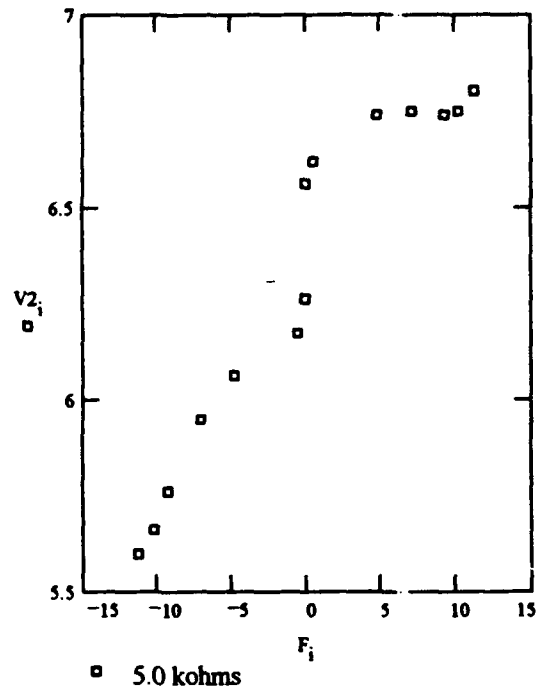
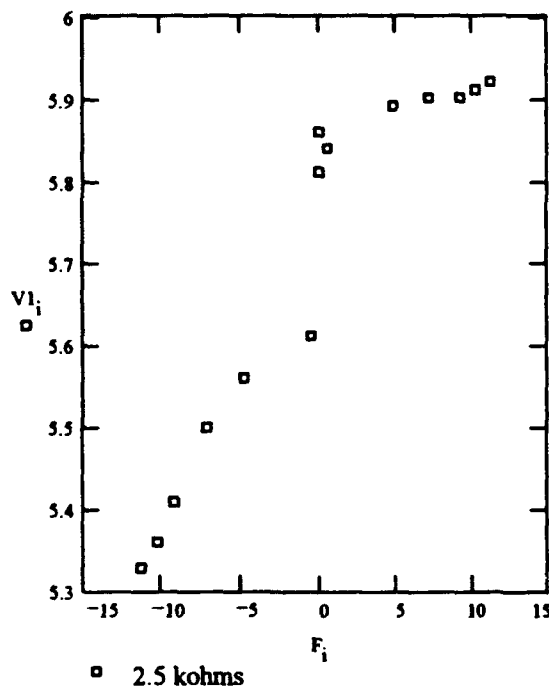
Where the corresponding resistances are (kohms):

R1 = 2.5
R2 = 5.0
R3 = 7.5
R4 = 10.0
R5 = 12.5

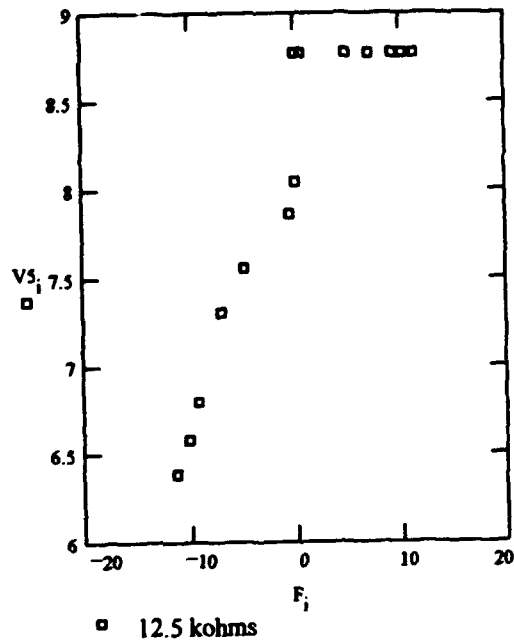
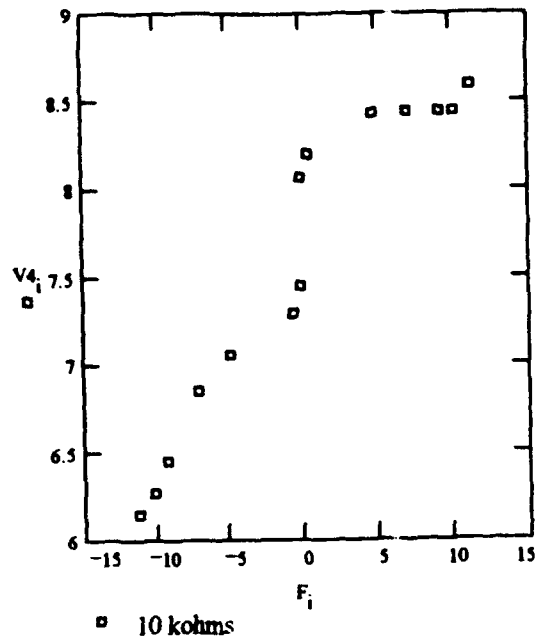
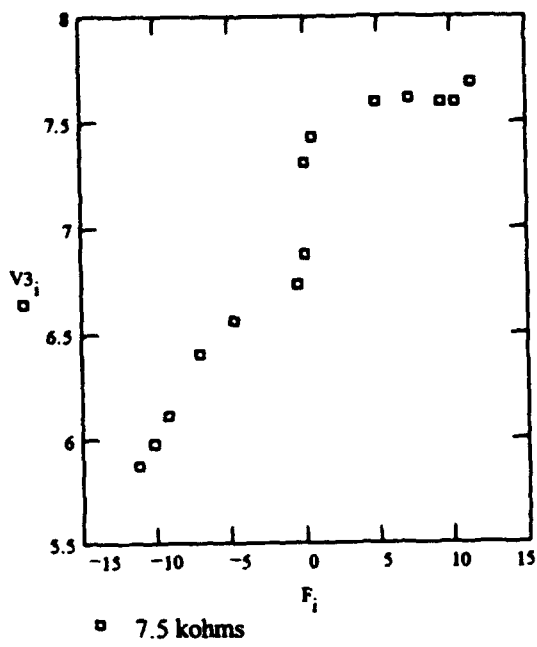
Force is:

$$F_i = m_i \cdot g \cdot 10^{-3} \text{ (N)}$$

Response Graphs:



Response Graphs cont...



APPENDIX B

```

C *****
C *
C *
C *      THESIS
C *      NAVAL ENGINEERING
C *      FSR FORCE/TORQUE TRANSDUCER
C *      REDUNDANCY ANALYSIS
C *
C *
C *      -- Charles A. Gunzel-III, LT, USN
C *
C *****

```

```

DATA (A(1,I),I=1,6) /7.5,0,0,0,-1,1/
DATA (A(2,I),I=1,6) /-1.5,0,0,0,1,-1/
DATA (A(3,I),I=1,6) /0,7.5,0,1,0,1/
DATA (A(4,I),I=1,6) /0,-1.5,0,-1,0,-1/
DATA (A(5,I),I=1,6) /4.5,4.5,3,1,-1,0/
DATA (A(17,I),I=1,6) /4.5,4.5,3,-1,1,0/

DATA (A(7,I),I=1,6) /-7.5,0,0,0,1,-1/
DATA (A(8,I),I=1,6) /1.5,0,0,0,-1,1/
DATA (A(9,I),I=1,6) /0,-7.5,0,-1,0,-1/
DATA (A(10,I),I=1,6) /0,1.5,0,1,0,1/
DATA (A(11,I),I=1,6) /-4.5,-4.5,-3,-1,1,0/
DATA (A(23,I),I=1,6) /4.5,4.5,-3,1,-1,0/

DATA (A(13,I),I=1,6) /7.5,0,0,0,-1,-1/
DATA (A(14,I),I=1,6) /-1.5,0,0,0,1,1/
DATA (A(15,I),I=1,6) /0,7.5,0,1,0,-1/
DATA (A(16,I),I=1,6) /0,-1.5,0,-1,0,1/
DATA (A(6,I),I=1,6) /-4.5,4.5,3,1,1,0/
DATA (A(18,I),I=1,6) /4.5,-4.5,3,-1,-1,0/

DATA (A(19,I),I=1,6) /-7.5,0,0,0,1,1/
DATA (A(20,I),I=1,6) /1.5,0,0,0,-1,-1/
DATA (A(21,I),I=1,6) /0,-7.5,0,-1,0,1/
DATA (A(22,I),I=1,6) /0,1.5,0,1,0,-1/
DATA (A(12,I),I=1,6) /4.5,-4.5,-3,-1,-1,0/
DATA (A(24,I),I=1,6) /-4.5,4.5,-3,1,1,0/

```

```

15  WRITE (*,*) 'The full matrix is as follows:'
    WRITE (20,*) 'The full matrix is as follows:'
    WRITE (*,*)
    WRITE (20,*)
    WRITE (*,400) ((A(ROW,COL),COL=1,6),ROW=1,24)

```

```
WRITE (20,400) ((A(ROW,COL),COL=1,6),ROW=1,24)
```

C VERIFY THE MATRIX

```
WRITE (*,*)  
WRITE (20,*)  
WRITE (*,*) 'Do you wish to change any elements?'  
WRITE (20,*) 'Do you wish to change any elements?'  
READ (*,300) ANS  
WRITE (20,350) ANS  
IF (ANS.EQ.'Y') THEN  
  GO TO 25  
ELSE  
  GO TO 35  
25 WRITE (*,*) 'Enter the row and column number of the element:'  
   WRITE (20,*) 'Enter the row and column number of the element:'  
   READ (*,*) ROW,COL  
   WRITE (20,*) ROW,COL  
   WRITE (*,*)  
   WRITE (20,*)  
   WRITE (*,100)  
+   'Enter the corrected value of element (',ROW,',',COL,'):'  
  WRITE (20,100)  
+   'Enter the corrected value of element (',ROW,',',COL,'):'  
  READ (*,*) A(ROW,COL)  
  WRITE (20,*) A(ROW,COL)  
  WRITE (*,*) 'Do you wish to change another element?'  
  WRITE (20,*) 'Do you wish to change another element?'  
  READ (*,300) ANS  
  WRITE (20,350) ANS  
  IF (ANS.EQ.'Y') THEN  
    GO TO 25  
  END IF  
  WRITE (*,*) 'Do you wish to view the matrix again?'  
  WRITE (20,*) 'Do you wish to view the matrix again?'  
  READ (*,300) ANS  
  WRITE (20,350) ANS  
  IF (ANS.EQ.'Y') THEN  
    GO TO 15  
  END IF  
35 CONTINUE
```

C BREAK FULL MATRIX INTO 4 SUB MATRICES

```
DO 37 ROW=1,6  
DO 36 COL=1,6  
  A1(ROW,COL)=A(ROW,COL)  
  A2(ROW,COL)=A((ROW+6),COL)  
  A3(ROW,COL)=A((ROW+12),COL)  
  A4(ROW,COL)=A((ROW+18),COL)  
36 CONTINUE  
37 CONTINUE
```

C DISPLAY THE 4 SUB-SYSTEMS

```
WRITE (*,*) 'The A-POSITIVE face system is:'  
WRITE (20,*) 'The A-POSITIVE face system is:'  
WRITE (*,400) ((A1(ROW,COL),COL=1,6),ROW=1,6)  
WRITE (20,400) ((A1(ROW,COL),COL=1,6),ROW=1,6)
```

```

WRITE (*,*)
WRITE (20,*)

WRITE (*,*) 'The A-NEGATIVE face system is:'
WRITE (20,*) 'The A-NEGATIVE face system is:'
WRITE (*,400) ((A2(ROW,COL),COL=1,6),ROW=1,6)
WRITE (20,400) ((A2(ROW,COL),COL=1,6),ROW=1,6)
WRITE (*,*)
WRITE (20,*)

WRITE (*,*) 'The B-POSITIVE face system is:'
WRITE (20,*) 'The B-POSITIVE face system is:'
WRITE (*,400) ((A3(ROW,COL),COL=1,6),ROW=1,6)
WRITE (20,400) ((A3(ROW,COL),COL=1,6),ROW=1,6)
WRITE (*,*)
WRITE (20,*)

WRITE (*,*) 'The B-NEGATIVE face system is:'
WRITE (20,*) 'The B-NEGATIVE face system is:'
WRITE (*,400) ((A4(ROW,COL),COL=1,6),ROW=1,6)
WRITE (20,400) ((A4(ROW,COL),COL=1,6),ROW=1,6)
WRITE (*,*)
WRITE (20,*)

```

C CHECK THE RANK OF EACH OF THESE SUBSYSTEMS

```

TOL=100*AMACH(4)

CALL LSGRR (NRA,NCA,A1,LDA,TOL,RANK1,GINVA1,LDGINV)
WRITE (*,500) 'The rank of the A-POSITIVE face
+ system is:',RANK1
WRITE (20,500) 'The rank of the A-POSITIVE face
+ system is:',RANK1

CALL LSGRR (NRA,NCA,A2,LDA,TOL,RANK2,GINVA2,LDGINV)
WRITE (*,500) 'The rank of the A-NEGATIVE face
+ system is:',RANK2
WRITE (20,500) 'The rank of the A-NEGATIVE face
+ system is:',RANK2

CALL LSGRR (NRA,NCA,A3,LDA,TOL,RANK3,GINVA3,LDGINV)
WRITE (*,500) 'The rank of the B-POSITIVE face
+ system is:',RANK3
WRITE (20,500) 'The rank of the B-POSITIVE face
+ system is:',RANK3

CALL LSGRR (NRA,NCA,A4,LDA,TOL,RANK4,GINVA4,LDGINV)
WRITE (*,500) 'The rank of the B-NEGATIVE face
+ system is:',RANK4
WRITE (20,500) 'The rank of the B-NEGATIVE face
+ system is:',RANK4

IF ((RANK1.EQ.6).AND.(RANK2.EQ.6).AND.
+ (RANK3.EQ.6).AND.(RANK4.EQ.6)) THEN
WRITE (*,*)
WRITE (20,*)
WRITE (*,*) 'Each of these subsystems is invertible.'
WRITE (20,*) 'Each of these subsystems is invertible.'

END IF

```

C INITIALIZE 24 FSR #'S TO ZERO

```
      DO 39 I=1,24
        FSR(I)=0
39    CONTINUE
```

C GENERATE A RANDOM FSR# FROM 1 TO 24

```
      GRP1=0
      GRP2=0
      GRP3=0
      GRP4=0
      XPOS=4
      XNEG=4
      YPOS=4
      YNEG=4
      ZPOS=4
      ZNEG=4
      J=0
45    J=J+1
      FSR(J)=24*RNUNF()
```

C ENSURE FSR# 0 IS NOT A CHOICE

```
      IF (FSR(J).EQ.0) THEN
        J=J-1
        GO TO 45
      END IF
```

C ENSURE THIS IS NOT A REPEAT VALUE

```
      DO 46 I=1,(J-1)
        IF (FSR(J).EQ.FSR(I)) THEN
          J=J-1
          GO TO 45
        END IF
46    CONTINUE
```

C REPORT THE FSR CHOSEN TO FAIL

```
      WRITE (*,*)
      WRITE (20,*)
      WRITE (*,500) 'The sensor I will simulate failed is FSR #',FSR(J)
      WRITE (20,500) 'The sensor I will simulate failed is FSR #',FSR(J)
```

C TERMINATE IF THERE ARE NOT ENOUGH FSR'S REMAINING

```
      IF (J.EQ.19) THEN
        WRITE(*,*) 'TERMINATION==> Sorry, there are not
+ enough remaining FSRs.'
        WRITE(20,*) 'TERMINATION==> Sorry, there are not
+ enough remaining FSRs.'
        GO TO 1000
      END IF
```

C CHECK WHICH SUBSYSTEM THIS FAILED FSR IS IN

```
      IF ((FSR(J).GE.1).AND.(FSR(J).LE.6)) THEN
        GRP1=1
        WRITE(*,600) 'This sensor is in the A-POSITIVE face system.'
```

```

WRITE(20,600)'This sensor is in the A-POSITIVE face system.'
ELSE IF ((FSR(J).GE.7).AND.(FSR(J).LE.12)) THEN
  GRP2=1
  WRITE(*,600) 'This sensor is in the A-NEGATIVE face system.'
  WRITE(20,600)'This sensor is in the A-NEGATIVE face system.'
ELSE IF ((FSR(J).GE.13).AND.(FSR(J).LE.18)) THEN
  GRP3=1
  WRITE(*,600) 'This sensor is in the B-POSITIVE face system.'
  WRITE(20,600)'This sensor is in the B-POSITIVE face system.'
ELSE
  GRP4=1
  WRITE(*,600) 'This sensor is in the B-NEGATIVE face system.'
  WRITE(20,600)'This sensor is in the B-NEGATIVE face system.'
END IF

```

C SET THIS FSR SIGNAL TO ZERO

```

DO 47 COL=1,6
  A(FSR(J),COL)=0.0
47 CONTINUE

```

C CHECK IF THERE ARE ANY COMPLETE INTACT SUBSETS REMAINING

```

WRITE (*,*)
WRITE (20,*)
IF (GRP1.EQ.0) THEN
  WRITE(*,*) 'The A-POSITIVE face system is still active.'
  WRITE(20,*) 'The A-POSITIVE face system is still active.'
END IF
IF (GRP2.EQ.0) THEN
  WRITE(*,*) 'The A-NEGATIVE face system is still active.'
  WRITE(20,*) 'The A-NEGATIVE face system is still active.'
END IF
IF (GRP3.EQ.0) THEN
  WRITE(*,*) 'The B-POSITIVE face system is still active.'
  WRITE(20,*) 'The B-POSITIVE face system is still active.'
END IF
IF (GRP4.EQ.0) THEN
  WRITE(*,*) 'The B-NEGATIVE face system is still active.'
  WRITE(20,*) 'The B-NEGATIVE face system is still active.'
END IF
IF ((GRP1.EQ.0).OR.(GRP2.EQ.0).OR.(GRP3.EQ.0).OR.(GRP4.EQ.0)) THEN
  GO TO 55
ELSE
  WRITE(*,*) 'None of the 4 initial subsystems remain intact.'
  WRITE(20,*) 'None of the 4 initial subsystems remain intact.'
  GO TO 56
END IF

```

C CHECK IF IT IS DESIRED TO TAKE OUT ANOTHER FSR

```

55 WRITE (*,*)
   WRITE (20,*)
   WRITE (*,*) 'Press 1 if you wish to eliminate another FSR?'
   WRITE (20,*) 'Press 1 if you wish to eliminate another FSR?'
   READ (*,*) I
   WRITE (20,*) I
   IF (I.EQ.1) THEN
     WRITE (*,*)
     WRITE (20,*)

```

```

        GO TO 45
      ELSE
        GO TO 1000
      END IF
56  CONTINUE
    WRITE(*,*) 'I will randomly pick 6 of the remaining FSRs to
+ generate another subsystem.'
    WRITE(20,*) 'I will randomly pick 6 of the remaining FSRs to
+ generate another subsystem.'
    WRITE(*,*)
    WRITE(20,*)

```

C CHECK IF THERE REMAINS AT LEAST ONE FSR'S IN EACH DIRECTION

```

      DO 57 I=1,J
        IF ((FSR(J).EQ.1).OR.(FSR(J).EQ.2)
+ .OR.(FSR(J).EQ.13).OR.(FSR(J).EQ.14)) THEN
          XPOS=XPOS-1
        END IF
        IF ((FSR(J).EQ.7).OR.(FSR(J).EQ.8)
+ .OR.(FSR(J).EQ.19).OR.(FSR(J).EQ.20)) THEN
          XNEG=XNEG-1
        END IF
        IF ((FSR(J).EQ.3).OR.(FSR(J).EQ.4)
+ .OR.(FSR(J).EQ.15).OR.(FSR(J).EQ.16)) THEN
          YPOS=YPOS-1
        END IF
        IF ((FSR(J).EQ.9).OR.(FSR(J).EQ.10)
+ .OR.(FSR(J).EQ.21).OR.(FSR(J).EQ.22)) THEN
          YNEG=YNEG-1
        END IF
        IF ((FSR(J).EQ.5).OR.(FSR(J).EQ.6)
+ .OR.(FSR(J).EQ.17).OR.(FSR(J).EQ.18)) THEN
          ZPOS=ZPOS-1
        END IF
        IF ((FSR(J).EQ.11).OR.(FSR(J).EQ.12)
+ .OR.(FSR(J).EQ.23).OR.(FSR(J).EQ.24)) THEN
          ZNEG=ZNEG-1
        END IF
57  CONTINUE

```

```

      IF ((XPOS.EQ.0).OR.(XNEG.EQ.0)
+ .OR.(YPOS.EQ.0).OR.(YNEG.EQ.0)
+ .OR.(ZPOS.EQ.0).OR.(ZNEG.EQ.0)) THEN
        WRITE (*,*)
        WRITE (20,*)
        WRITE (*,*) 'TERMINATION==> There are not enough FSRs
+ remaining in each direction.'
        WRITE (20,*) 'TERMINATION==> There are not enough FSRs
+ remaining in each direction.'
        GO TO 1000
      END IF

```

C TERMINATE IF THERE ARE NOT ENOUGH FSR'S REMAINING

```

      IF (J.EQ.19) THEN
        WRITE (*,*)
        WRITE (20,*)
        WRITE (*,*) 'TERMINATION==> There are not enough FSRs
+ remaining to continue.'

```

```

        WRITE (20,*) 'TERMINATION==> There are not enough FSRs
+ remaining to continue.'
        GO TO 1000
    END IF

```

C RANDOMLY PICK 6 OF THE REMAINING FSR'S

```

65     N1=0
        N2=1
66     CONTINUE
        XPOS=0
        XNEG=0
        YPOS=0
        YNEG=0
        ZPOS=0
        ZNEG=0
        DO 69 K=(J+1),24
67         FSR(K)=24*RNUNF()
C ENSURE FSR# 0 IS NOT A CHOICE

```

```

        IF (FSR(K).EQ.0) THEN
            GO TO 67
        END IF

```

C ENSURE THIS IS NOT A REPEAT VALUE

```

        DO 68 I=1,J
            IF ((FSR(I)).EQ.(FSR(K))) THEN
                GO TO 67
            END IF
68     CONTINUE

```

C ENSURE THERE IS ONLY ONE FSR PER FACE

```

        IF ((FSR(K).EQ.1).OR.(FSR(K).EQ.2)
+ .OR.(FSR(K).EQ.13).OR.(FSR(K).EQ.14)) THEN
            XPOS=XPOS+1
        END IF
        IF ((FSR(K).EQ.7).OR.(FSR(K).EQ.8)
+ .OR.(FSR(K).EQ.19).OR.(FSR(K).EQ.20)) THEN
            XNEG=XNEG+1
        END IF
        IF ((FSR(K).EQ.3).OR.(FSR(K).EQ.4)
+ .OR.(FSR(K).EQ.15).OR.(FSR(K).EQ.16)) THEN
            YPOS=YPOS+1
        END IF
        IF ((FSR(K).EQ.9).OR.(FSR(K).EQ.10)
+ .OR.(FSR(K).EQ.21).OR.(FSR(K).EQ.22)) THEN
            YNEG=YNEG+1
        END IF
        IF ((FSR(K).EQ.5).OR.(FSR(K).EQ.6)
+ .OR.(FSR(K).EQ.17).OR.(FSR(K).EQ.18)) THEN
            ZPOS=ZPOS+1
        END IF
        IF ((FSR(K).EQ.11).OR.(FSR(K).EQ.12)
+ .OR.(FSR(K).EQ.23).OR.(FSR(K).EQ.24)) THEN
            ZNEG=ZNEG+1
        END IF

        IF ((XPOS1.GT.1).OR.(XNEG1.GT.1)

```

```

      + .OR. (YPOS1.GT.1) .OR. (YNEG1.GT.1)
      + .OR. (ZPOS1.GT.1) .OR. (ZNEG1.GT.1)) THEN
        GO TO 66
      ELSE IF (N1.EQ.6) THEN
        GO TO 70
      END IF
69    CONTINUE

C SET UP NEW 6x6 MATRIX

70    CONTINUE
      DO 72 ROW=(J+1),K
      DO 71 COL=1,6
        A5((ROW-J),COL)=A(FSR(ROW),COL)
71    CONTINUE
72    CONTINUE

C CHECK RANK & PRINT NEW MATRIX IF RANK=6

      CALL LSGRR (NRA,NCA,A5,LDA,TOL,RANK5,GINVA5,LDGINV)

      IF (RANK5.LT.6) THEN
        N1=N1+1
        IF (N1.EQ.N2*(10**4)) THEN
          N2=N2+1
          WRITE(*,800) 'There have been',N1,' iterations attempting to
+ find an invertible matrix with the remaining FSRs.'
          WRITE(20,800) 'There have been',N1,' iterations attempting to
+ find an invertible matrix with the remaining FSRs.'
        END IF
        GO TO 66
      END IF

      WRITE (*,*)
      WRITE (20,*)
      WRITE (*,800) 'After',N1,' iterations, the randomly
+ generated subsystem is:'
      WRITE (20,800) 'After',N1,' iterations, the randomly
+ generated subsystem is:'
      WRITE (*,400) ((A5(ROW,COL),COL=1,6),ROW=1,6)
      WRITE (20,400) ((A5(ROW,COL),COL=1,6),ROW=1,6)
      WRITE (*,*)
      WRITE (20,*)
      WRITE (*,500) 'The rank of this new subsystem is:',RANK5
      WRITE (20,500) 'The rank of this new subsystem is:',RANK5
      WRITE (*,*) 'This subsystem provides an invertible matrix.'
      WRITE (20,*) 'This subsystem provides an invertible matrix.'

C CHECK IF IT IS DESIRED TO TAKE OUT ANOTHER FSR

      WRITE (*,*)
      WRITE (20,*)
      WRITE (*,*) 'Press 1 if you wish to eliminate another FSR?'
      WRITE (20,*) 'Press 1 if you wish to eliminate another FSR?'
      READ (*,*) I
      WRITE (20,*) I
      IF (I.EQ.1) THEN
        J=J+1
        XPOS=4
        XNEG=4

```

```

      YPOS=4
      YNEG=4
      ZPOS=4
      ZNEG=4
73     FSR(J)=24*RNUNF()
C ENSURE FSR# 0 IS NOT A CHOICE

      IF (FSR(J).EQ.0) THEN
        GO TO 73
      END IF

C ENSURE THIS IS NOT A REPEAT VALUE

      DO 74 I=1, (J-1)
        IF ((FSR(I)).EQ.(FSR(J))) THEN
          GO TO 73
        END IF
74     CONTINUE

      GO TO 56
    ELSE
      GO TO 1000
    END IF

C FORMAT LIBRARY

100  FORMAT (1X,A,I2,A,I2,A)
200  FORMAT (1X,24(1X,F6.3))
300  FORMAT (A)
350  FORMAT (10X,A)
400  FORMAT ((T18,6(F5.1,3X)))
500  FORMAT (1X,A,I3)
600  FORMAT (1X,A,I2,A)
700  FORMAT (1X,I2)
800  FORMAT (1X,A,I7,A)

1000 CONTINUE
      STOP
      END

```

Sample Output...

The full matrix is as follows:

7.5	0.0	0.0	0.0	-1.0	1.0
-1.5	0.0	0.0	0.0	1.0	-1.0
0.0	7.5	0.0	1.0	0.0	1.0
0.0	-1.5	0.0	-1.0	0.0	-1.0
4.5	4.5	3.0	1.0	-1.0	0.0
-4.5	4.5	3.0	1.0	1.0	0.0
-7.5	0.0	0.0	0.0	1.0	-1.0
1.5	0.0	0.0	0.0	-1.0	1.0
0.0	-7.5	0.0	-1.0	0.0	-1.0
0.0	1.5	0.0	1.0	0.0	1.0
-4.5	-4.5	-3.0	-1.0	1.0	0.0
4.5	-4.5	-3.0	-1.0	-1.0	0.0
7.5	0.0	0.0	0.0	-1.0	-1.0
-1.5	0.0	0.0	0.0	1.0	1.0
0.0	7.5	0.0	1.0	0.0	-1.0
0.0	-1.5	0.0	-1.0	0.0	1.0
4.5	4.5	3.0	-1.0	1.0	0.0
4.5	-4.5	3.0	-1.0	-1.0	0.0
-7.5	0.0	0.0	0.0	1.0	1.0
1.5	0.0	0.0	0.0	-1.0	-1.0
0.0	-7.5	0.0	-1.0	0.0	1.0
0.0	1.5	0.0	1.0	0.0	-1.0
4.5	4.5	-3.0	1.0	-1.0	0.0
-4.5	4.5	-3.0	1.0	1.0	0.0

Do you wish to change any elements?

N

The A-POSITIVE face system is:

7.5	0.0	0.0	0.0	-1.0	1.0
-1.5	0.0	0.0	0.0	1.0	-1.0
0.0	7.5	0.0	1.0	0.0	1.0
0.0	-1.5	0.0	-1.0	0.0	-1.0
4.5	4.5	3.0	1.0	-1.0	0.0
-4.5	4.5	3.0	1.0	1.0	0.0

The A-NEGATIVE face system is:

-7.5	0.0	0.0	0.0	1.0	-1.0
1.5	0.0	0.0	0.0	-1.0	1.0
0.0	-7.5	0.0	-1.0	0.0	-1.0
0.0	1.5	0.0	1.0	0.0	1.0
-4.5	-4.5	-3.0	-1.0	1.0	0.0
4.5	-4.5	-3.0	-1.0	-1.0	0.0

The B-POSITIVE face system is:

7.5	0.0	0.0	0.0	-1.0	-1.0
-1.5	0.0	0.0	0.0	1.0	1.0
0.0	7.5	0.0	1.0	0.0	-1.0
0.0	-1.5	0.0	-1.0	0.0	1.0
4.5	4.5	3.0	-1.0	1.0	0.0
4.5	-4.5	3.0	-1.0	-1.0	0.0

The B-NEGATIVE face system is:

-7.5	0.0	0.0	0.0	1.0	1.0
1.5	0.0	0.0	0.0	-1.0	-1.0
0.0	-7.5	0.0	-1.0	0.0	1.0
0.0	1.5	0.0	1.0	0.0	-1.0
4.5	4.5	-3.0	1.0	-1.0	0.0
-4.5	4.5	-3.0	1.0	1.0	0.0

The rank of the A-POSITIVE face system is: 6
The rank of the A-NEGATIVE face system is: 6
The rank of the B-POSITIVE face system is: 6
The rank of the B-NEGATIVE face system is: 6

Each of these subsystems is invertible.

The sensor I will simulate failed is FSR # 4
This sensor is in the A-POSITIVE face system.

The A-NEGATIVE face system is still active.
The B-POSITIVE face system is still active.
The B-NEGATIVE face system is still active.

Press 1 if you wish to eliminate another FSR?
1

The sensor I will simulate failed is FSR # 3
This sensor is in the A-POSITIVE face system.

The A-NEGATIVE face system is still active.
The B-POSITIVE face system is still active.
The B-NEGATIVE face system is still active.

Press 1 if you wish to eliminate another FSR?
1

The sensor I will simulate failed is FSR # 18
This sensor is in the B-POSITIVE face system.

The A-NEGATIVE face system is still active.
The B-NEGATIVE face system is still active.

Press 1 if you wish to eliminate another FSR?
1

The sensor I will simulate failed is FSR # 22
This sensor is in the B-NEGATIVE face system.

The A-NEGATIVE face system is still active.

Press 1 if you wish to eliminate another FSR?
1

The sensor I will simulate failed is FSR # 16
This sensor is in the B-POSITIVE face system.

The A-NEGATIVE face system is still active.

Press 1 if you wish to eliminate another FSR?
1

The sensor I will simulate failed is FSR # 21
This sensor is in the B-NEGATIVE face system.

The A-NEGATIVE face system is still active.

Press 1 if you wish to eliminate another FSR?

1

The sensor I will simulate failed is FSR # 1
This sensor is in the A-POSITIVE face system.

The A-NEGATIVE face system is still active.

Press 1 if you wish to eliminate another FSR?

1

The sensor I will simulate failed is FSR # 20
This sensor is in the B-NEGATIVE face system.

The A-NEGATIVE face system is still active.

Press 1 if you wish to eliminate another FSR?

1

The sensor I will simulate failed is FSR # 19
This sensor is in the B-NEGATIVE face system.

The A-NEGATIVE face system is still active.

Press 1 if you wish to eliminate another FSR?

1

The sensor I will simulate failed is FSR # 2
This sensor is in the A-POSITIVE face system.

The A-NEGATIVE face system is still active.

Press 1 if you wish to eliminate another FSR?

1

The sensor I will simulate failed is FSR # 23
This sensor is in the B-NEGATIVE face system.

The A-NEGATIVE face system is still active.

Press 1 if you wish to eliminate another FSR?

1

The sensor I will simulate failed is FSR # 11
This sensor is in the A-NEGATIVE face system.

None of the 4 initial subsystems remain intact.

I will randomly pick 6 of the remaining FSRs to generate another subsystem.

After 0 iterations, the randomly generated subsystem is:

4.5	7.5	1.0	1.0	0.0	-4.5
1.5	0.0	-7.5	0.0	-1.0	0.0
-4.5	-7.5	0.0	0.0	0.0	1.0
7.5	4.5	4.5	3.0	1.0	-1.0
0.0	7.5	0.0	0.0	0.0	-1.0
1.5	1.5	0.0	0.0	0.0	-1.0

The rank of this new subsystem is: 6
This subsystem provides an invertible matrix.

Press 1 if you wish to eliminate another FSR?

1

I will randomly pick 6 of the remaining FSRs to generate another subsystem.

After 1 iterations, the randomly generated subsystem is:

-7.5	0.0	-7.5	0.0	-1.0	0.0
1.5	4.5	4.5	3.0	-1.0	1.0
-7.5	-7.5	0.0	0.0	0.0	1.0
0.0	-4.5	4.5	3.0	1.0	1.0
-7.5	-4.5	4.5	3.0	1.0	1.0
4.5	1.0	1.0	0.0	-4.5	1.0

The rank of this new subsystem is: 6
This subsystem provides an invertible matrix.

Press 1 if you wish to eliminate another FSR?

1

I will randomly pick 6 of the remaining FSRs to generate another subsystem.

After 1 iterations, the randomly generated subsystem is:

-4.5	4.5	-4.5	-3.0	-1.0	-1.0
4.5	-1.5	0.0	0.0	0.0	1.0
4.5	0.0	-7.5	0.0	-1.0	0.0
-1.5	0.0	1.5	0.0	1.0	0.0
-1.5	1.0	1.0	0.0	-4.5	1.0
-4.5	4.5	3.0	1.0	1.0	0.0

The rank of this new subsystem is: 6
This subsystem provides an invertible matrix.

Press 1 if you wish to eliminate another FSR?

1

I will randomly pick 6 of the remaining FSRs to generate another subsystem.

After 0 iterations, the randomly generated subsystem is:

4.5	0.0	1.5	0.0	1.0	0.0
-4.5	4.5	4.5	3.0	1.0	-1.0
4.5	4.5	4.5	3.0	1.0	-1.0
-1.5	1.0	1.0	0.0	-4.5	1.0
-4.5	4.5	3.0	1.0	1.0	0.0
-1.5	0.0	0.0	0.0	1.0	1.0

The rank of this new subsystem is: 6
This subsystem provides an invertible matrix.

Press 1 if you wish to eliminate another FSR?

1

I will randomly pick 6 of the remaining FSRs to generate another subsystem.

After 1 iterations, the randomly generated subsystem is:

4.5	0.0	-7.5	0.0	-1.0	0.0
-1.5	4.5	4.5	3.0	1.0	-1.0
4.5	1.0	1.0	0.0	-4.5	1.0
4.5	4.5	3.0	-1.0	1.0	0.0
0.0	-7.5	0.0	-1.0	0.0	-1.0
1.5	0.0	0.0	0.0	-1.0	1.0

The rank of this new subsystem is: 6
This subsystem provides an invertible matrix.

Press 1 if you wish to eliminate another FSR?

1

I will randomly pick 6 of the remaining FSRs to generate another subsystem.

After 1 iterations, the randomly generated subsystem is:

0.0	1.5	0.0	0.0	0.0	-1.0
-4.5	1.0	1.0	0.0	-4.5	1.0
-4.5	4.5	3.0	1.0	1.0	0.0
1.5	0.0	0.0	0.0	-1.0	1.0
4.5	4.5	3.0	-1.0	1.0	0.0
-1.5	0.0	0.0	0.0	1.0	1.0

The rank of this new subsystem is: 6
This subsystem provides an invertible matrix.

Press 1 if you wish to eliminate another FSR?

1

I will randomly pick 6 of the remaining FSRs to generate another subsystem.

After 27 iterations, the randomly generated subsystem is:

-1.5	1.0	1.0	0.0	-4.5	1.0
0.0	-7.5	0.0	-1.0	0.0	-1.0
-1.5	0.0	0.0	0.0	1.0	1.0
0.0	1.5	0.0	1.0	0.0	1.0
4.5	4.5	3.0	-1.0	1.0	0.0
1.5	0.0	0.0	0.0	-1.0	1.0

The rank of this new subsystem is: 6
This subsystem provides an invertible matrix.

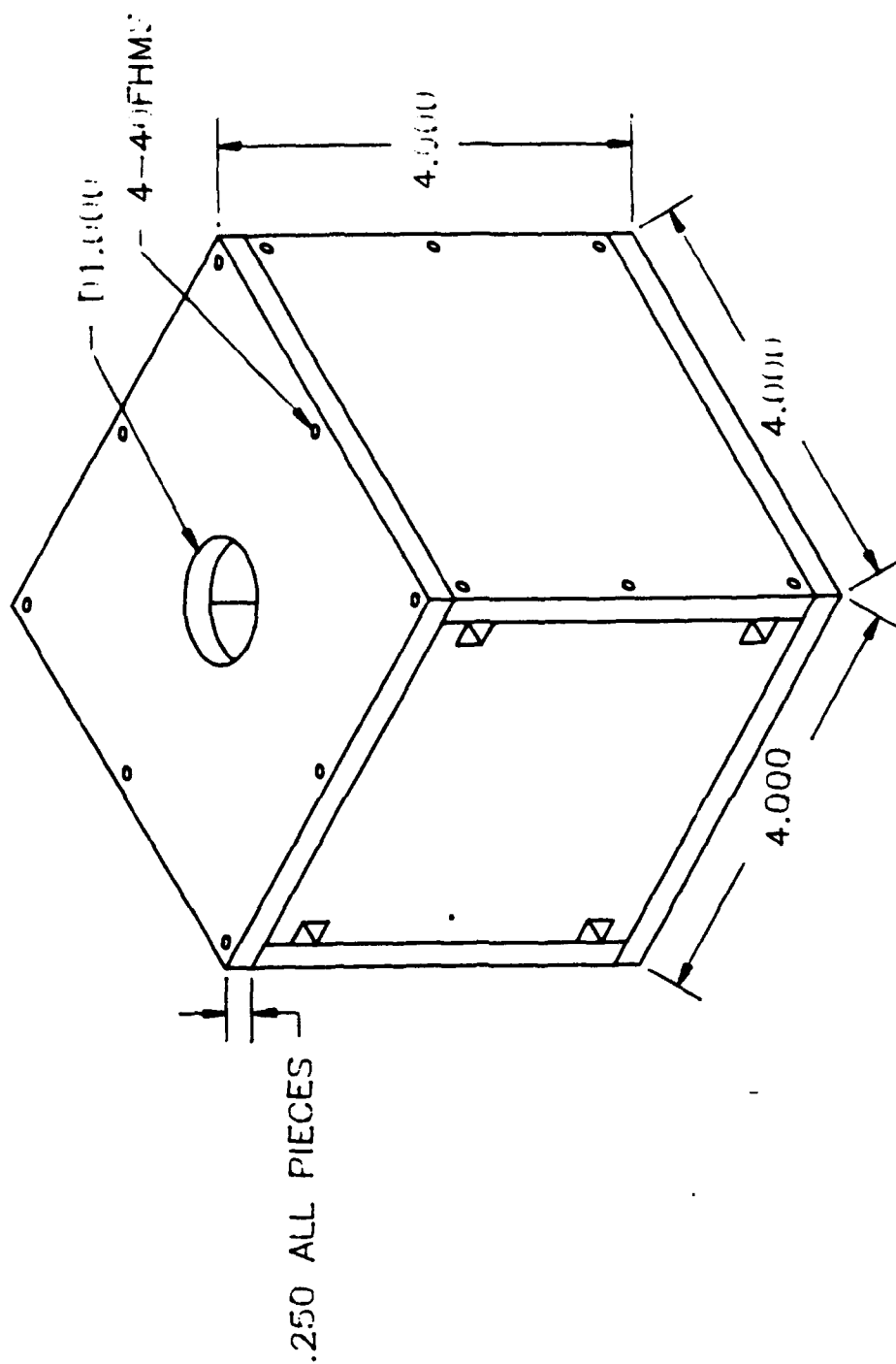
Press 1 if you wish to eliminate another FSR?

1

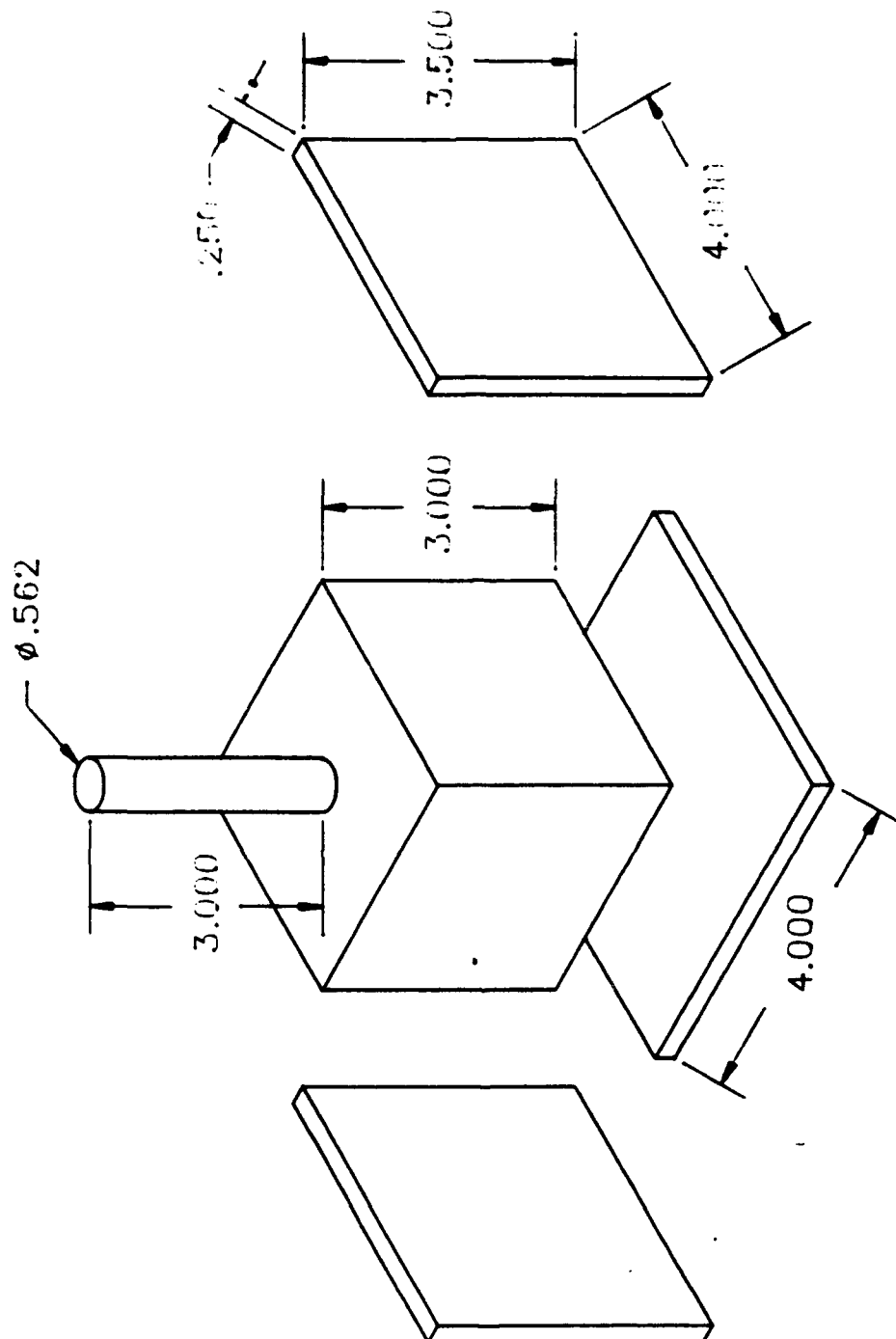
I will randomly pick 6 of the remaining FSRs to generate another subsystem.

TERMINATION==> There are not enough FSRs remaining to continue.

APPENDIX C



FORCE-TORQUE TRANSDUCER
(OUTSIDE BOX)



FORCE-TORQUE TRANSDUCER
(INSIDE CUBE)

APPENDIX D

DRIFT ANALYSIS TEST #1:

RESISTANCE: various (kohms)

i = 1..17

DATE/TIME ELAPSED TIME (hrs)

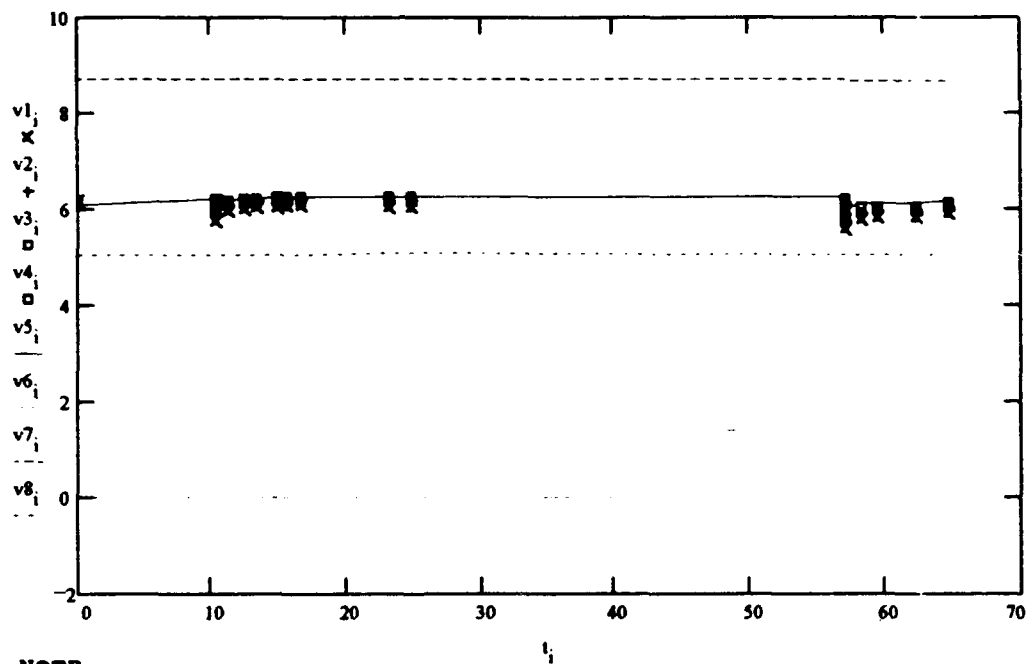
VOLTAGE (v)

dtg_i =

t_i =

v1_i = v2_i = v3_i = v4_i = v5_i = v6_i = v7_i = v8_i =

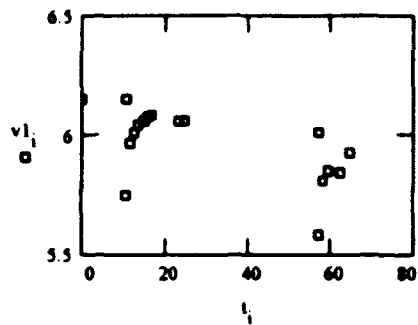
232247	0	6.149	6.090	6.161	6.187	6.087	.004	8.704	5.059
240908	10.35	6.149	6.102	6.176	6.220	6.216	.004	8.704	5.059
240909	10.37	5.749	6.060	5.975	6.089	6.089	.004	8.701	5.059
241007	11.34	5.963	6.092	6.085	6.170	6.168	.004	8.709	5.060
241113	12.44	6.009	6.113	6.115	6.197	6.193	.004	8.714	5.062
241210	13.39	6.041	6.128	6.140	6.210	6.211	.004	8.719	5.062
241332	14.76	6.060	6.138	6.164	6.238	6.230	.004	8.722	5.062
241425	15.64	6.074	6.142	6.174	6.248	6.232	.004	8.724	5.062
241527	16.67	6.083	6.147	6.187	6.255	6.240	.004	8.724	5.062
242153	23.10	6.062	6.106	6.182	6.240	6.236	.004	8.709	5.064
242334	24.78	6.060	6.104	6.178	6.234	6.234	.004	8.704	5.064
260752	57.08	6.011	6.050	6.174	6.197	6.253	.004	8.691	5.060
260754	57.11	5.585	5.759	5.745	5.906	6.006	.004	8.679	5.060
260901	58.23	5.811	5.880	5.929	6.035	6.109	.004	8.681	5.060
261015	59.46	5.852	5.902	5.963	6.060	6.138	.004	8.684	5.060
261308	62.34	5.844	5.887	5.967	6.048	6.121	.004	8.646	5.057
261527	64.67	5.923	5.950	6.031	6.115	6.176	.004	8.686	5.060



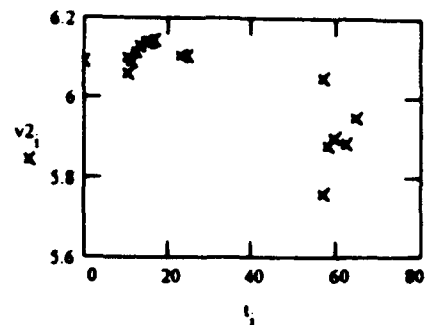
NOTE:

- CH1--joystick FSR#1,10kohms
- CH2--joystick FSR#2,10kohms
- CH3--joystick FSR#12,10kohms
- CH4--joystick FSR#6,10kohms
- CH5--uncut FSR in beam prototype,30kohms
- CH6--uncut FSR w/ no applied load,1Mohms
- CH7--shortened FSR loaded with vice grips,1Mohms
- CH8--no FSR, just 5v directly applied,1Mohms

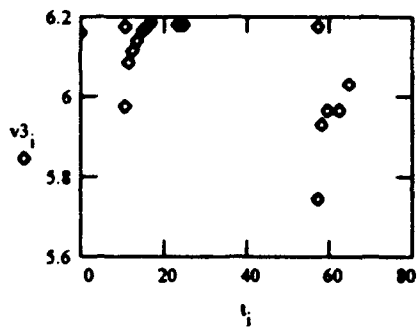
CHANNEL 1



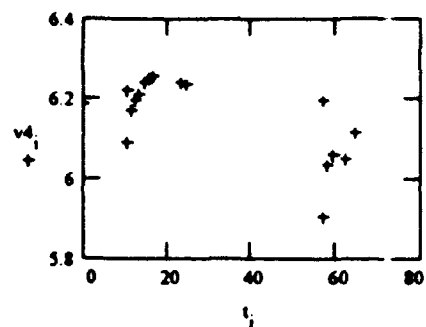
CHANNEL 2



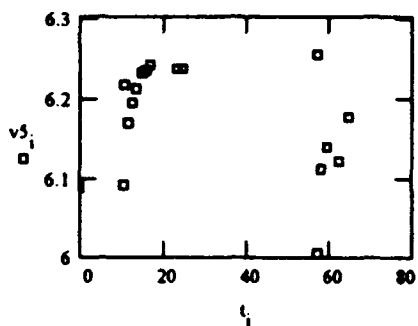
CHANNEL 3



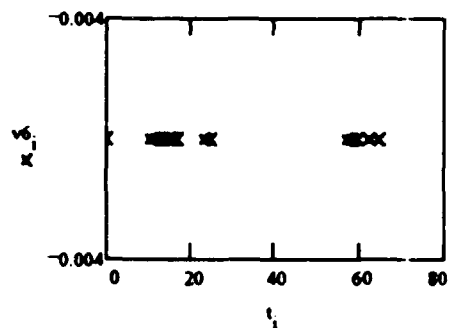
CHANNEL 4



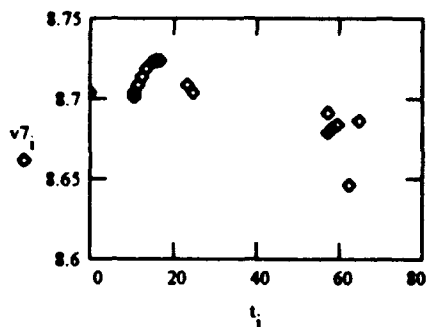
CHANNEL 5



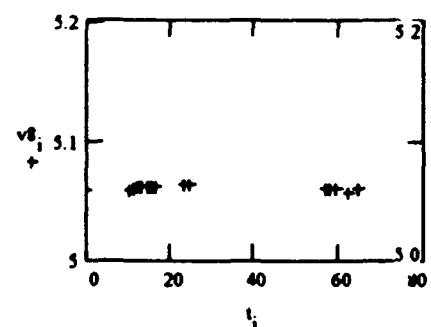
CHANNEL 6



CHANNEL 7



CHANNEL 8



DRIFT ANALYSIS TEST #2:

RESISTANCE: various (kohms) $i = 1.21$

DATE/TIME ELAPSED TIME(min)

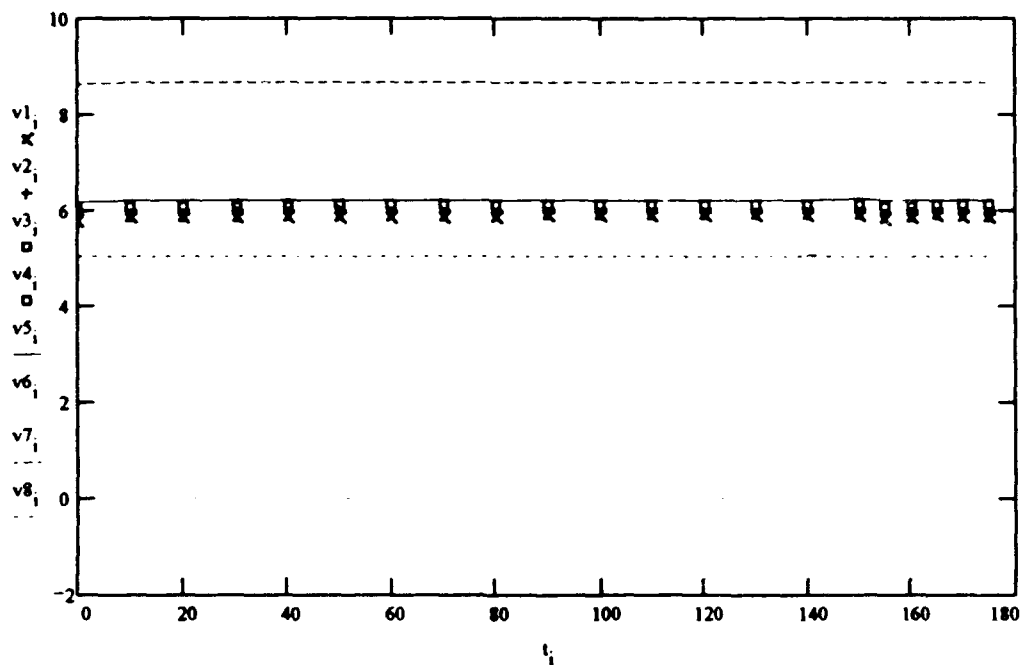
VOLTAGE (v)

$dtg_i =$

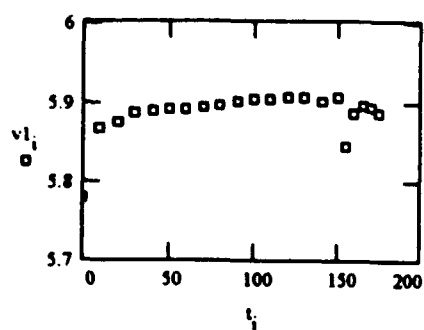
$t_i =$

$v1_i = v2_i = v3_i = v4_i = v5_i = v6_i = v7_i = v8_i =$

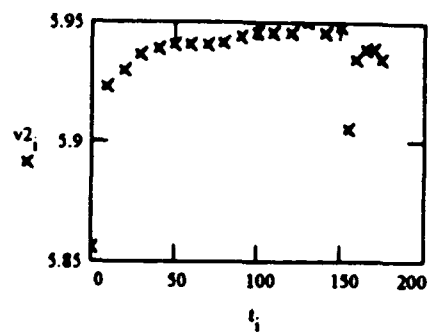
282010	0	5.778	5.856	6.031	6.027	6.147	.004	8.631	5.058
282020	10	5.865	5.923	6.089	6.091	6.203	.004	8.671	5.058
282030	20	5.872	5.930	6.096	6.100	6.207	.004	8.676	5.058
282040	30	5.886	5.937	6.102	6.106	6.213	.004	8.678	5.059
282050	40	5.887	5.939	6.104	6.108	6.217	.004	8.681	5.059
282100	50	5.891	5.941	6.106	6.113	6.217	.004	8.681	5.059
282110	60	5.889	5.941	6.110	6.113	6.221	.004	8.681	5.059
282120	70	5.893	5.941	6.110	6.113	6.222	.004	8.681	5.059
282130	80	5.895	5.942	6.110	6.115	6.222	.004	8.683	5.059
282140	90	5.899	5.944	6.110	6.117	6.224	.004	8.683	5.059
282150	100	5.903	5.946	6.110	6.120	6.226	.004	8.683	5.059
282200	110	5.903	5.946	6.111	6.121	6.226	.004	8.683	5.059
282210	120	5.904	5.946	6.115	6.123	6.228	.004	8.683	5.059
282220	130	5.904	5.950	6.117	6.125	6.228	.004	8.683	5.059
282230	140	5.901	5.946	6.117	6.123	6.228	.004	8.683	5.059
282240	150	5.904	5.948	6.117	6.127	6.230	.004	8.686	5.059
282245	155	5.843	5.906	6.087	6.083	6.205	.004	8.663	5.059
282250	160	5.884	5.935	6.106	6.104	6.224	.004	8.681	5.059
282255	165	5.896	5.939	6.110	6.110	6.228	.004	8.681	5.059
282300	170	5.893	5.939	6.110	6.110	6.228	.004	8.683	5.059
282305	175	5.884	5.935	6.110	6.110	6.228	.004	8.683	5.059



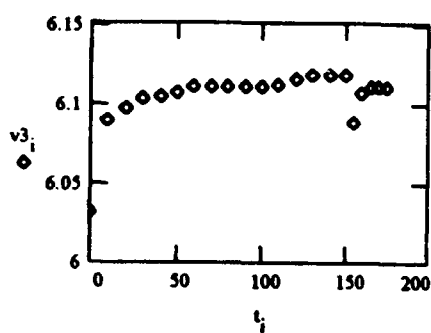
CHANNEL 1



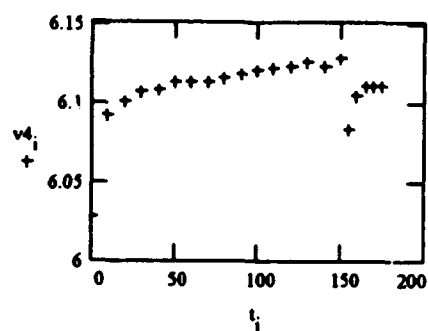
CHANNEL 2



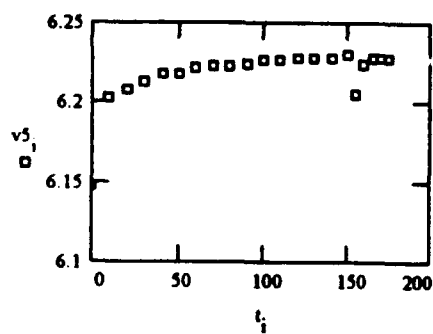
CHANNEL 3



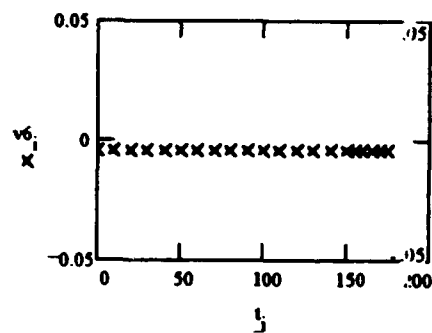
CHANNEL 4



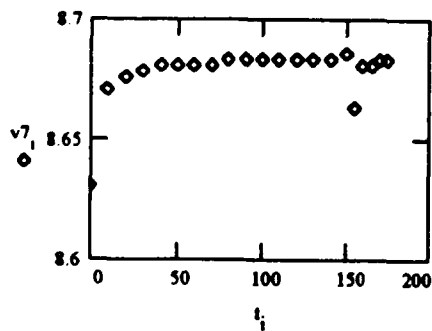
CHANNEL 5



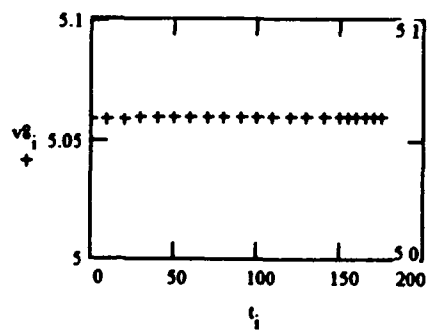
CHANNEL 6



CHANNEL 7



CHANNEL 8



DRIFT ANALYSIS TEST #3:

RESISTANCE: 1 (Mohms) $i = 1.13$

DATE/TIME ELAPSED TIME(min) VOLTAGE (v)

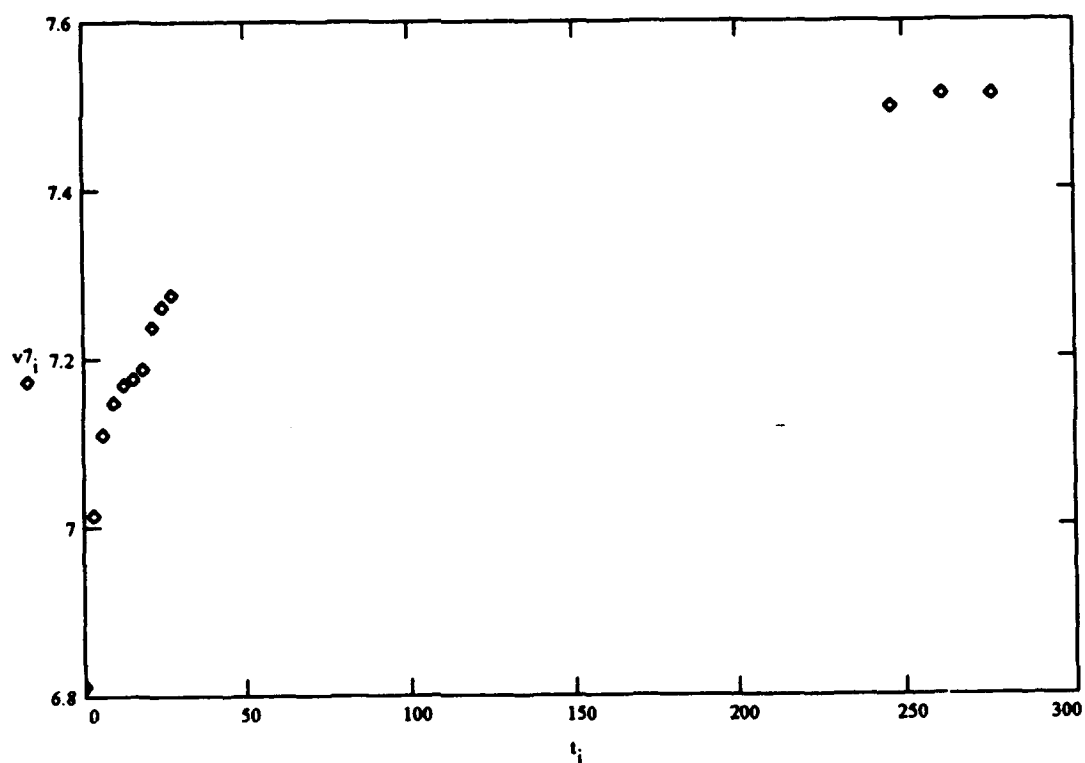
$dtg_i =$

$t_i =$

$v7_i =$

031611	0	6.811
031614	3	7.015
031617	6	7.109
031620	9	7.148
031623	12	7.168
031626	15	7.176
031629	18	7.187
031632	21	7.238
031635	24	7.263
031638	27	7.276
032017	246	7.498
032032	261	7.511
032047	276	7.513

CHANNEL 7

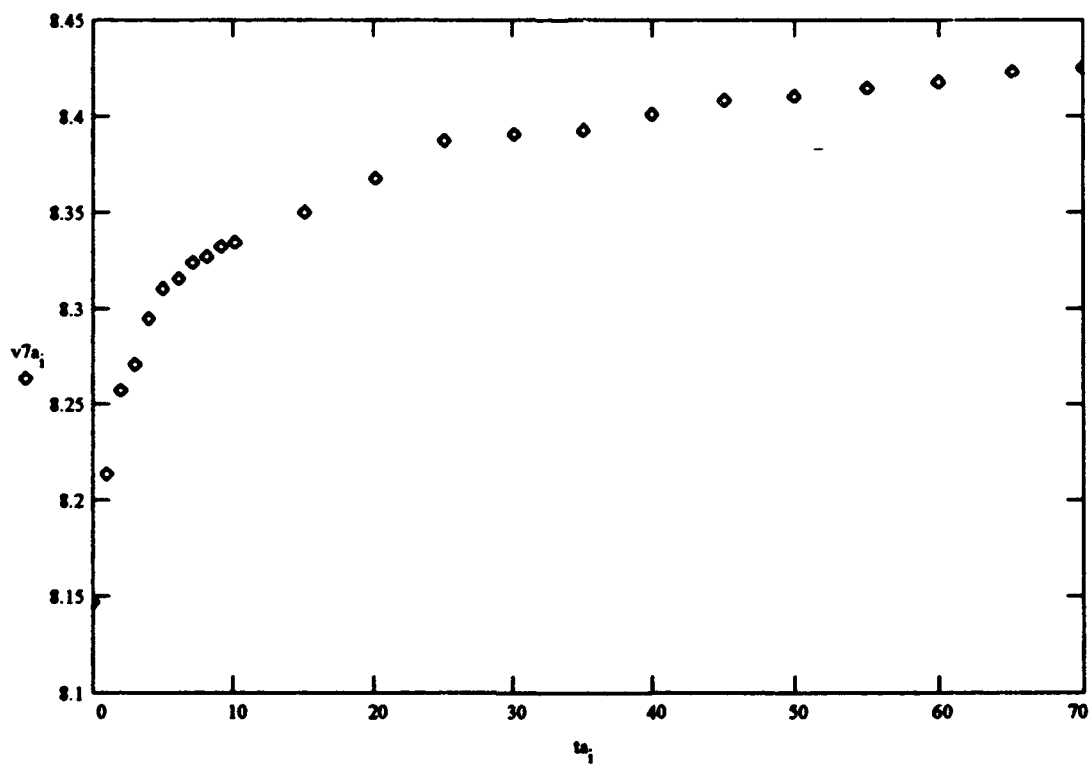


DRIFT ANALYSIS TEST #4:

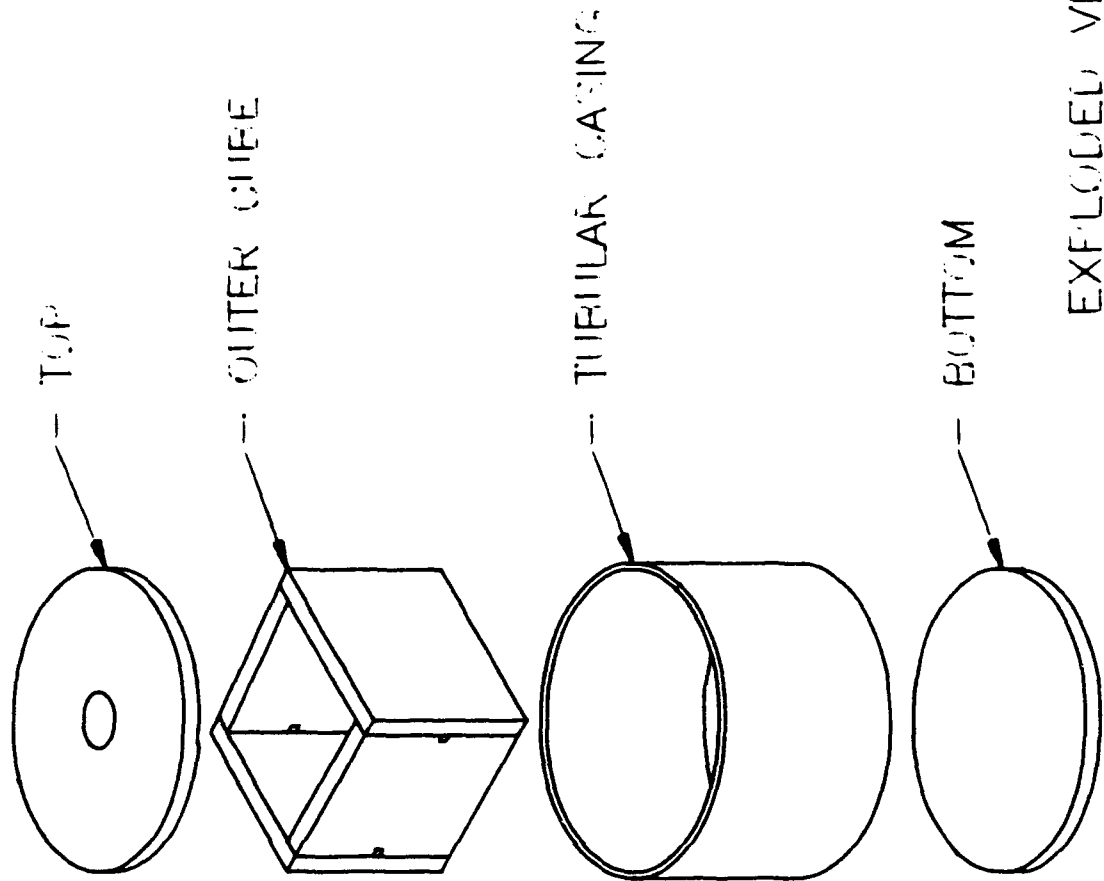
RESISTANCE: 1 (Mohms) $i = 0.22$

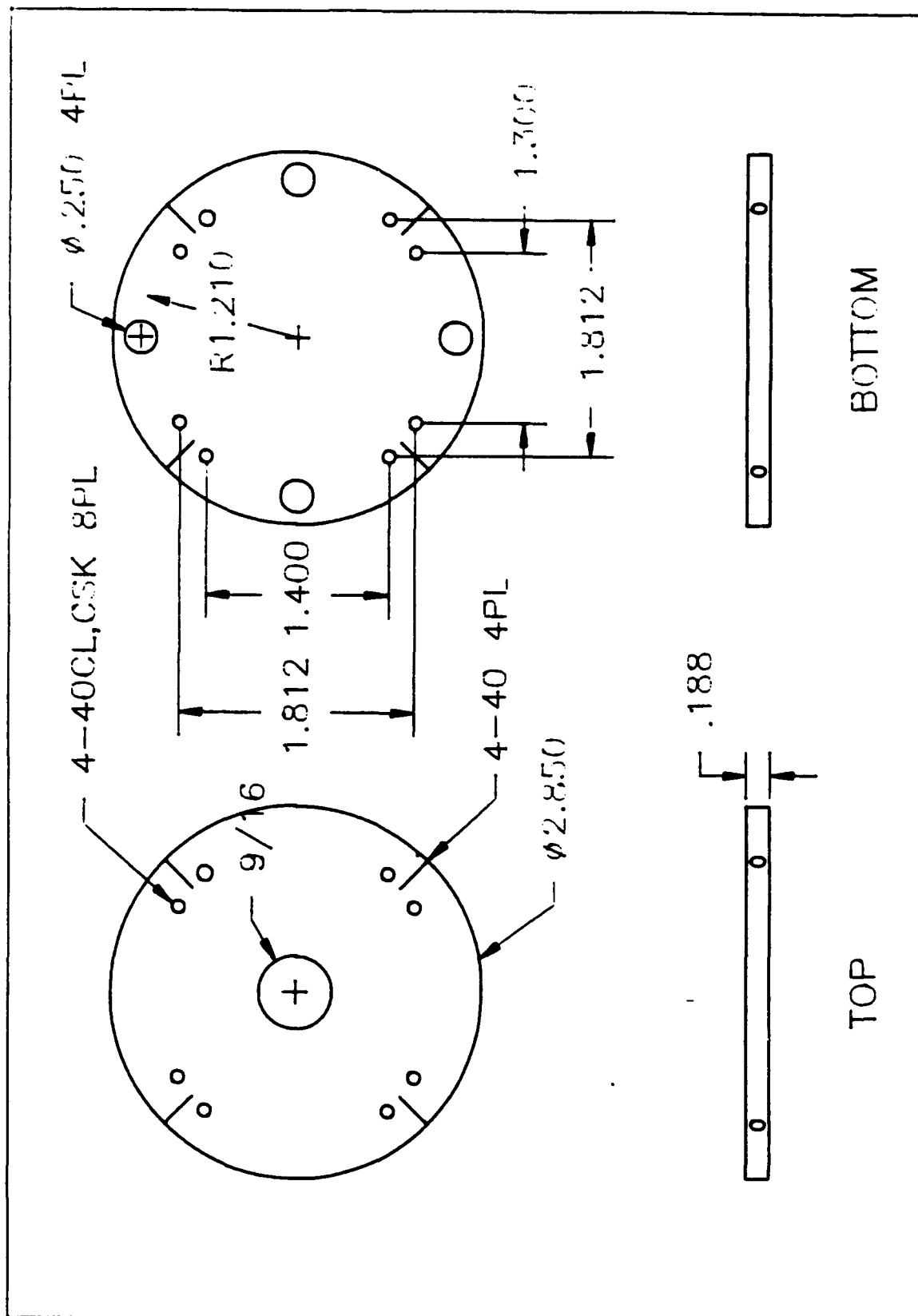
DATE/TIME ELAPSED TIME(min) VOLTAGE (v)

$dt_{a_1} =$	$ta_1 =$	$v7a_1 =$
032115	0	8.147
032116	1	8.214
032117	2	8.257
032118	3	8.271
032119	4	8.295
032120	5	8.310
032121	6	8.316
032122	7	8.324
032123	8	8.327
032124	9	8.332
032125	10	8.334
032130	15	8.350
032135	20	8.368
032140	25	8.388
032145	30	8.391
032150	35	8.393
032155	40	8.401
032200	45	8.408
032205	50	8.410
032210	55	8.415
032215	60	8.418
032220	65	8.423
032225	70	8.425



APPENDIX E





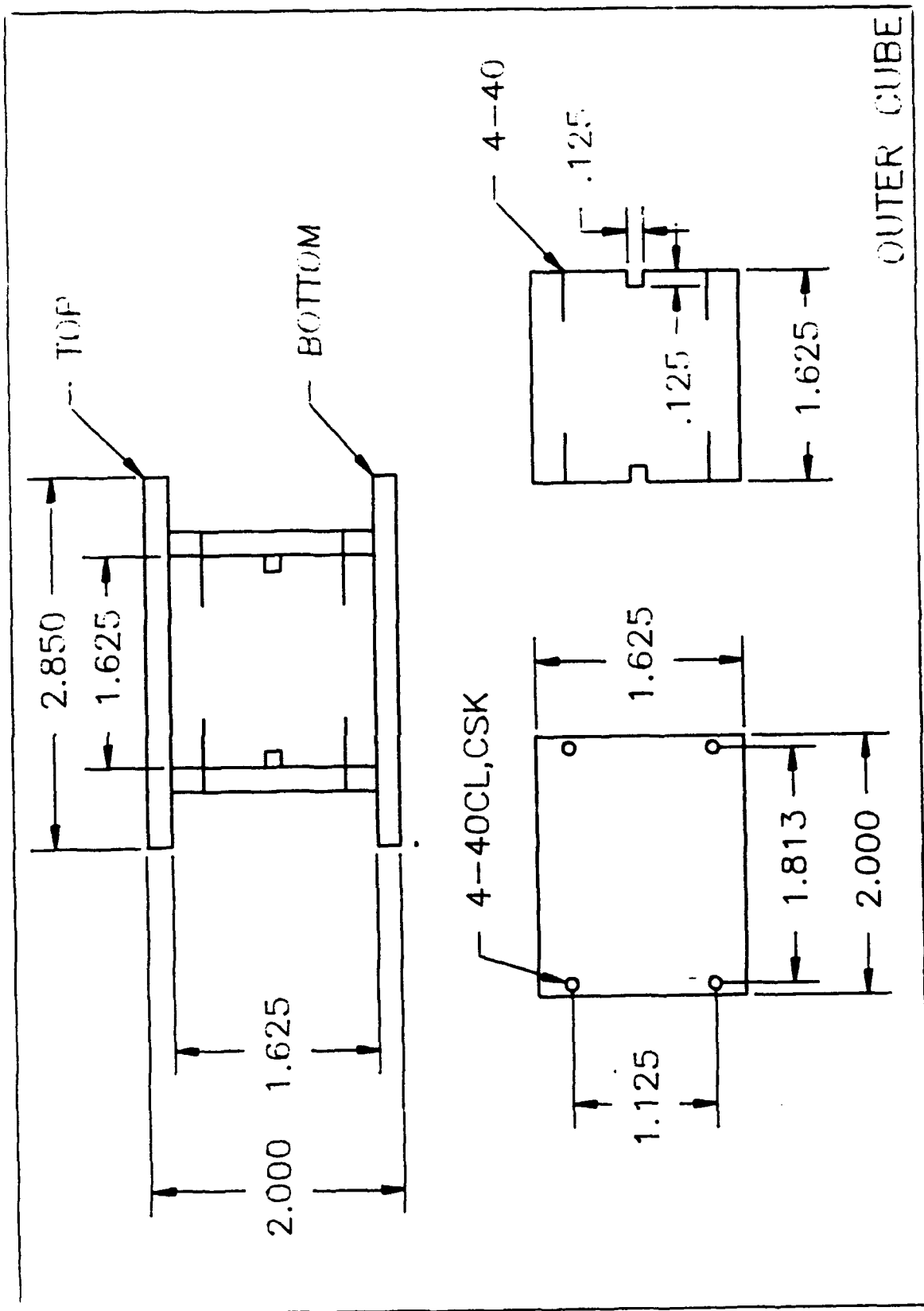
3.00 ODX.075 WALL

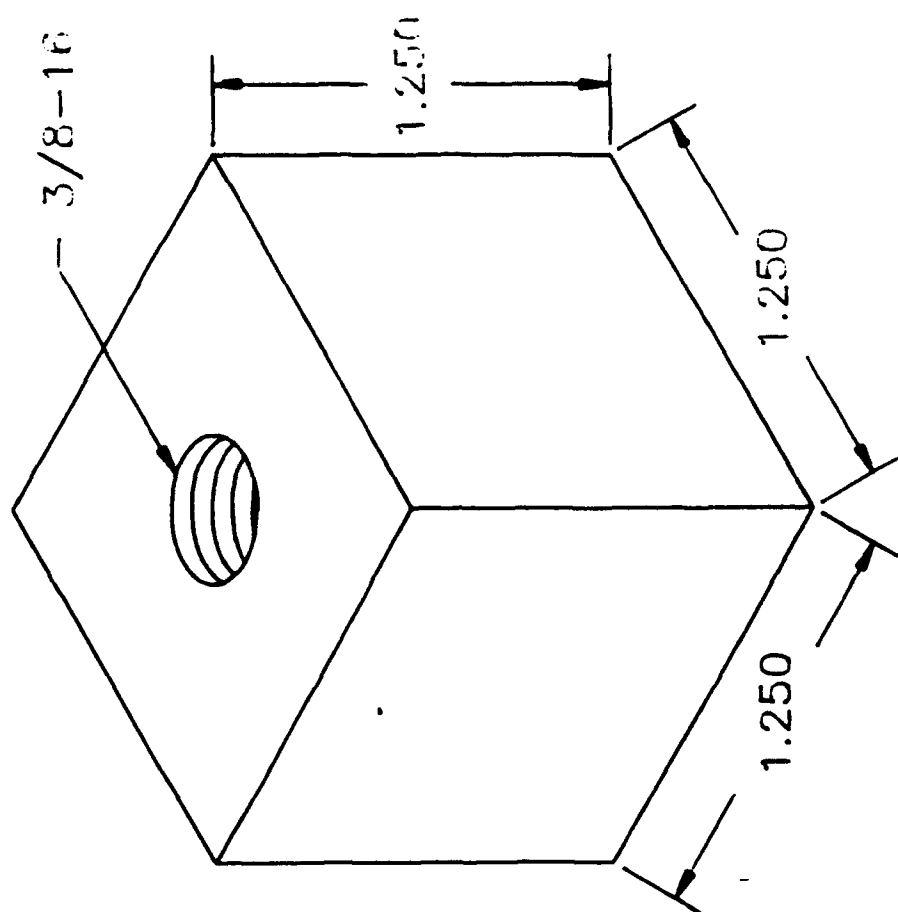
4-40CL,CSK 8FL

.094

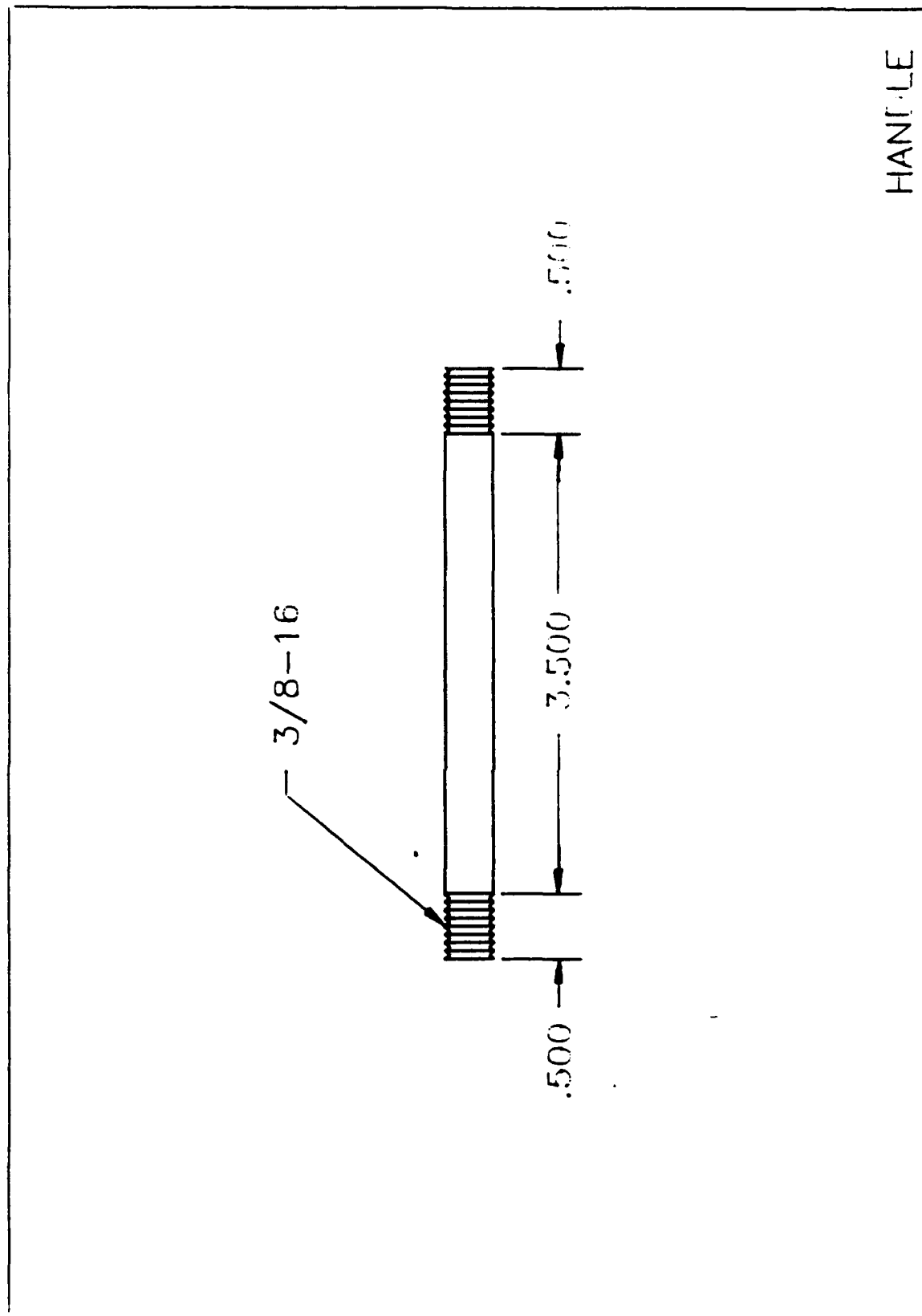
2.000

TUBULAR CASING





INNER CUBE



HANDLE

LIST OF REFERENCES

1. Syvertsen, James M., *Force Override Rate Controller for Remote Actuation*, Master's Thesis, Naval Postgraduate School, September 1992.
2. Ondrey, Larry P., *Three Axis Override Rate Control of a PUMA 560 Manipulator*, Master's Thesis, Naval Postgraduate School, March 1993.
3. Driels, Morris R., *Force Override Rate Controller For Remote Actuation: Final Report FY92*, Unpublished report, Naval Postgraduate School, 1992.
4. *Force and Position Sensing Resistors*, Interlink Electronics, Revision 2/90.
5. *Force Sensing Resistors Technote 1*, Interlink Electronics, Release 9/90.
6. Liu, C.L., *Introduction to Combinatorial Mathematics*, McGraw-Hill Book Company, 1968.

INITIAL DISTRIBUTION LIST

	No. Copies
1. Defense Technical Information Center Cameron Station Alexandria VA 22304-6145	2
2. Library, Code 052 Naval Postgraduate School Monterey CA 93943-5002	2
3. Mr. Jim Moore New Initiatives Office NASA Johnson Space Center 2101 NASA Road 1 Houston TX 77058-3691	1
4. Mr. L. Monford NASA Johnson Space Center Mail Stop ER Houston TX 77058	1
5. Naval Engineering Curricular Office Code 34 Department of Mechanical Engineering Naval Postgraduate School Monterey CA 93943-5000	1
6. Department Chairman, Code ME Department of Mechanical Engineering Naval Postgraduate School Monterey CA 93943-5000	1
7. Professor Morris Driels, Code ME/dr Department of Mechanical Engineering Naval Postgraduate School Monterey CA 93943-5000	3
8. LT Charles A. Gunzel-III Navy Dive and Salvage Training Center 350 South Crag Road Panama City FL 32407	2